universität wien

MASTERARBEIT

The effects of UV irradiation on alternative splicing in *Arabidopsis thaliana* and *Physcomitrella patens*

Armin Fuchs, Bakk.Biol.

angestrebter akademischer Grad
Master of Science (MSc)

Wien, 2011

Studienkennzahl:	A 066 830
Studienrichtung:	Masterstudium Molekulare Mikrobiologie und Immunbiologie
Betreuerin:	Prof. Dr.rer.nat. Andrea Barta

Dedicated to my parents, my sister and my grandparents

Acknowledgements

I often imagined this particular moment, forming my acknowledgments to thank everybody who accompanied me on this journey and now this time has finally arrived.

Of course, in the process of tossing out thanks, I have to show gratitude to the universe for not getting rid of me even though I spam entropy all over the place. Besides untouchable entities, I'd like to thank my mom and dad, who not only created me, but also did everything they could to support me in my efforts of becoming a scientist. Without your help, nothing of this would have been possible. I'd also like to thank my beloved sister and grandparents, who never gave up on a seemingly hopeless case such as myself.

As you, dear reader, (hopefully) know, a person is always majorly defined by its environment, most importantly and foremost by good, oldschool friends. In this department I have been blessed with wonderful people who sometimes willingly, sometimes not so much willingly supported and accompanied me all along the way. I'd like to thank my closest friends for their everlasting support and utter madness across all these splendid years.

Thanks to Dave, my dear friend and flat-mate, without whom I would have definitely gone crazy. Without a doubt, many more good years will follow as we both progress in our (hopefully only partially scientific) lives. Thanks to Dominicus, who significantly influenced my life and train of thoughts across all these years. Even though we had a lot of fights, we had even more conciliations. I am grateful for your sincere friendship. I'd like to thank my good old friend Daniel, who is with me since the earliest of days my crude brain is still able to recall (as of 2011). You are a true friend, who supported me during all these years. Thanks to the crazy physician and my brilliant friend (or maybe the other way round, I can never remember) Simon, who always cheered me up in times of need. You are, without a doubt, one of a kind. Thanks to Michael for being a great friend during all these years and for your occasional loss at tennis (so I would not give up on this sport). Thanks to Sebastian for a smorgasboard of entertaining evenings, filled with movies, discussions and the occasional, yet infinitely awesome RockBand session. I'd also like to thank my friend Matthias for being an utterly crazy and yet beloved person in my live. We had countless feverish discussions

on almost anything this universe has to offer and yet we still talk to each other, which is odd to begin with. Of course, thanks to Marion for being such an inspiring friend, who's (almost) always in a fun-contagious mood. Last but not least I'd like to thank Teddy. You've become a good friend during my short period in Vienna.

Obviously, I could not have done this thesis without the support and opportunity given to me by the great lab of Andrea Barta. My sincere thanks go to Andrea for offering me the chance to learn and work in your lab and to get to know you as a kind and brilliant person. Infinite thanks to Maria for your everlasting patience and support during my time in the lab. You are definitely the best mentor one can possibly hope for. I'd also like to thank Janett for tons of fun in the lab and for helping me a great deal during my thesis work and especially for your help on LaTeX. Thanks also to Yamile, Olga, Nicola, Claudia, Stefanie, Jarek, Branislav and Franz for your support and friendship during my time in Vienna.

Last but not least I'd like to thank a few individuals for what they do. Thanks to Sean "Day9" and Nick "Tasteless" Plott, Husky, Artosis and the whole crew of Team Liquid for being such inspiring, utterly crazy, funny and hardworking guys in the scene of Starcraft II. Of course, also thanks to Blizzard for creating this very game. Thanks to Roger Federer for being an inspiration on and off the tennis court. Thanks to Chuck Lorre, Bill Prady and the whole crew of the Big Bang Theory for this ingenious Sitcom. Thanks to Dylan Moran for being an unbelievable stand-up comedian. Thanks to Masamune Shirow and Mamoru Oshii for writing and filming Ghost in the Shell. Thanks to the Dave Brubeck Quartet for writing and recording Take Five, which got me through numerous almost-freak-out moments. Thanks to Kenji Kawai, Nobuo Uematsu and Mogwai for making music and of course, thanks to Douglas Adams for writing "The Hitchhiker's Guide to the Galaxy" [1].

Of course I have to end this acknowledgements section in style, so I'll quote Albert Einstein with an interesting and hopefully not entirely true conclusion: "Science is a wonderful thing if one does not have to earn one's living at it."

Contents

Abstract

Alternative splicing is a powerful mechanism to fine tune gene expression and significantly increase transcriptome complexity of most eukaryotic organisms. A plenitude of cis- and trans-acting factors are necessary to appropriately redirect the spliceosome to weaker splice sites in times of need. The well known family of SR proteins plays a considerable part during splice site selection and spliceosome assembly. Previous studies have demonstrated that SR proteins extensively influence alternative splicing of downstream genes during stress conditions. Furthermore, it has been shown that SR pre-mRNAs themselves undergo alternative splicing, which in turn is partially regulated by SR proteins, therefore giving rise to a complex network that enables an organism to quickly react to environmental stimuli. Here we show that SR pre-mRNAS in *Arabidopsis thaliana* and *Physcomitrella patens* experience extensive alternative splicing events upon UV-C treatment. In addition to UV-C radiation, we simultaneously subjected *A.thaliana* cell suspension cultures to starvation as an additional stress factor. As a result, we show that unique splicing and regulatory events arise upon combination of these potent stresses. Interestingly, regulation of orthologous SR pre-mRNAs partially differs between the flowering plant *A.thaliana* and the ancient moss *P.patens*, which implicates diverging adaptations to changing evolutionary pressures over millions of years. Furthermore, we demonstrate that splicing of specific DNA-repair pre-mRNAs in *A.thaliana* and *P.patens* is partially regulated by SR proteins. Previous studies have been able to show that slowing down or pausing of the Pol II possibly increases alternative splicing rates due to the exclusive presence of weak 3' splice sites before stronger ones can be transcribed and become available to the spliceosome. Here we try to uncover a possible connection between alternative splicing and the transcription process of the stalled RNA polymerase II during UV-C induced DNA damage in plants. Last but not least, we make use of artificial microRNAs to effectively knock down specific SR genes in *A.thaliana*, which will enable follow-up studies that further analyse this complex regulatory network.

Zusammenfassung

Alternatives Spleißen ist ein wichtiger Mechanismus zur Feinregulation der Genexpression und Erweiterung der Transkriptomkomplexität in den meisten eukaryotischen Organismen. Eine Vielzahl an cis- und trans-agierenden Faktoren ist notwendig um das Spleißosom bei Bedarf korrekt zu schwächeren Spleißstellen zu dirigieren. Die wohlbekannte Familie der SR Proteine spielt eine bedeutende Rolle während der Spleißstellenselektion und dem Aufbau des Spleißosoms. Frühere Studien haben gezeigt, dass SR Proteine während Stresssituationen einen umfangreichen Einfluss auf alternatives Spleißen von nachgeschalteten Genen haben. Darüber hinaus wurde demonstriert, dass SR prä-mRNAs selber alternativ gespleißt werden, teils sogar unter der Regulation von SR Proteinen, was wiederum auf ein komplexes und verstricktes Netzwerk hindeutet, welches es einem Organismus erlaubt schnell auf umweltbedingte Stimuli zu reagieren. In dieser Arbeit zeigen wir, dass SR prä-mRNAs in *Arabidopsis thaliana* und *Physcomitrella patens* unter dem Einfluss von UV-C Bestrahlung alternativ gespleißt werden. Zusätzlich zur UV-C Strahlung haben wir *A.thaliana* Zellsuspensionskulturen simultan einem weiteren Stressfaktor ausgesetzt, nämlich dem Hungern. Als Resultat demonstrieren wir spezifische Spleiß- und Regulationsereignisse, welche durch die Kombination dieser Stressfaktoren ausgelöst wurden. Interessanterweise unterscheidet sich hierbei die Regulation von orthologen SR prä-mRNAs in der Blütenpflanze *A.thaliana* und dem Moos *P.patens*, was auf divergierende Adaptionen auf wechselnde evolutionäre Selektionsdrücke über Millionen von Jahren hinweist. Des Weiteren zeigen wir, dass Spleißen von DNA-Reparatur prä-mRNAs in *A.thaliana* und *P.patens* teilweise von SR Proteinen reguliert wird. Frühere Studien haben gezeigt, dass ein Abdrosseln oder Pausieren der RNA Polymerase II zu einer Steigerung von alternativem Spleißen führen kann, hauptsächlich durch die frühere Verfügbarkeit von schwachen 3' Spleißstellen bevor stärkere Spleißstellen transkribiert und dadurch für das Spleißosom verfügbar sind. In dieser Arbeit versuchen wir eine mögliche Verbindung zwischen alternativem Spleißen und dem Transkriptionsprozess der gedrosselten RNA Polymerase II während UV-C induziertem DNA Schaden in Pflanzen zu identifizieren. Zu guter Letzt nutzen wir künstliche Mikro-RNAs um die Expression von spezifischen SR Genen in *A.thaliana* effektiv zu unterdrücken, wodurch zukünftige Studien ermöglicht werden, welche dieses komplexe regulatorische Netzwerk weiter analysieren können.

Chapter 1

Introduction

1.1 *Arabidopsis thaliana*

Arabidopsis thaliana is the most intensively researched plant species. Considering that *A.thaliana* is a relatively unremarkable species, its development from an insignificant weed to the classical plant model organism is quite peculiar and certainly not self-mandatory. Initial studies, which evoked first interests in *A.thaliana* as a model organism, were conducted in the 1940s by Friedrich Laibach (Frankfurt) and George Rédei (University of Missouri, Columbia) in Germany and the United States, respectively (Figure 1) [2].

In this pre-molecular era, when gene cloning was but a dream, Laibach was drawn to *A.thaliana* due to its exceptional phenotypical natural variation and the responsible underlying mechanisms. Inspired by Laibachs' work, the following three decades attracted a number of enthusiastic and gifted scientists who conducted pioneer work in the area of X-ray induced mutations and biochemical genetics (Reinholz, Roebbelen, Jacobs), thus further promoting the influx of able researchers into this emerging field

Figure 1: **Important figures in the history of *A.thaliana* as a model organism.** Left to right: Friedrich Laibach, Gerhard Röbbelen and George Rédei. Adopted from [3].

[4]. When Rédei published a paper on *A.thaliana* as a genetic organism in the Annual Review of Genetics in 1975, the molecular era had dawned for *Arabidopsis* [5]. Positively alarmed by this publication, a plethora of scientists realised that *A.thaliana* offered unique research opportunities in a less competitive and more interdisciplinary connected environment [2]. After all, probably the most significant feature about *A.thaliana* is the supportive and encouraging research community in the background that might have made the difference between an insignificant weed and the classical plant model organism that is *Arabidopsis thaliana*.

Besides opportunity and community, also biological facts helped *A.thaliana* along the way. It is a member of the mustard family (Brassicaceae) and can be found all across Europe, Asia and North Africa [6]. A plenitude of different ecotypes (accessions), acquired from natural populations, can be accessed for experimental analysis. Among all these variations, the Columbia and Landsberg ecotypes are the most commonly used for studies and thus are considered the references. The plant itself can easily be adopted to the lab environment because of its ease of maintenance. *A.thaliana* is on average only about 10 cm tall (roots excluded) with self-pollinating flowers which give rise to tens of thousands of seeds, thus ensuring a high number of viable progeny. The life cycle of this plant, from seed germination to flowering to seed maturation, is completed within six weeks. Furthermore, plants can be grown on either petri dishes containing different growth media or simply in pots filled with soil [7, 3, 2]. *A.thaliana* cells may also be kept in a cell-culture orientated fashion and cell walls can be enzymatically digested, thus generating protoplasts, which can be easily manipulated for genetic, biochemical and microscopical analysis.

With only 125 Mb and five chromosomes the genome of *A.thaliana* is one of the smallest among flowering plants. It contains an estimated 27.000 protein-coding genes and duplicated several times over millions of years [8]. Even though flowering plants, like *A.thaliana*, lack the necessary genetic prerequisites for homologous recombination and thus targeted gene manipulation, insertional mutagenesis through *Agrobacterium tumefaciens* mediated T-DNA transformation can be achieved [9]. However, T-DNA insertion lines are not arbitrarily available for each and every gene, as these lines are generated through random insertions of T-DNA into the genome of *A.thaliana*. Luckily, necessity begets ingenuity. Taking advantage of microRNAs (miRNAs) allows for specific targeting of mRNAs transcribed from desired genes. MicroRNAs are 21-24

Figure 2: ***Arabidopsis thaliana.*** Painted by Janet Wehr, 1995 (image courtesy of C. Somerville). Adopted from [4].

nucleotides (nt) short endogenous non-coding RNA molecules, which regulate gene expression on a post-transcriptional level by binding to and repressing / degrading mature mRNA transcripts [10, 11, 12, 13]. By replacing the original miRNA sequence within the pre-miRNA construct with a specifically designed sequence complementary to the mRNA of any given target gene, it is possible to effectively knock-down target gene expression. This sophisticated modification of miRNAs gives rise to the term artificial microRNAs (amiRNAs). Thus, this approach enables the efficient targeting of single genes in closely related families and between close homologues [13].

Taken together, multiple reasons account for *A.thaliana* as the classical plant model organism. Last but not least, an ever growing, interdisciplinary community has formed around *A.thaliana*, which supports an encouraging atmosphere to do science.

1.2 *Physcomitrella patens*

The moss *Physcomitrella patens* is an emerging model organism in plant science. *P.patens* belongs to bryophytes, which cover mosses, liverworts and hornworts. These ancient lineages diverged from vascular land plants over 450 million years ago and thus reflect perfect research opportunities on the conservation and evolution of genetic and

physiological features [14, 15]. *P.patens* belongs to the family of Funariaceae, a class of Bryopsida. Funariaceae are described as a family of short-lived, small to medium-sized annual and biennial plants. P. patens itself has been described beautifully by Lang et al. as "a monoecious, self-fertile, annual opportunist growing in late summer to autumn in open, unshaded, limy, loamy, moist and disturbed but nutrient-rich habitats, often close to the waterline" [16]. *P.patens* can be found mainly in temperate zones across Europe, North America, Japan, Africa and Australia [17, 18].

The life cycle of *P.patens* is predominately haploid, which is fortunate for genetic studies. The diploid phase only spans the time frame from fertilization of the sexual organs to the release of roughly 4000 mature, haploid spores [19]. The gametophyte of *P.patens* is, in opposite to vascular plants, the larger plant, which comprises almost all tissues. After the germination of a haploid spore, a connected layer of single cells is formed, the protonema (Figure 3B, 3C). As the moss ages, shoots, also known as gametophytes or gametophores (Figure 3D), emerge from the protonemata. These gametophytes, induced by the phytohormon cytokinin, form both male and female sexual organs to initiate the brief, diploid phase of *P.patens* [20].

The haploid genome of *P.patens* contains roughly 500 Mb and consists of 27 chromosomes, which harbour around 36.000 predicted genes [21]. A gene structure of *P.patens* is comparable to the structure in *Arabidopsis*. However, the G/C content in *P.patens* genes is almost equal to the A/T portion, which is not the case in *Arabidopsis*. This is an indication that mosses seem to evolve at rather slow rates, which is partially due to their predominant haploid genome (see [22] for a detailed analysis).

Over the last two decades *P.patens* emerged as a model organism due to its ease of maintenance, simple body plan and unique genetic, phylogenetic and physiological features. Only the mosses *P.patens* and *Ceratodon purpureus* harbour the genetic prerequisites needed for homologous recombination and thus make reverse genetic approaches possible [23, 24, 25, 26].

Taken together, *P.patens* resembles an ideal plant model organism due to its unique phylogenetic position, unusual high frequency of gene targeting, simple body plan and thus ease of maintenance.

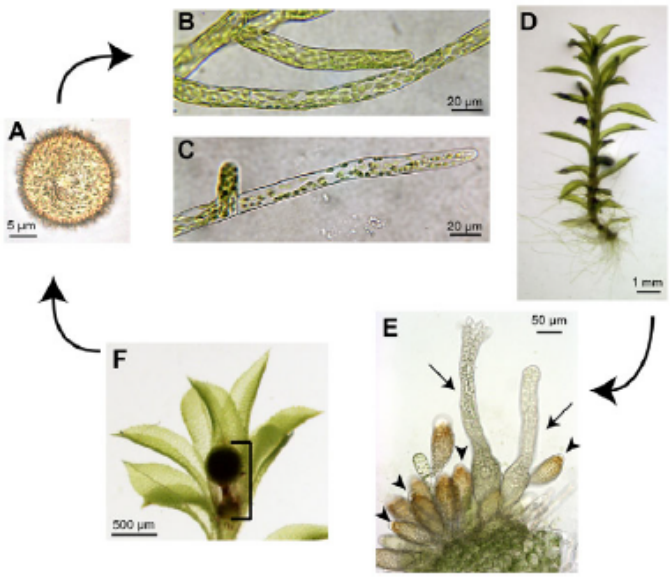

Figure 3: **Life cycle of *Physcomitrella patens*. A** Haploid spore, which subsequently transforms into **B** chloronemal cells. These cells eventually differentiate into **C** caulonemal cells. **D** A gametophore, grown from protonemata. **E** Gametophores house female (archegonia, see arrows) and male (antheridia, see arrowheads) reproduction organs. **F** Sporophyte (see bracket) at the tip of a gametophore. Adopted from [20].

1.3 Pre-mRNA splicing

Eukaryotic genes contain coding exonic and non-coding intronic sequences, which are also present on nascent pre-mRNA transcripts [27, 28]. A vast ribonucleoprotein (RNP) complex, the spliceosome, is able to recognize and bind rather degenerate consensus sequences on any given pre-mRNA to remove introns and ligate exons with remarkable precision [29, 30]. This process has been termed pre-mRNA splicing.

1.3.1 The spliceosome and key steps in pre-mRNA splicing

The spliceosome is a large and highly dynamic RNA-protein complex, which consists of five different small nuclear RNAs (snRNAs), namely U1, U2, U4, U5 and U6, and roughly 300 proteins [31]. The biological functions of RNP machineries such as the spliceosome or the ribosome are the result of an intensive cooperation between RNAs and proteins. Although these macromolecules are different in nature, they still share overlapping biological functions, such as reaction catalysis or the formation of binding platforms. If it were not for the dynamic collaborations between RNAs and proteins,

Figure 4: **Conserved sequences in metazoan pre-mRNAs.** Shown are the conserved consensus sequences in metazoan pre-mRNA introns (grey). Letters in red represent the highly conserved dinucleotides. R represents a purine while Y is a pyrimidine. N can be any nucleotide. Adopted from [32].

fundamental cellular processes could not be facilitated [32].

During the dynamic process of pre-mRNA splicing, the spliceosome undergoes vast structural rearrangements to facilitate the excision of introns and ligation of adjacent exons [32].

Two chemical reactions, called SN2-type transesterifications, as well as specific sequences, known as splice sites, are needed to do so. Splice sites are rather degenerate consensus sequences at the borders of intron/exon junctions (Figure 4). The 5' splice site is located at the 5' end of the intron and is characterized by a highly conserved GU dinucleotide, embedded in a less conserved consensus sequence, which varies between different organisms [31]. Three consecutive consensus sequences are located at the 3' end of the intron. First, the branch point, which harbours a specific A residue important for the first transesterification reaction to occur. The second conserved sequence is the polypyrimidine tract, followed by the third sequence, a highly conserved AG dinucleotide at the 3' end of the intron [33]. Only after the assembly of the spliceosomal components onto these splice sites may the transesterification reactions be catalysed (Figure 5).

The first step is characterized by an attack of the 2'-hydroxyl of the specific adenosine residue located in the branch point. The attack targets the phosphodiester bond at the 5' splice site, which results in a free 5' exon, while the intron forms a lariat structure with the adjacent 3' exon. The now exposed hydroxyl-group at 3' end of the 5' exon attacks the phosphodiester bond at the 3' splice site of the intron, thus leading to exon ligation and the ultimate release of the intron-lariat structure [32].

These cis-acting splice sites located in introns form, unlike self-splicing group II in-

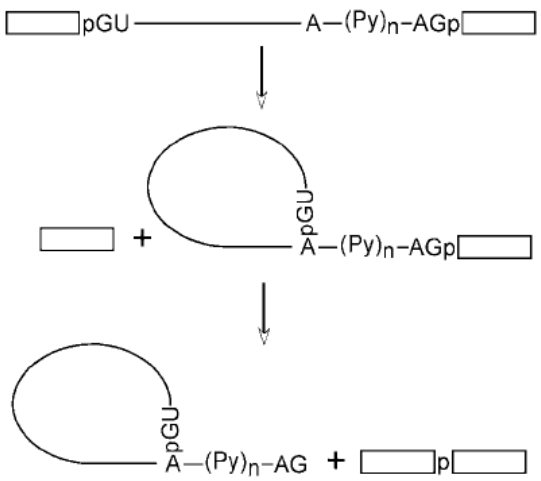

Figure 5: **Transesterification reactions.** Shown are schematics of the two transesterification reactions, which happen during pre-mRNA splicing. Open boxes represent exons while the intervening line represents an intron. Py is a pyrimidine and p is a phosphate. After the first step, the 5' exon is detached while the intron forms a lariat structure. The second step releases the intron lariat from the attached 3' exon and ligates the two exons. Details can be extracted from the text. Adopted from [33].

trons, very little secondary and tertiary structures and thus are dependent on additional trans-acting factors like the spliceosome [34]. This implicates that the spliceosome rearranges its own and the structure of the pre-mRNA in a way that the reactive groups come into close contact, which is in fact the case.

As mentioned above, the major spliceosome (for details on the minor spliceosome refer to [35]) consists of the snRNPs U1, U2, U4/U6 and U5. Each snRNP is composed of one snRNA (two snRNAs for U4/U6) and numerous specific proteins. Unlike the ribosomal snRNPs, the spliceosomal complexes do not harness any preformed active centers and undergo significant structural rearrangements along the splicing of pre-mRNAs (Figure 6) [32].

The assembly of the spliceosome begins with the ATP-independent base-pairing between the 5' end of the U1 snRNA and the 5' splice site of the intron. This initial interaction is supported by serine-arginine-rich (SR) proteins, which will be described in detail later on. Next, the protein SF1/BBP and the heterodimer U2AF bind to the branch point sequence and AG dinucleotide at the 3' end of the intron, respectively. Simultaneously, these two proteins are connected with each other and thus bind the

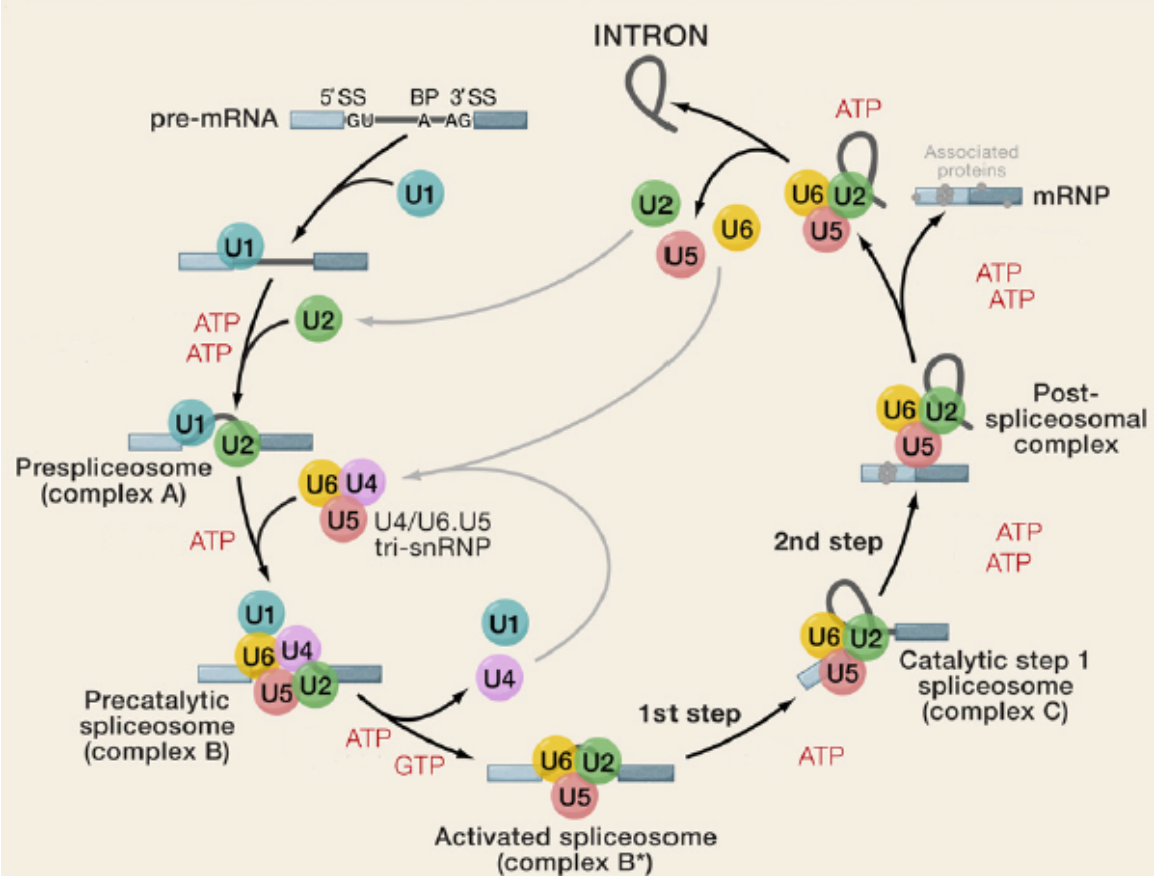

Figure 6: **Assembly of the major spliceosome across introns.** The assembly and disassembly cycle of the major spliceosome, but without any details on proteins, derived from mammalian splicing extracts, is shown. Blue rectangles represent exons while the intervening grey lines represent introns. Colored circles represent the individual components of the major spliceosome. See text for a detailed description. Adopted from [32].

pre-mRNA cooperatively. With U1, SF1/BBP and U2AF bound to the pre-mRNA, the spliceosomal E complex is formed, which plays a vital role in the recognition of the 5' and 3' splice sites of introns [32].

The spliceosomal E complex is transformed into the A complex upon ATP-dependent base-pairing interactions of the U2 snRNP with the branch point sequence located on the pre-mRNA. Subsequently, the bound SF1/BBP protein is being replaced by the U2 snRNP [32]. To form the catalytically still inactive B complex, the preassembled tri-snRNP U4/U6-U5 joins the A complex. Now all necessary snRNPs are present.

However, the B complex has to be massively rearranged in order to carry out the

first transesterification reaction. Upon activation of the spliceosome, U1 and U4 are released to give rise to the catalytically activate B* complex [32]. After facilitating the first transesterification reaction, the B* complex is henceforth known as the C complex, which has to undergo additional structural rearrangements before the second reaction can occur [36].

After releasing the intron lariat, the spliceosome dissociates from the nascent messenger RNA. Subsequently, the snRNPs U2, U5 and U6 are also released from the spliceosome to be re-used in additional rounds of splicing [32].

1.3.2 Alternative splicing

Constitutive pre-mRNA splicing is described by the removal of introns and ligation of exons. Considering that, for example, the human genome contains roughly 24.000 protein-coding genes which express far more than 100.000 proteins, a crucial step in between seems amiss [37]. In fact, the assembly of the spliceosome across a pre-mRNA cannot be solely facilitated by cis-acting splice sites, but is also dependent on additional cis-regulatory sequences as well as trans-acting splicing factors, which will be described in detail later on [38]. Subsequently, these additional factors can alter the process of pre-mRNA splicing in such a way that the spliceosome assembles across weaker, alternative splice sites. This in turn may lead to different combinations of inclusions and exclusions of exons and introns, thus giving rise to alternatively spliced mRNA isoforms. This mechanism has been termed alternative splicing.

Alternative splice isoforms ultimately lead to the production of functionally altered and often truncated proteins, thus enormously enhancing the transcriptome and proteome complexity. Furthermore, isoforms may contain premature termination codons (PTCs) which may subject the mature mRNA to RNA degradation through nonsense-mediated-decay (NMD) [39, 40]. In fact, alternative splicing has been shown to influence almost every aspect of RNA metabolism, such as transcription, nuclear transport, degradation or even translation efficiency [31].

When alternative splicing was first discovered it was considered a rather rare event. Today it is known that at least 90% of human genes are subjected to alternative splicing. Estimates in *A.thaliana* indicate an alternative splicing ratio of roughly 42% [41].

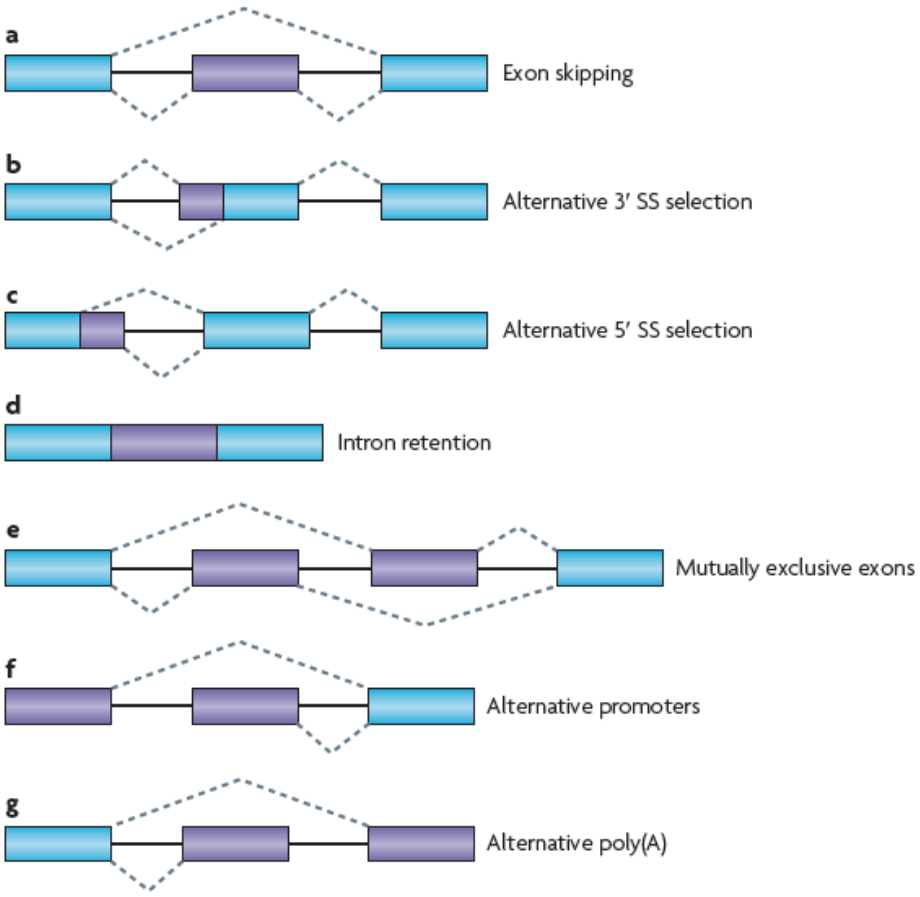

Figure 7: **Different types of alternative splicing events.** Blue boxes depict constitutive- and purple boxes alternative exons while intervening lines represent introns. Dashed lines are indicative for splicing options. **a-g** depict different types of alternative splicing events. See text for details. Adopted from [38].

Alternative splicing of pre-mRNAs may be classified into four main subgroups, depending on the nature of the splicing event (Figure 7) [38].

The first event is called exon skipping, which accounts for roughly 40% of all alternative splicing events in humans, but only for 8% in *A.thaliana* (Figure 7a) [31]. Exon skipping describes the process of splicing a specific type of exon, known as a cassette exon, and its flanking introns out of the transcript. Alternative 3' and 5' splice site selection (3'/5' SS) account for the second and third examples of alternative splicing events (Figure 7b, 7c). These types of splicing rely on the utilization of weaker splice sites located at any one end (3' or 5') of an exon. Alternative 3' and 5' splice site se-

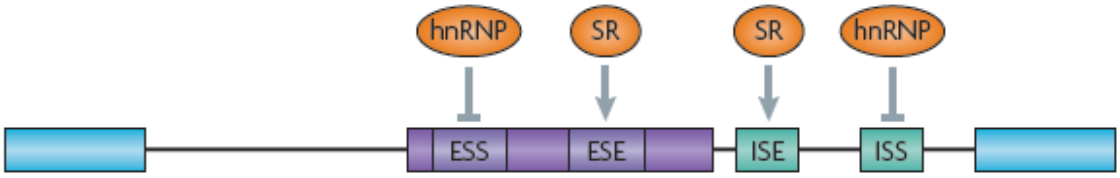

Figure 8: **Cis-acting auxiliary elements.** Blue boxes depict constitutive- and purple boxes alternative exons while intervening lines represent introns. Teal boxes depict specific sequence stretches within an intron. Arrows indicate activating- and stamps repressing interactions between proteins and auxiliary elements. Refer to the text for further details. Adopted from [38].

lection is quite abundant in higher eukaryotes with around 18% and 8% of all splicing events, respectively. The forth type is the most prevalent one in plants and at the same time the rarest one in vertebrates and invertebrates. Intron retention occurs when introns are not spliced out of the mature mRNA transcript (Figure 7d). Besides these four subgroups of alternative splicing events exist a number of less frequent but more complex types, which will only be named here for completeness; Mutually exclusive exons, alternative promoter usage, alternative polyadenylation (Figure 7e, 7f, 7g) [38].

The nature of alternative splicing events depends on additional cis- and trans-acting factors, as strong splice sites alone are not sufficient to define exons and promote effective splicing [31]. Auxiliary elements acting in cis are exonic and intronic splicing enhancers and silencers (ESE, ESS, ISE, and ISS, respectively). These factors are highly variable sequence stretches, either located in exons or introns. Specific trans-acting factors, such as SR proteins and hnRNPs, are able to bind these regions and thus influence the spliceosomal splice site choice (Figure 8) [33].

To further complicate the matter at hand, a plenitude of studies have shown that alternative splicing patterns of genes vary in dependence on multiple factors; splicing events are highly tissue- and cell-type specific. Additionally, they are changing along developmental stages and stress conditions as well as between different signaling pathways. An attempt to account for the complexity of alternative splicing is the very interesting idea of a "cellular code" [29]. This train of thought implies that the regulation of alternative splicing is dependent on the abundance and interactions of multiple positively and negatively acting factors, which may be individually expressed both in different cell types and throughout a myriad of varying conditions

and developmental stages. By intergrating this idea, one might be able to grasp the fact that the Dscam gene of *Drosophila melanogaster* can be expressed as 38.016 alternatively spliced isoforms [42]. However, the task of identifying minor changes in protein and RNA ratios intertwined in such a vast network will prove mighty difficult.

Nevertheless, ongoing research has revealed many a functions and pivotal roles of alternative splicing in disease development (humans) as well as defensive mechanisms (plants) (please refer to [30, 31, 43, 44, 45] for further details).

In order to close in on the topic of this thesis, it should be noted that a number of publications have shown that alternative splicing of plant pre-mRNAs is affected by various biotic and abiotic stresses [31, 46, 47]. Unusual heat and cold conditions exhibit a strong effect on alternative splicing from maize over rice to *A.thaliana*. For example, elevated temperatures inhibit splicing of maize and *A.thaliana* heat-shock genes alongside others [46, 48]. Furthermore, temperature stress significantly affects alternative splicing of SR pre-mRNAs (see subchapter Serine/arginine-rich proteins) [49, 50]. Since plants are sessile organisms, they are bound to cope with incoming stresses rather than just walk away. By altering the splicing situations of a myriad of downstream genes, plants instantly adapt to most given conditions.

1.3.3 Serine/arginine-rich proteins

The following subchapter will largely focus on the properties of serine/arginine-rich proteins (SR) in plants since this thesis is based on experimental work conducted in the plant model organisms *A.thaliana* and *P.patens*.

SR proteins are a highly conserved family of RNA binding partners [51]. Ever since their discovery around 20 years ago, an extensive amount of studies have identified a myriad of processes in which they are involved [52]. SR proteins influence the nuclear export of mRNA, its stability and even its translation efficiency. Furthermore, they are involved in genome maintenance as well as oncogenic transformation [53, 54, 51, 30]. However, SR proteins play their most prominent role as essential splicing factors in the regulation of constitutive and alternative splicing. SR proteins function as trans-acting splicing activators or repressors by binding to regulatory sequences in cis, namely exonic and intronic splicing enhancers and silencers, on the

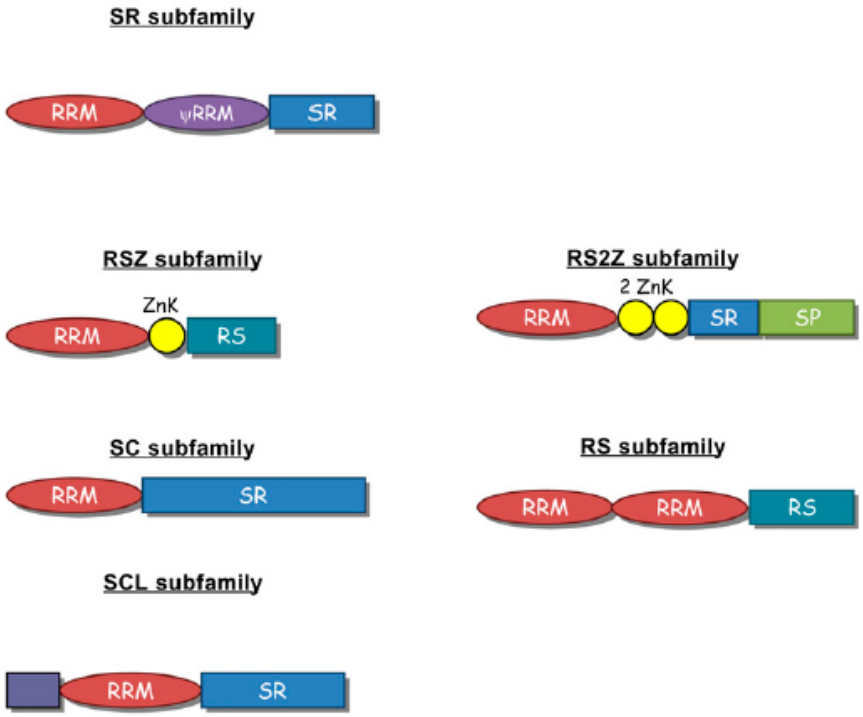

Figure 9: **SR protein subfamilies.** Shown are the modular structures of SR protein subfamilies in *A.thaliana*. The RS2Z, RS and SCL subfamilies are plant-specific. See text for a detailed description. Adopted from [62].

pre-mRNA transcript. Their ability to interact with RNA derives from one to two RNA recognition motifs (RRMs) located at the N terminus. Simultaneously, SR proteins are able to interact with proteins, such as spliceosomal ones, through their C-terminal arginine/serine-rich (RS) domain. Additionally, since SR proteins are in essence phosphoproteins, the RS domain is subjected to phosphorylation and dephosphorylation by specific kinases and phosphatases, respectively, which significantly influences their interaction properties (RNA binding, localization, splicing activities, etc.) [55, 56, 57, 58, 59, 60, 61, 50]. Thus, SR proteins lie at the center of pre-mRNA-spliceosome interactions by recruiting the spliceosome to nascent transcripts, enabling either constitutive or alternative splicing.

The human genome codes for 12 SR genes, while *A.thaliana* encompasses 18 and rice (*Oryza sativa*) even 22 SR genes [63, 64, 65, 31, 62]. This significant expansion of SR genes in *A.thaliana* originates most probably from at least three rounds of genome duplication events, either of the entire ancestral genome or of particular

regions [66, 67]. While there do exist clear orthologs to some human SR proteins, such as SRSF1, SRSF2 and SRSF7, there are also plant-specific SR proteins, which show unique domain architectures [68].

Following this expansion of SR proteins in plants, the establishment of plant-specific subfamilies has become a necessity to acknowledge their additional functions in plants. To date, six SR subfamilies have been identified in *A.thaliana*, three of which do not have orthologs in mammals (Figure 9). The SR subfamily comprises proteins which are orthologs of mammalian SRSF1. A highly conserved SWQDLKD motif in the second RRM, as well as a SR dipeptide-rich RS domain is characteristic for this family. Proteins of the RSZ subfamily contain one zinc knuckle and are orthologs of mammalian SRSF7. Proteins of the SC subfamily are ortholog to SRSF2 in mammals. Their structure encompasses one RRM- followed by a RS domain. The SCL subfamily is plant-specific and quite similar to the SC subfamily, except that it possesses a charged extension at the N terminus. Proteins of the RS2Z subfamily show quite unique structural features. They incorporate two zinc knuckles, a classical RS domain and an additional SP-rich region. The RS subfamily is the last plant-specific one. Proteins of this subfamily are characterized by two RRM domains, which, however, lack the SWQDLKD motif. Additionally, they contain a RS domain which is rich in RS dipeptides (References to this paragraph: [62, 69, 58, 63, 64, 66, 70, 61, 71, 50, 72, 73]).

The expansion of SR genes in *A.thaliana* imposes the question whether these genes show redundant or unique features regarding their functions. Since proteins of paralogous genes show a high level of homology, the important differences can be found in the regulatory regions, which ultimately control the expression patterns on the transcriptional level. Detailed analyses of paralogous promoter regions of SR genes have shown both redundant and varying cis-acting regulatory sequences. Thus, by analysing the expression patterns of *A.thaliana* SR genes through Northern-blot and RT-PCR approaches, it has become evident that numerous paralogous SR genes are indeed differentially controlled in a spatiotemporal fashion [66].

At-SR30 and At-SR34, both members of the SR subfamily, are generally expressed in all plant tissues [70, 74, 50]. Nevertheless, data derived from promoter-reporter gene fusion experiments indicates that their expression patterns are actually complementary during the early stages of *A.thaliana* seedling development. The first stages

of the formation of lateral roots is accompanied by the expression of both At-SR30 and At-SR34. However, as development progresses, their expression patterns start to deviate, indicated by the sole presence of At-SR34 in growing root tip cells, which hints for specific roles of At-SR30 and At-SR34 proteins during root development [66, 50].

The paralogous pair of genes At-RS40 and At-RS41 belong to the plant-specific RS subfamily. They are located on duplicated regions on the chromosomes IV and V and hence these SR genes pose an interesting subject of investigation [66]. By conducting reporter gene fusion experiments, a strong expression of At-RS41 can be observed throughout all tissues of *A.thaliana*, whereas At-RS40 shows comparable expression levels only in roots and cotyledons (Kalyna M., Barta A., unpublished work). These differential expression patterns indicate diverging and most probably distinct roles of At-RS40 and At-RS41 during plant development.

The RS2Z subfamily comprises the members At-RS2Z32 and At-RS2Z33. As of yet, data on At-RS2Z32 is rather scarce, however, derived from informations regarding EST clones, it is very likely that At-RS2Z32 is expressed in flowers, siliques, roots and rosette leaves. On the contrary, data on At-RS2Z33 is quite abundant. It is know that expression of At-RS2Z33 happens during embryogenesis, seedling formation, as well as in flower and root development [66]. Additionally, it is known that At-RS2Z33 regulates splicing of its own pre-mRNA in an autoregulatory feedback-loop fashion [49].

Another paralogous gene pair belonging to the plant-RS subfamily is At-RS31 and At-RS31a, which are 72% identical to one another. Interestingly, despite the common presence of an unusual long intron in the genes At-RS2Z32, At-RS2Z33, At-RS40, At-RS41, At-RS31 and At-RS31a, only At-RS2Z33 has been shown to autoregulate splicing of this particular long intron. None of the other previously listed genes has yet been shown (to the authors best knowledge) to regulate splicing of its own pre-mRNA. However, it has been shown that At-RS2Z33 regulates splicing of At-RS31 [75]. These findings once again point out that the vast network of SR genes and proteins interacts with one another to fine tune gene expression. Furthermore, these results demonstrate that paralogous pair of genes are not strictly redundant in regard to their functions, but are likely to diverge and acquire additional and/or new

functions.

In this regard our lab is also interested in the presence of homologous SR genes present in *P.patens*. Since it has been shown numerous times that SR genes and proteins are intertwined in complex networks of positive and negative regulatory actions, it is thrilling to find out whether SR genes and proteins acquired different functions and expression patterns during the evolution of two such contrary plants such as *A.thaliana* and *P.patens*. In 2006, Kalyna et al. have been able to identify two homologous SR genes present in *P.patens*. Pp-RS27 inherits a high degree of resemblence to the RS subfamily present in *A.thaliana*. The SR gene Pp-RS2Z38 shows homologies to the RS2Z subfamily [75]. Additionally, our lab was able to identify Pp-RS2Z37 as another homologous SR gene most fittingly placed in the RS2Z subfamily (Maronova M., Kalyna M. and Barta A., unpublished work). However, despite the presence of the characteristic long intron in Pp-RS27, Pp-RS2Z37 and Pp-RS2Z38, no evidence is yet available whether these long introns are spliced in a similiar way to *A.thaliana* [75]. In fact, very little data is available on alternative splicing and the nature of SR genes in *P.patens*. A problem this thesis is trying to, at least partially, correct.

While SR proteins are major players in splicing, it is interesting to note that SR pre-mRNAs themselves undergo extensive alternative splicing. Even though genes of virtually every functional category undergo alternative splicing in *A.thaliana*, as has been shown by gene ontology analysis, non-random patterns do emerge. Few of these categories are over-represented and one of them enfolds splicing regulators, such as SR genes [76]. In fact, Palusa et al. have shown that 15 out of 18 SR genes undergo alternative splicing, producing 95 splicing isoforms, thereby increasing the SR transcriptome complexity by six-fold [46]. Additionally, it has been shown that splicing events of SR pre-mRNAs are tightly controlled across different tissues and even at distinct developmental stages, thus adding another layer of complexity [70, 50, 77, 69, 71]. Analysis of splice isoforms has shown that, due to the modular nature of SR genes, predicted proteins may lack functional domains or contain additional amino acids, thus giving rise to a, at least theoretical, chance of functional manipulation [64, 46]. Also, protein isoforms may be truncated due to the nature of alternatively spliced mRNA isoforms, which has been shown to be quite abundantly present in the SR subfamily of SR genes [50].

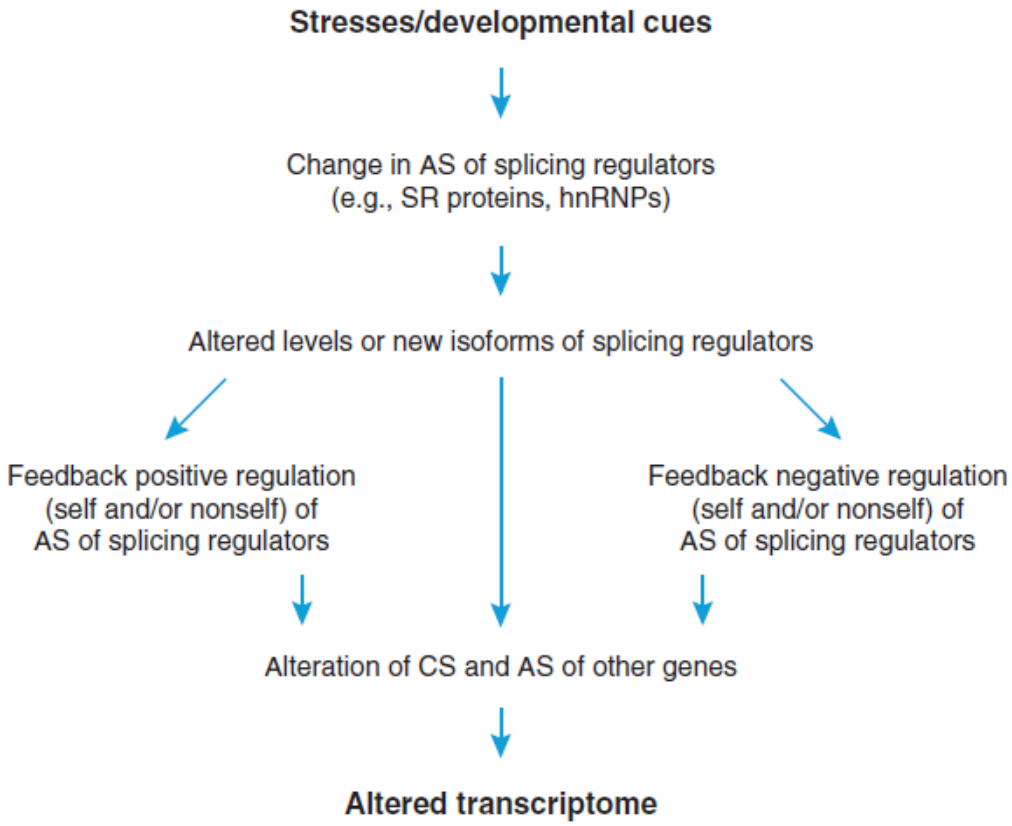

Figure 10: **Responses to the environment.** Depicted is a scheme which illustrates how stresses and developmental cues may alter the transcriptome by influencing the splicing patterns of essential splicing regulators. Abbreviations: AS - alternative splicing; CS - constitutive splicing. Adopted from [31].

Previous studies have also shown that biotic and abiotic stresses exhibit an impact on alternative splicing patterns of genes [44, 78, 79, 46, 47, 45]. Furthermore, several SR genes undergo alternative splicing due to various stress sources, which results in the appearance of some and loss of other splice isoforms, subsequently influencing the organisms stress response [46]. These findings clearly point to the existence of a fundamental regulation network, which is activated upon stress (Figure 10). By modifying the functions of essential splicing regulators through alternative splicing, they themselves alter the splicing patterns of downstream genes and even of other SR genes, thus allowing an organism to quickly react to stress by regulating splicing and subsequently expression patterns of affected genes [31, 80, 49, 50].

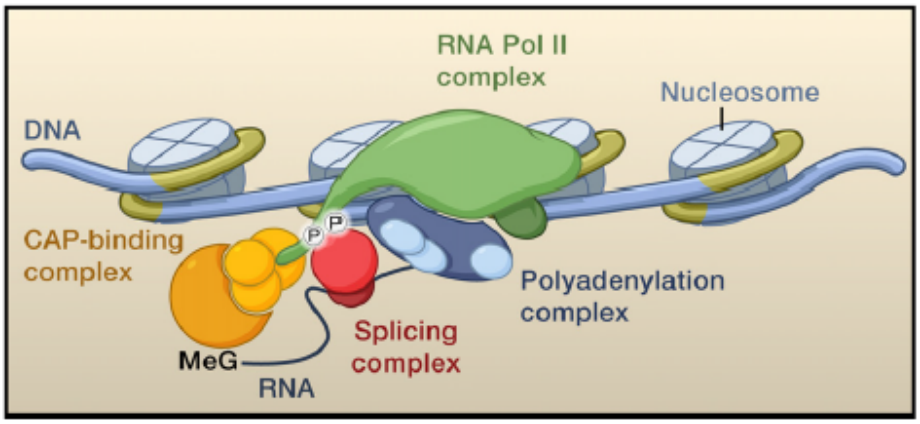

Figure 11: **RNA processing and transcription is coupled.** During transcription the RNA polymerase II recruits multiple RNA-processing factors, which take up work while transcription is still happening. This cotranscriptionality is the result of massive recruiting actions initiated by the RNA polymerase II C-terminal domain. See text for further details. Adopted from [43].

Expression studies in *A.thaliana* using various methods have revealed that SR genes are expressed in all tissues, however at different levels [81, 69, 58, 49, 74, 77, 71]. To determine the function of any given SR gene, plant biologists may use three different approaches. The first one implements an animal in-vitro splicing assay using splicing-deficient HeLa cell S100 extracts. This method obviously inherits a crux, since it employs an animal system while plants express plant-specific SR proteins. Nevertheless, studies were able to show that a number of plant SR proteins, even plant-specific ones, did complement the splicing-deficient extract and promote splice site switching in vitro [70, 75]. The second option is to either constitutively or transiently overexpress SR proteins and monitor changes in splicing patterns. A handful of studies have shown alterations in alternative splicing patterns and have even observed specific phenotypes. For example, when At-SR30 is overexpressed, the protein manipulates the alternative splicing patterns of At-SR34 and of its own pre-mRNAs along other endogenous genes [50]. Another prominent example is the overexpression of At-RS2Z33, which alters alternative splicing of two additional SR genes. Furthermore, as already mentioned before, it also regulates the splicing pattern of its own pre-mRNA [49]. The third method is to generate SR gene knockout lines, which allows analysis of alternative splicing patterns in the absence of a specific SR protein. However, since plants are known for genome duplication events, at least some SR proteins might show redundant functions, thus substituting for the knocked-out protein. Studies in *Caenorhabditis elegans* have shown that double or even triple knockouts

of SR genes exhibit severe to lethal effects while single knockouts have shown no phenotype at all [82]. Thus, functional redundancy proves to be quite a thorn when analysing the functions of SR genes, even more so since reverse genetic approaches in *A.thaliana* might prove difficult, to say the least (authors own observation). Thus, one might consider the application of amiRNA mediated approaches, as mentioned before in the subchapter on *A.thaliana* (Subchapter 1.1)

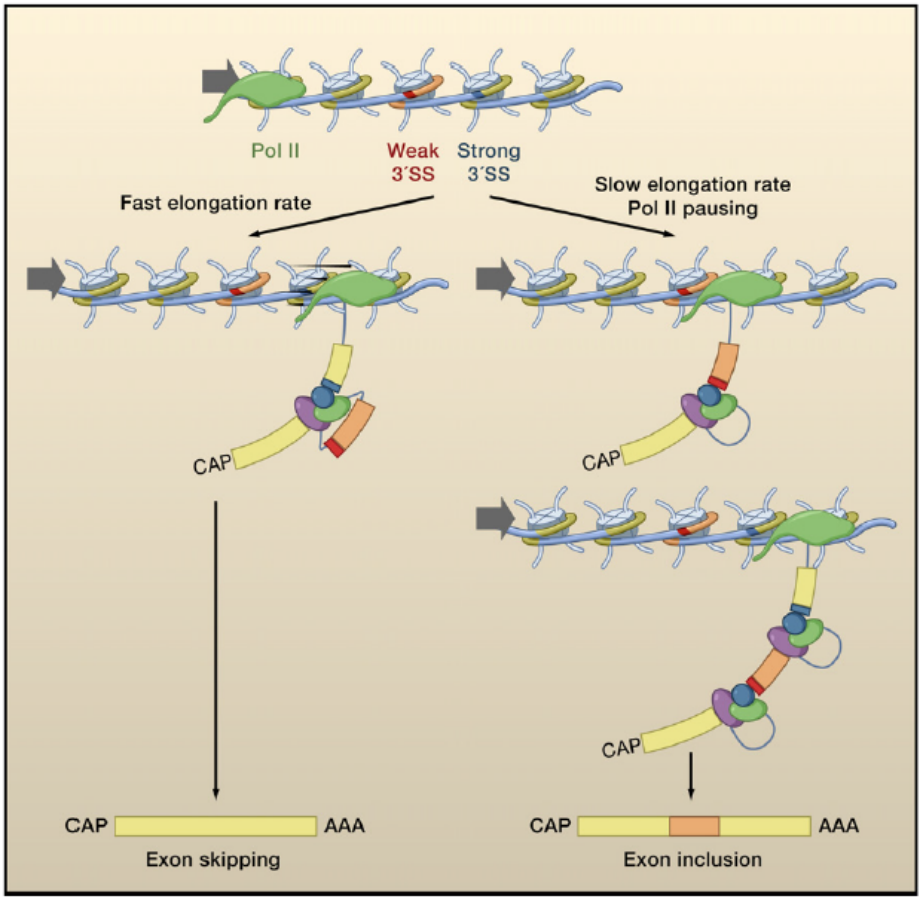

Figure 12: **RNA polymerase II kinetics influence splice site choice.** Fast and fluent transcription by the RNA polymerase II allows the simultaneous presence of weak (red) and strong (blue) splice sites in the emerging pre-mRNA transcript. This subsequently influences the spliceosomal splice site choice towards the stronger site. If the RNA polymerase II is slowed down, weaker splice sites might be already present in the nascent transcript while strong splice sites are not yet transcribed, which leads to the inclusion of a weaker exon. This model has been termed "first served, first commited". Adopted from [43].

SR proteins are mostly located in the nucleus and more precisely in speckles, which are nuclear compartments that seem to act primarily as storage sites for splicing

factors [83]. As transcription happens, SR proteins are recruited from the center of speckles to the periphery, where the RNA polymerase II (Pol II) stands ready to transcribe. In fact, more than 20 years ago Beyer and Osheim were able to show that splicing can occur cotranscriptionally, which means that splicing occurs before the Pol II releases the nascent pre-mRNA transcript (Figure 11) [84, 43]. This elaborate cooperation is coordinated by the carboxy-terminal domain (CTD) of the Pol II. It is well established that the phosphorylation status of the CTD greatly influences the activity of the Pol II and it has been shown that the CTD needs to be phosphorylated in order to recruit splicing factors, such as SR proteins, thus enabling cotranscriptional splicing [85, 86]. As the nascent pre-mRNA is synthesized, the splicing machinery already goes to work and selects appropriate splice sites. However, this process is not strict in a way that introns are spliced out in the order that they emerge from the Pol II, since this would render alternative splicing impossible [87, 88, 89, 90]. This whole fine-tuned process rather depends on a multitude of varying factors. One of them is the elongation rate of the Pol II. A number of elegant studies have shown that the rate of RNA synthesis by the Pol II might influence the RNA secondary structure, which subsequently might affect splice site choices and splicing [91, 92, 93, 94, 95]. Thereby, if the rate of RNA synthesis is manipulated, alternative splicing patterns will likely be altered. In fact, there are various ways to affect RNA synthesis, for example through biotic and abiotic stresses, such as UV light. Muñoz et al. have shown that UV light induced DNA-damage leads to hyperphosphorylation of the CTD, which inhibits the elongation rate of the Pol II, ultimately resulting in alternative splicing of downstream genes (Figure 12) [96]. Further emerging evidence suggests that also chromatin and histone modifications play vital parts in the regulation of alternative splicing (refer to [43] for further details).

1.4 Genotoxic stress

Every organism is constantly subjected to environmental and cellular stress of some sort. The term genotoxic stress comprises a whole smorgasboard of stress sources across abiotic and biotic stresses, which are able to substantially hinder an organism to reach its full potential [97]. In the case of this thesis the focus will rely on stress sources affecting plants. Abiotic stress for plants results from extreme temperatures, such as freezing or unusual heat, from water starvation or flooding, from ion toxic-

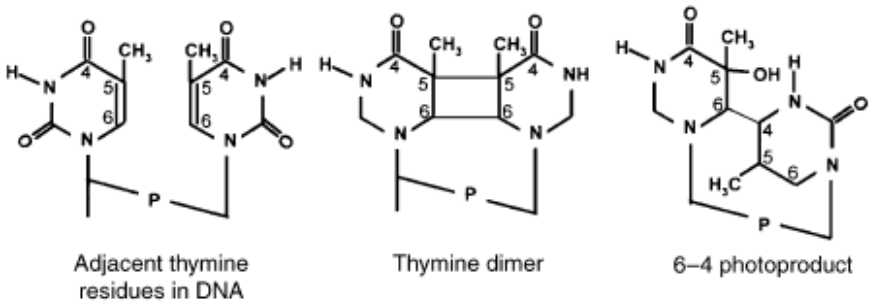

Figure 13: **UV induced DNA damage.** The two DNA damage induced photoproducts, CPDs and 6-4PPs, are depicted. The adjacent thymines on the left side represent the default status in DNA, while the chemical structure in the middle represents a CPD and the structure on the right side depicts a 6-4PP. Adopted from [102].

ity or from ultraviolet radiation, such as UV-B. Biotic stresses derive from invading pathogens, such as fungi, bacteria, viri or insects [98]. Prolonged exposure to abiotic and biotic stress sources has severe effects on plants, such as growth and development retardation, which, in case of economic plants, leads to significant harvest failures [99].

DNA can easily be damaged through a plenitude of harmful agents, commonly known as mutagens [97]. Chemical mutagens alter the integrity of DNA in multiple ways. Some are integrated as base analogs, others alter the characteristics of incorporated bases, again others may intercalate into DNA, thus causing detrimental frame shifts and some simply alter the structure of DNA, making it inaccessible to DNA-binding proteins [100, 101].

The most common and first known mutagenic source is radiation, which in fact splits up into two kinds of radiation [97]. First, ionizing radiation, which comprises X- and gamma-rays. The second one is UV radiation, which includes UV-A (320-400 nm), UV-B (290-320 nm) and UV-C (180-290 nm). UV-B accounts for a significant mutagenic fraction of sunlight and UV-C is characterized by being the most energetic and thus lethal wavelength of UV-radiation. UV-B is an intrinsic part of sunlight, which reaches the surface of the earth while UV-C is successfully absorbed below wavelengths of 280 nm by the atmosphere [15]. However, both UV-B and UV-C induce the formation of pyrimidine-dimers in the DNA (Figure 13) [100, 101]. These dimers are formed between two adjacent pyrimidines, thus resulting in cyclobutane pyrimidine dimers (CPDs) and pyrimidine-pyrimidone (6-4) photoproducts (6-4PPs), with

the first one being far more prevalent [101, 103, 104, 102]. Both of these photoproducts promote mutagenesis and distort the structure of DNA, which further inhibits DNA replication as well as transcription by stalling DNA- and RNA-polymerases [105]. Additionally, UV radiation directly affects the stability of RNA and proteins, which often results in elevated levels of RNA and protein degradation. Besides inducing the formation of UV-photoproducts, UV-B and UV-C also cause oxidative damage through the induction of reactive oxygen species (ROS) [106]. ROS are free radicals which react with and damage DNA, RNA, proteins and lipids, thus further hampering the metabolism and genome stability of an organism [107].

However, since UV radiation is an intrinsic part of sunlight, its mode of action is not strictly detrimental to plants [108]. In fact, UV-B acts as a key environmental signal, which significantly regulates a myriad of downstream processes [109]. Therefore, the response of a plant is heavily based on the wavelength and dose of UV irradiation.

Low doses of UV-B radiation are said to predominantly trigger photomorphogenic reactions, while high doses lead to DNA damage signaling. Photomorphogenic UV-B signaling comprises specific, intertwined pathways, which are triggered after UV-B light is perceived by its receptor, the UV RESISTANCE LOCUS8 (UVR8). UVR8 holds 14 tryptophan residues, which are able to absorb UV radiation and further trigger a dimer to monomer structural rearrangement, which in turn leads to interractions of UVR8 and CONSTITUTIVELY PHOTOMORPHOGENIC 1 (COP1), the central regulator of light signaling [110]. In fact, these tryptophan residues seem to be highly conserved across other plant species, including *P.patens* [109]. Ultimately, signaling iniated by low doses of UV radiation lead to adaptive changes in metabolism, morphology and UV protection. *A.thaliana* mutants lacking key components of these pathways, such as UVR8, COP1 or the transcription factors HY5 and HYH, are very sensitive to UV radiation and respond with severe necrosis [111, 112, 113].

Elevated doses of UV radiation lead to the initiation of nonspecific signaling pathways, which promote DNA repair mechanisms alongside wounding and defense responses [114, 115, 109]. A possible explanation for the puzzling triggering of the two latter pathways is that UV radiation stimulates the accumulation of a wide variety of signaling molecules, such as jasmonic acid, ethylene, salicylic acid and ROS, which in turn initiate wounding and pathogen-related defense mechanisms in plants [116, 117, 109].

In yeast and mammalian cells, UV radiation has been shown to trigger the arrest of the cell cycle and subsequent promotion of DNA repair mechanisms [118]. Distinct components involved in these DNA damage signaling processes are conserved in plants and thus similiar reactions are likely to occur [109]. In fact, various UV-B related responses in plants are initiated by DNA damage signaling [109].

1.5 DNA repair mechanisms

Plants inevitably have to cope with any environmental stress thrown at them since they are sessile organisms. The most common stress source for plants is UV radiation, however it is quite seldom to see UV damaged plants in the wild and therefore they must have evolved elaborate protective mechanisms [15]. In fact, plants have developed two distinct ways to cope with UV-radiation. The first one is meant to avoid DNA and further cell damage before it even happens by expressing and incorporating UV-absorbing and reflecting compounds like flavonoids, anthocyanins or epicuticular waxes [119, 120]. The second mechanism comprises a number of effective DNA repair mechanisms.

Upon infliction of DNA damage, organisms react by activating damage response signaling pathways, which in turn activate essential downstream factors [97]. Cells may be arrested in their cell-cycle progression to repair any harm done if the damage severity is not overwhelming [121]. Several events and signaling reactions responsible for these interactions have been summed up under the fitting description of a DNA-damage response (DDR) pathway [101]. DDR signaling activates a number of protein kinases, which in turn interact with check point kinases and cell-cycle associated proteins [122, 123]. In the end, depending on the specific interactions between the DDR pathway effectors and cellular components, the cell is either arrested and repaired or left to die if the inflicted damage is too severe. Components involved in the DDR pathway are highly conserved throughout higher eukaryotes, which exemplifies the pivotal role these genes play in DNA-damage connected signaling.

Interestingly, studies, carried out predominantly in mammalian cell systems, have shown that alternative splicing seems to play a pivotal role in the responses to DNA damage [96]. Apparently, a large number of genes involved in cell survival and apopto-

sis are alternatively spliced, often in a way that two isoforms deploy contrary functions [124]. As already mentioned before, the transcription and splicing of pre-mRNAs is coupled, meaning that pre-mRNA processing happens cotranscriptionally. Furthermore, it has been shown that RNA polymerase II arrest during transcription follows UV treatment [125]. Additionally, it is evident that slowing down transcriptional elongation promotes alternative splicing by favouring weaker splice sites over strong ones in a spatiotemporal manner [126]. Taken together, these previous findings strongly indicate an important function of alternative splicing during DNA damage signaling in connection to the RNA polymerase II transcription status, at least in mammalian cell systems. Therefore, it is intriguing to find out whether these pivotal roles are conserved also in plants, such as *A.thaliana* and *P.patens*.

1.5.1 Photoreactivation

The term photoreactivation (PR) describes a very elegant method to directly revert UV-induced pyrimidine dimers to their monomer configuration through the action of enzymes called photolyases (Figure 14) [127]. Photolyases are highly specific proteins, which are able to disband pyrimidine dimers by absorbing blue light in the range of 300 600 nm, thus PR is a light-dependent repair pathway [128]. It has been shown that PR is most prominent in nonproliferating cells and only if the UV-inflicted damage is not too severe [100, 101]. Furthermore, this repair mechanism is not conserved among every species. PR is active across pro-, eukaryotic and archaic organisms, such as *Escherichia coli*, yeast, plants and specific animal species, but not in humans [127, 129, 130].

1.5.2 Nucleotide excision repair

Nucleotide excision repair (NER) is a light-independent, dark repair pathway, which generally removes DNA lesions caused by UV radiation (Figure 15). Opposite to PR, which specifically reverts dealt damage, NER removes a damage-containing stretch of 24-32 base oligonucleotides and replaces it through DNA synthesis and nick ligation [131, 132]. It has been shown that the NER pathway actually comprises two sub-pathways termed global genome repair (GGR) and transcription-coupled repair (TCR) [97]. GGR deals with damage across the whole genome while TCR is specifically recruited to the actively transcribed DNA strand when the RNA polymerase

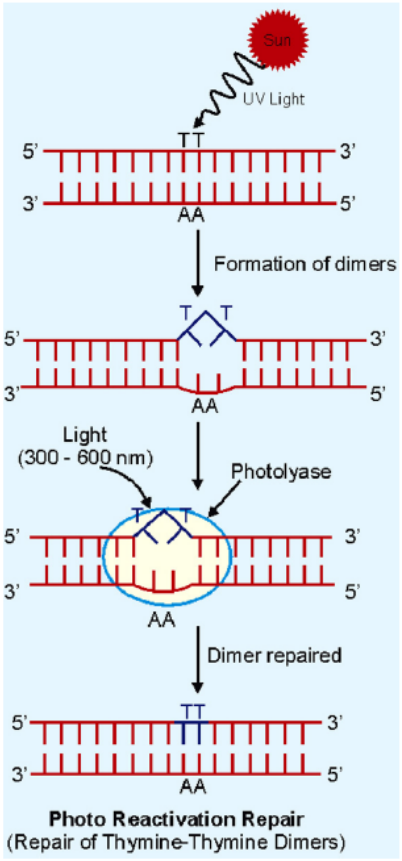

Figure 14: **Photoreactivation.** Shown is a schematic overview of photoreactivation (PR). UV light induces the formation of a thymine-dimer in the DNA, which is subsequently repaired by the action of a photolyase. In order to carry out its function, a photolyase needs to absorb blue light in the range of 300 - 600 nm. Photoreactivation directly reverts the induced DNA damage, leaving no traces behind. See text for relevant details. Adopted from [97].

II is stalled due to UV-photoproducts [133]. After the DNA-damage site has been recognized, XPA and TFIIH bind and unwind the stretch of DNA so that additional repair proteins can enter the scene. Next, ERCC1/XPF (At-RAD1, UVH1) and XPG bind to the site and remove the damaged strand by introducing a nick on both the 5' and 3' side. Gap filling occurs through DNA synthesis based on the complementary, undamaged strand [101, 134]. NER is highly conserved among animals, yeast and plants [135]. In fact, it has been shown that *A.thaliana* uvh1 mutants are unable to repair UV induced DNA damage in the dark [136]. Moreover, Liu et al. were able to complement the uvh1-1 mutation by introducing a cosmid carrying the functional At-RAD1 repair gene, thus conclusively proving that At-RAD1 is a true homolog of the *S.cerevisiae* Rad1 and the human XPF genes. Besides its evident role in the NER pathway, At-RAD1 is also suspected to inherit additional functions throughout plant

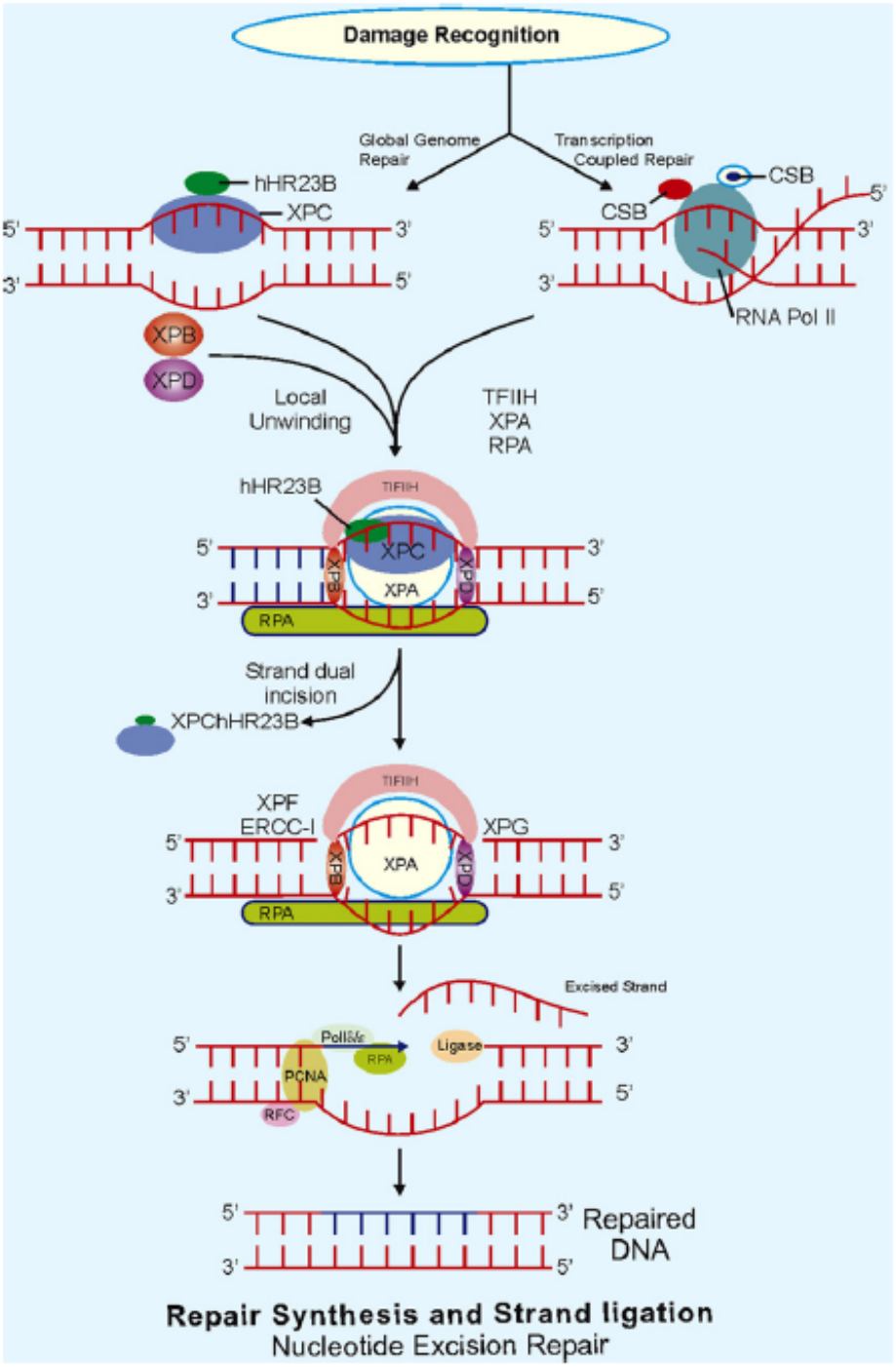

Figure 15: **Nucleotide excision repair.** This figure depicts the most important steps of the nucleotide excision repair pathway (NER) in detail. Note that at the top of the model, GGR and TGR are shown, which then both follow the same path towards DNA damage repair. See text for relevant details. Adopted from [97].

growth and metabolism [136]. Transgenic mice, which lack a functional nucleotide excision repair mechanism, show aberrant developmental traits, such as premature senescence. In agreement to these findings, *A.thaliana* uvh mutants seem to exhibit an early senescence phenotype and show a delay in the growth of new tissues when uvh1-1 mutant seeds are germinated [136]. Interestingly, the uvh1 mutation published by Liu et al. changes the splicing pattern of At-RAD1 in a way that an in-frame stop codon is produced. Following this train of thought, we were eager to identify and analyse possible alternative splice isoforms of At-RAD1, as well as the regulation of alternative splicing of At-RAD1 by SR proteins.

1.5.3 Base excision repair

Spontaneous or oxidative damage leads to the modification of a single base residue in the DNA, which can be quite detrimental for a cell. Manipulation of a single base may lead to mutations during DNA replication or even block replication and transcription as a whole [137, 138]. Such aberrant bases are removed by the base excision repair (BER) pathway, which simply replaces the damaged base by an undamaged one (Figure 16) [101, 100, 134, 139].

Just like NER, BER also comprises two sub-pathways, namely the short-patch and long-patch BER. The short-patch BER is divided into three steps. First, a specific DNA glycosylase (At-FPG1), which scans the minor groove of the DNA, recognizes a particular base adduct and subsequently cleaves the corrupt base from the sugar-phosphate backbone, thus creating an abasic AP site [140, 141]. The second step starts with an AP-endonuclease, which recognizes the abasic site and introduces a nick in the DNA-backbone at the 5' end [142]. In the third and last step, a DNA polymerase removes the deoxyribose-phosphate residue and fills the one-nucleotide gap, which is then sealed by a DNA ligase [143]. The long patch BER reaction includes the more general removal of two to ten nucleotides, which contain the modified base. The resulting gap is filled and sealed by a DNA polymerase and ligase, respectively [144]. A prominent example for the activity of BER is the removal of the guanine oxidation product 7, 8-dihyrdo-8-oxoguanine (8-oxoG), which is read as a thymidine and thus introduces a G-T mutation.

In *A.thaliana* it has been shown that at least seven different At-FPG1 mRNA vari-

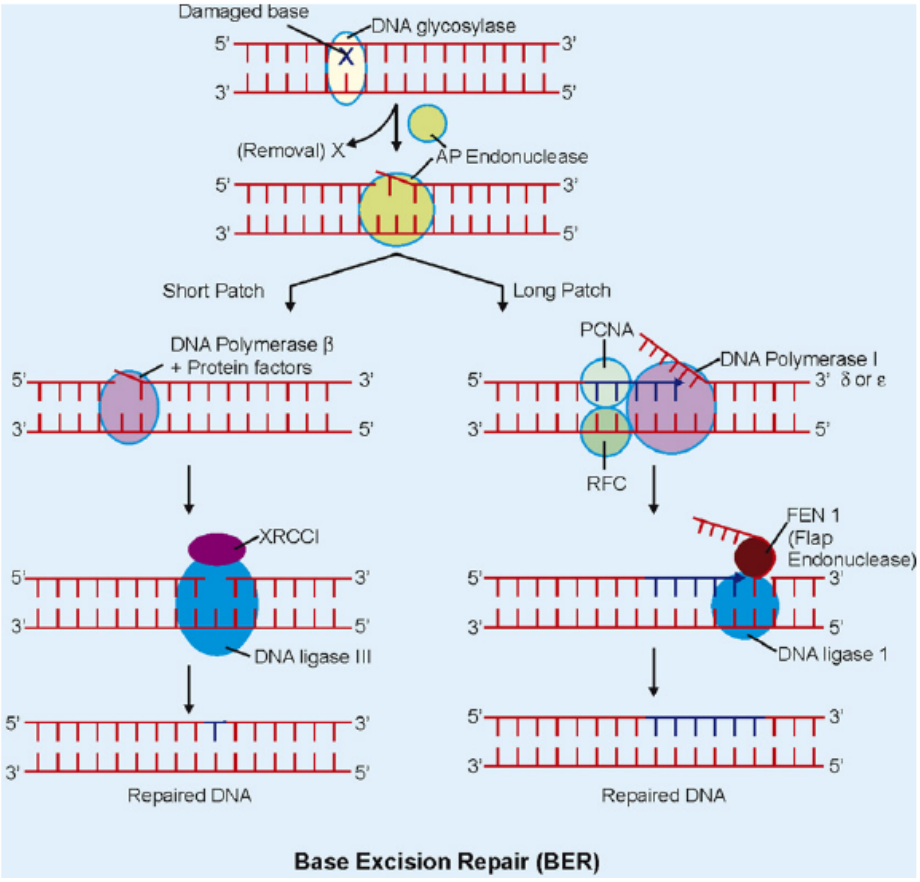

Figure 16: **Base excision repair.** Shown is a schematic illustration which depicts the most important steps in the base excision repair pathway (BER). Both the short and long patch subpathways are shown. See text for relevant details. Adopted from [97].

ants are expressed [145, 146, 147, 148]. While it is not clear whether every single splice isoform codes for a functional protein, at least two of them are confirmed to translate into actual proteins. Moreover, while both produced proteins consist of a similarly conserved N-terminal amino acid sequence, their C-terminal regions differ significantly. In fact, only one of these isoforms is able to cleave oligonucleotides containing 8-oxo-Gs, which strongly suggests that alternative splicing indeed alters the functions of At-FPG1 protein isoforms [147]. Furthermore, only one isoform contains a nuclear localisation signal, which indicates a difference in the subcellular localisation of these two isoforms [146]. Taken together, these fascinating findings most likely explain our interest in the regulation and alternative splicing patterns of At-FPG1 during stress conditions in *A.thaliana*. Additionally, we analysed the expression and splicing patterns of potential homologs in the moss *P.patens*.

1.6 Objectives and motivation

The efforts captured in this thesis focus on the complex roles and interactions of SR genes, which are intertwined in the fascinating mechanism of alternative splicing. We conduct our experiments in the model organisms *A.thaliana* and *P.patens* and use UV-C radiation as a stress source. Our goal is to elicit novel interplays between SR and DNA repair genes and also to take a closer look on the role of the RNA polymerase II in alternative splicing and DNA damage repair. To realise these eager goals we take advantage of various overexpression and knockout lines in *A.thaliana* and *P.patens* to analyse expression and splicing patterns of SR genes and their possible interaction partners, such as SR genes themselves and surprisingly also DNA repair genes. Furthermore, we circumvent the lack of specific knockout lines in *A.thaliana* by applying an artifical microRNA approach to knockdown desired SR genes.

Evolutionary speaking, *A.thaliana* and *P.patens* are very distinct organisms. Therefore, we are also interested in the possible conservation or acquirement of new functions and interactions of SR and DNA repair genes along evolution. Additionally, we analyse alternative splicing events of orthologous genes in these two organisms to find out whether splicing patterns evolved over time. To elucidate this topic we analyse different tissues, specific growth stages and pheno/genotypes, both in *A.thaliana* and *P.patens*.

Ultimately, the aim of this thesis is to be part of the mission to elucidate the functions of SR genes in alternative splicing.

Chapter 2

Materials

2.1 Chemicals

Chemical	Source
2-(*N*-morpholino)ethanesulfonic acid	Duchefa Biochemie
2'-deoxynucleoside 5'-triphosphate	Invitrogen, Promega
2-Mercaptoethanol	Merck
Acetic acid, glacial	Merck
Aceton p.a.	Merck
Acrylamide	Sigma
Adenosine triphosphate (ATP)	Invitrogen, Promega
Agarose	genXpress
Ampicillin	Sigma
Bactotryptone	Sigma
Calcofluor	Sigma
D(+)-Sucrose Ph.Eur.	Carl Roth
Di-ammonium tartrate p.a.	Fluka, Sigma - Aldrich
Dimethyl sulfoxide (DMSO)	Merck
D-Mannitol	Sigma
Ethanol	Merck
Ethidium bromide	Sigma
Ethylenediaminetetraacetic acid	Merck
Glufosinate-ammonium (BASTA)	Sigma

Continue on next side

Chemical	**Source**
Glycerol	Sigma
Hydrochloric acid fuming 37%	Merck
Hypochlorite	Merck
Isopropyl-β-thiogalactopyranoside (IPTG)	Peqlab
Kanamycin	Sigma
Methanol	Merck
MOPS SDS running buffer	Invitrogen
Murashige and Skoog vitamin mixture	Duchefa Biochemie
Murashige and Skoog Medium 1A Micro and 1/2 Macro elements	Duchefa Biochemie
N,*N*'-Methylenebisacrylamide	Sigma
NuPAGE Antioxidant	Invitrogen
NuPAGE LDS sample buffer 4x	Invitrogen
NuPAGE Reducing agent 10x	Invitrogen
NuPAGE Transfer buffer 20x	Invitrogen
o-Phenylenediamine-dihydrochloride tablet, 10mg/tablet	Sigma
Piperazine-*N*,*N*'-bis(2-ethanesulfonic acid) (PIPES)	Sigma
Plant agar	Duchefa Biochemie
Protamine sulfate	Sigma
Rifampicin	Sigma
Rnase ZAP	Ambion
Silwett L-77	Lehle Seeds
Sodium chloride (NaCl)	Merck
Spectinomycin	Sigma
Tetracycline	Sigma
Tetramethylethylenediamine (TEMED)	BioRad
Tris(hydroxymethyl)aminomethane (TRIS)	Appli-chem
Triton X-100	Sigma
Tryptone	Oxoid
Tween-20	Sigma

Continue on next side

Chemical	**Source**
Yeast extract	Oxoid

2.2 Auxiliary materials

Material	**Source**
Celophane discs	A.A. Packaging Limited
Cover glasses	Marienfeld
Falcon tubes (15 mL, 50 mL)	Falcon
Filter paper	Marcherey-Nagel
Glass bottles	Schott
Glass pipettes	Brand
Leukopor	BSN Medical
Microscope slides	Marienfeld
Millex-GP 0.2 μm filter unit	Millipore
Parafilm M	Parafilm
PCR reaction tubes	Biozym
Petri dish 150 mm	Falcon
Petri dish 90 mm single vent	Sterilin
Petri dish 90 mm triple vent	Sterilin
Pipette tips	Greiner
PVDF Filter Paper Sandwich	Invitrogen
Reaction tubes (1.5 mL, 2 mL)	Eppendorf
Serological pipettes (2 mL, 5 mL, 10 mL, 25 mL)	Becton Dickinson Labware
Square petri dish 100 mm	Sterilin
Universal tubes (10 mL)	Falcon

2.3 Instruments

Instrument	Source
Axioskop microscope	Zeiss
Bandelin electronic UW200	Bandelin
Centrifuge 5424, 5418, 5810R	Eppendorf
Certoclav table autoclave	Certoclav
Criterion Cell	BioRad
Curix 60	AGFA
Dremel 300	Dremel Europe
Geldoc-it TS Imaging System	UVP
Gilson pipetman P2, P20, P100, P200, P1000, P5000, P10000	Gilson
Julabo TWB14 water bath	Bartelt
Lab therm / shaker	Adolf Kühner AG
MaxiSorp ELISA plates	Nunc
Mini-SubCell GT	BioRad
NanoDrop ND1000 spectrophotometer	Peqlab
Novex Semi dry blotter	Invitrogen
Piko-Thermocycler	Finnzymes Instruments
Power pac 300	BioRad
Spot RT3 camera	Visitron Systems
TyphoonTM	GE Healthcare
UV stratalinker 4200	Stratagene
UVT-20M UV screen	Herolab
Water deionization system	Millipore
Wide Mini-SubCell GT	BioRad
Xcell SureLock Mini cell	Invitrogen

2.4 Commercially available systems

System	Source
Amersham ECL Western Blotting detection reagents	GE Healthcare
Dneasy Plant Mini Kit	Qiagen
MiniElute Gel Extraction Kit	Qiagen
NuPAGE Novex Bis-Tris 4-12% Mini Gels	Invitrogen
pGEM-T Easy Vector System I	Promega
QIAprep Spin Miniprep Kit	Qiagen
Reverse Transcription System	Promega
Rnase-free Dnase Set	Qiagen
Rneasy Plant Mini Kit	Qiagen
Wizard SV Gel and PCR clean up system	Promega

2.5 Proteins and enzymes

Protein/Enzyme	Source
AMV Reverse Transcriptase	Promega
Driselase	Sigma
Dynazyme II DNA Polymerase	Finnzymes
Horseradish-Peroxidase-Streptavidin	Sigma
PhusionTM High-fidelity DNA polymerase	Finnzymes
Restriction endonucleases	Fermentas, New England Biolabs
T4-DNA-Ligase	Promega

2.6 Antibodies

2.6.1 Primary antibodies

Primary antibody	Dilution	Application	Source
TDM-2 anti-CPD	1:1000	ELISA	Cosmo Bio Co.
Pol II (aN-15, sc-34092)	1:500	Western Blotting	Santa Cruz Biotechnology, Inc.
Anti-α-tubulin (DM1A, T9026)	1:5000	Western Blotting	Sigma

2.6.2 Secondary antibodies

Secondary antibody	Dilution	Application	Source
Biotin-XX F(ab')2 fragment of goat anti mouse IgG (H+L)	1:2000	ELISA	Invitrogen
Donkey anti-goat IgG-HRP (sc-2020)	1:10000	Western Blotting	Santa Cruz Biotechnology, Inc.
Goat anti-mouse IgG-HRP (CatN 170-6516)	1:10000	Western Blotting	BioRad

2.7 Primers

Primers were designed by using Primer-BLAST (http://www.ncbi.nlm.nih.gov) or iSct Primers (http://signal.salk.edu/tdnaprimers.2.html).

The primers were ordered at Sigma-Aldrich and dissolved in sterile, deionized water.

Information on the primer ID contains the primer name, the running number as well as the position on the gene and its orientation. See supplementary data for gene schemes and primer locations. Abbrevations: At - *Arabidopsis thaliana*; Pp - *Physcomitrella patens*; F - Forward; R - Reverse; E - Exon; I - Intron; Ex - Extension; C - Cycles;

2.7.1 Primers used in connection to *A.thaliana*

Primer ID	Sequence 5' - 3'	Gene	Extension, cycles
1. UBQ_101fwd (E1, F)	ACACCATCGACAATGTCAAGGCCA	At3g52590, At-Ubiquitin	Ex-15, C-22, Leaf-PCR: Ex-30, C-35
2. UBQ_923rev (E4, R)	CCTGCAGTTGACAGCTCTTGGGT		
3. RSp31SacI (E2, F)	AATGAGCTCGAATTGCGAATTAAGATAA	At3g61860, At-RS31	Ex-75, C-35
4. G47B73 (E6, R)	CTTTGAGTAGCTTCAAGGG		
5. 31II (E2, F)	ATAAAGCTTGAACTTTTCTTCAAAGG		

Primer ID	**Sequence 5' - 3'**	**Gene**	**Extension, cycles**
6. 47B7BamH (E6, R)	ATATAGGGATCCCATTG ATCAAGGTCTTCCTC		
7. RSp31a_LP2238 (E2, F)	CGATTGCTTTTGCAAGAAT GAGAC	At2g46610, At-RS31a	Ex-75, C-35
8. RSp31a_RP4094 (E6, R)	CCACATAGAGTGCAAAGCA CATAC		
9. 40E2HS (E2. F)	AACGAATTCATGAAGCCAG TCTTCTG	At4g25500, At-RS40	Ex-30, C-30
10. RSp35Bam (E5, R)	ATAGGATCCTAGGGCTTGC GACTCTCTCCC		
11. 41E2HS (E1, F)	AACGAATTCATGAAGCCTG TCTTTTGC	At5g52040, At-RS41	Ex-30, C-30
12. RSp41_2577 (E5, R)	TCCTACGGTCATCCCTCTTG		
13. RSZ32LP595fwd (E1, F)	TTAGGGTTACTGCGTATTT GCACTCTC	At3g53500, At-RS2Z32	Ex-40, C-35
14. RSZ32rp2390 (E6, F)	TGTAGCTGCGACCTCGACT GTAAC		
15. RSp33Sal (E2, F)	AAAGTCGACTATGCCTCGC TATGATGA	At2g37340, At-RS2Z33	Ex-40, C-35
16. RS2Z33_rp2527 (E6, R)	TAGCTTCGGCTACGGCTAA GACTC		
17. atSRp55Nco (E1, F)	ATATACCATGGGTAGCCGA TGGAATCGTAC	At1g09140, At-SR30	Ex-30, C-30, Leaf-PCR: C-35
18. AtribncBamHI (E11, R)	ATATAGGATCCTATCTTGAT CTTGATCTTG		
19. SRp34XbaI (E1, F)	AAATATCTAGAGATCTCAA ATCGACGACC	At1g02840, At-SR34	Ex-30, C-35
20. AtribnciBamHI (E12, R)	ATATAGGATCCCATTTTACC TCGATGGAC		
21. SC35_73fwd (E1, F)	CGCCGGCGGGAAAACCAT GT	At5g64200, At-SC35	Ex-30, C-25
22. SC35_900rev (E5, R)	TAGGCGGGCTACGGCTCC TC		
23. FPG-F1716pan (E7, F)	CCCGTTGCAGACTGCTTCT AGCC	At1g52500, At-FPG1	Ex-15-30, C-35
24. FPG-R2173pan (E8, R)	CCATCAACAAAGGCCTTT CC		
25. FPG-R2692rev (E10, R)	CGACCACCTCTGGGTTTC TG	At1g52500, At-FPG1	Ex-15-30, C-35

Primer ID	**Sequence 5' - 3'**	**Gene**	**Extension, cycles**
26. RAD1forw (E5, F)	CCATCCTGACATGGGTTT TGTC	At5g41150, At-RAD1	Ex-30, C-33
27. RAD1rev (E6, R)	CCAGTTCCTTTCTTCCGCC TGC		
28. RAD1-F3137 (E7, F)	CACCAGAAAGGCATGAAGA TAATAC		
29. RAD1-R3533 (E8, R)	CTTAACCGAGGAAAATGCA GAAC		
30. RAD23-F583pan (E2, F)	GGAGAACAAAGTTACGGA GG	At1g79650.4, At-RAD23	Ex-15, C-33
31. RAD23-R1133pan (E5, R)	GGAACAGGTGAAGACTGGG		
32. RAD23-F1730 (E8, F)	CATCTGGAGGACCTAACT CA		
33. RAD23-R2394 (E11, R)	CTCAGAAGTTGAGGGTTT TG		
34. PHR2_580fwd (E1, F)	AACGGGGCCTTTTCGTGC CC	At2g47590, At-PHR2	Ex-40, C-27
35. PHR2_1719rev (E3, R)	TGAGTCCTGTATCTCCCGG TCCG		
36. UVR2_1518fwd (E4, F)	GAGCTTGGGAGTGGGCAC GC	At1g12370, At-PHR1/UVR2	Ex-15, C-30
37. UVR2_1977rev (E7, R)	GCCTCTTCAGGTCCCTTGG TCC		
38. UVR3_2135fwd (E10, F)	GCGCGTCACTGTGTAGCCT GT	At3g15620, At-UVR3	Ex-15, C-30
39. UVR3_2714rev (E13, R)	ACGCTCAATGGTGCTGTCC ATGG		

Primer ID	Sequence 5' - 3'	Gene	Extension, cycles
40. CaMVPrcon (F)	CCACTATCCTTCGCAAGACCCTTCCT	35S rRNA CaMV promoter, octopine synthase terminator; used to verify transgenic plants containing CSHL-amiRNA constructs	Leaf-PCR: Ex-30, C-35, colony-PCR: Ex-15, C-30
41. OCSterm (R)	ACCGGCGGTAAGGATCTGAGC		

2.7.2 Primers used in connection to *P.patens*

Primer ID	Sequence 5' - 3'	Gene	Extension, cycles
43. Actin_fwd (E2, F)	GTCGAGCATGAAGATCAAAGTGG	PHYPA-DRAFT_109052, Pp-Actin	Ex-15, C-25
44. Actin_rev (E2. R)	ACCAGCCGTTAGAATTGAGCCCAG		
45. ppRSp27_F574 (E2, F)	CCGGTGTATTGTGGGAACTTTG	PHYPA-DRAFT_167387, Pp-RS27	Ex-75, C-30
46. ppRSp27_R2322 (E3, R)	CATCACGCTCATCTTCCATG		
47. ppRSZ37a_F1243 (E1, F)	CTCTGTTCATTCCAGTGAGTGTCTC	Pp-RS2Z37	Ex-75, C-30
48. ppRSZ37a_R5784 (E7, R)	AAGTATTTTCATTCACAGGTCATGG		
49. ppFPG1_1158fwd (E3, F)	CTCCAAAGTCGATGACACAGAAGAGTT	PHYPA-DRAFT_198646, Pp-FPG1	Ex-30, C-30
50. ppFPG1_2100rev (E5, R)	ACCCCAACTCAGAAATTGGCGGC		

Primer ID	Sequence 5' - 3'	Gene	Extension, cycles
51. ppFPG1_2711fwd (E7, F)	TGCACCAGGTTACACACCGCC	PHYPADRAFT_198646, PpFPG1	Ex-30, C-30
52. ppFPG1_3176rev (E8, R)	TCCCTGGCTTCCTGTCCCAACG		
53. ppFPG1_3941rev (E10, R)	TGCCTCACCTGCGTCCTCCA		
54. ppRAD1_990fwd (E1, F)	GGCGGATGGTACTCGCGTCG	PHYPADRAFT_201653, PpRAD1	Ex-30, C-30
55. ppRAD1_2116rev (E3, R)	TGCGTTCGTCCTTGCATGCTACA		
56. ppRAD1_2712fwd (E4, F)	TGGAGAAGATGCGGCTCCACGA		
57. ppRAD1_3399rev (E5, R)	CCGAGACCTCATTTCCAGACTCAGA		
58. ppRAD1_3327fwd (E5, F)	GCGCTAGACCCTTCCGAAGTTGC		
59. ppRAD1_3984rev (E6, R)	ACGTCACACCTGTTGCAGTGGC		
60. ppRAD1_4189fwd (E7, F)	TCCTTCCGTGCTTCATCAGCAG		
61. ppRAD1_4706rev (E8, R)	CCCAACACGCATGGCTCGGT		

2.8 Plasmids

Plasmid	Reference
CSHL_011244	Palatnik (2005), Ossowski (2006)
CSHL_078707	Palatnik (2005), Ossowski (2006)
CSHL_082339	Palatnik (2005), Ossowski (2006)
pSOUP/CD3-1124	Palatnik (2005), Ossowski (2006)

2.9 Bacterial strains

Strain	**Reference**
Agrobacterium tumefaciens AGL1	Lazo (1991)
Escherichia coli DH5α	Meselson and Yuan (1968)

2.10 Media

Media and buffers were prepared with deionized water and autoclaved for 20 minutes at 125°C, 1.5 bar. Temperature sensitive solutions were filter-sterilized (0.2 μm pore size).

2.10.1 Bacterial media

LB (Lysogeny Broth) medium	**1 L**
Tryptone	10 g
Yeast extract	5 g
Sodium chloride	10 g
Agar (for solid agar plates)	15 g
H_2O (deion.)	Up to 1 L
- autoclaved for 20 minutes	

SOB (Super Optimal Broth) medium	**1 L**
Bactotryptone	20 g
Yeast extract	5 g
NaCl	0.5 g
KCl	2.5 g
$MgCl_2$	2 g
$MgSO_4$	2.5 g
10M NaOH	20 μl
H_2O (deion.)	Up to 1 L
Adjusted ph to 6.7 - 7.0	
- autoclaved for 20 minutes	

2.10.2 *A.thaliana* media

1/2 GM [149]	**1 L**
1A Micro and 1/2 and Macro elements	2.2 g
MES monohydrate	0.5 g
MS vitamins	1 mL (x1000 stock)
D(+)-Sucrose	10 g
Plant agar	7 g
H_2O (deion.)	Up to 1 L
Adjusted pH to 5.6 with 1 M KOH	
- autoclaved for 20 minutes	

Liquid cell culture medium with 3% sucrose	**1 L**
Murashige and Skoog (MS) salts, including vitamins	4.4 g
2,4-dichlorophenoxyacetic acid (Auxin)	1 mg
D(+)-Sucrose	30 g
Adjusted pH to 5.5 with 1 M KOH	
H_2O (deion.)	Up to 1 L
- autoclaved for 20 minutes	

Liquid cell culture medium with / without 1% sucrose	**1 L**
Murashige and Skoog (MS) salts, including vitamins	4.4 g
2,4-dichlorophenoxyacetic acid (Auxin)	1 mg
(D(+)-Sucrose	10 g)
Adjusted pH to 5.5 with 1 M KOH	
H_2O (deion.)	Up to 1 L
- autoclaved for 20 minutes	

Solid cell culture medium with / without 1% sucrose	**1 L**
Murashige and Skoog (MS) salts, including vitamins	4.4 g
2,4-dichlorophenoxyacetic acid (Auxin)	1 mg
(D(+)-Sucrose	10 g)
Adjusted pH to 5.5 with 1 M KOH	
Plant agar	7 g
H_2O (deion.)	Up to 1 L
- autoclaved for 20 minutes	

2.10.3 *P.patens* media

BCDAT medium	**1 L**
Stock solution B 100x	10 mL
Stock solution C 100x	10 mL
Stock solution D 100x	10 mL
Trace element solution 1000x	1 mL
Di-ammonium-tartrate	920 mg
Plant agar	8 g
H_2O (deion.)	Up to 1 L
- autoclaved for 20 minutes	
1M $CaCl_2$ (sterile filtered)	1 mL

Solution B 100x	**1 L**
$MgSO_4 \times 7H2O$	25 g
H_2O (deion.)	Up to 1 L

Solution C 100x	**1 L**
KH_2PO_4	25 g
H_2O (deion.)	Up to 1 L
Adjusted pH to 6.5 with 4 M KOH	

Solution D 100x	**1 L**
KNO_3	101 g
$FeSO_4 \times 7H2O$	1.25 g
H_2O (deion.)	Up to 1 L

Trace element solution	**1 L**
H_3BO_3	614 mg
$AlK(SO_4)_2 \times 12H_2O$	110 mg
$CuSO_4 \times 5H_2O$	55 mg
KBr	28 mg
LiCl	28 mg
$Na_2MoO_4 \times 2H_2O$	25 mg
$MnCl_2 \times 4H_2O$	389 mg
$CoCl_2 \times 6H_2O$	55 mg
$ZnSO_4 \times 7H_2O$	55 mg
Kl	28 mg
$SnCl_2 \times 2H_2O$	28 mg
$NiCl_2 \times 6H_2O$	59 mg

Driselase in mannitol	**10 mL**
Driselase Basidiomycetes sp.	100 mg
8% mannitol	Up to 10 mL

The solution of driselase in mannitol was dissolved over 15 minutes in a 50 mL falcon tube by occasional inversions. When dissolved, the mixture was centrifuged at 2500 rpm for five minutes at room temperature and subsequently filter sterilized by using a 0.22 μm filter.

PRM-L	**100 mL**
Stock solution B 100x	1 mL
Stock solution C 100x	1 mL

Continue on next side

PRM-L	**100 mL**
Stock solution D 100x	1 mL
Trace element solution 1000x	100 μL
Di-ammonium-tartrate	92 mg
Mannitol	6 g
H_2O (deion.)	Up to 99 mL
- autoclaved for 20 minutes	
1M $CaCl_2$ (sterile filtered)	1 mL

PRM-B	**500 mL**
Stock solution B 100x	5 mL
Stock solution C 100x	5 mL
Stock solution D 100x	5 mL
Trace element solution 1000x	500 μL
Di-ammonium-tartrate	92 mg
Mannitol	30 g
Plant agar	2.75 g
H_2O (deion.)	Up to 495 mL
- autoclaved for 20 minutes	
1M $CaCl_2$ (sterile filtered)	5 mL

20 mL were used per PRM-B agar plate. Plates were subsequently covered with cellophane after agar solidified.

PRM-T	**100 mL**
Stock solution B 100x	1 mL
Stock solution C 100x	1 mL
Stock solution D 100x	1 mL
Trace element solution 1000x	100 μL
Di-ammonium-tartrate	92 mg
Mannitol	6 g
Plant agar	400 mg

Continue on next side

PRM-T	**100 mL**
H_2O (deion.)	Up to 99 mL
- autoclaved for 20 minutes	
1M $CaCl_2$ (sterile filtered)	1 mL

PRM-T medium was split into 10 mL aliquots and stored at 60°C for further use.

8% mannitol	**200 mL**
Mannitol	16 g
H_2O (deion.)	Up to 200 mL
- Sterile filtered	

2.11 Solutions, buffers and standards

Diverse additives were dissolved in water, subsequently filter sterilized and stored at -20°C. After the temperature of the media dropped to approximately 60°C, additives were added to the final concentration as indicated below.

Additive	**Solvent**	**Stock solution**	**End concentration**
Ampicillin	ddH_2O	50 mg/mL	50 μg/mL
Auxin	96% EtOH	200 mg/mL	1 μg/mL
BASTA	ddH_2O	5 mg/mL	6 μg/mL
Kanamycin	ddH_2O	100 mg/mL	100 μg/mL
Rifampicin	ddH_2O	50 mg/mL	100 μg/mL
Spectinomycin	ddH_2O	50 mg/mL	50 μg/mL (*E.coli*)
			100 μg/mL (*A.tumefaciens*)
Tetracyclin	ddH_2O	12.5 mg/mL	12.5 μg/mL (*E.coli*)
			2.5 μg/mL (*A.tumefaciens*)
Vancomycin	ddH_2O	200 mg/mL	300 mg/L
X-Gal	ddH_2O	20 mg/mL	60 μl per 10 cm plate

TB (Transformation Buffer)	**100 mL**
PIPES	0.3 g
$CaCl_2$	0.16 g
KCl	1.8 g
Adjusted pH to 6.7 with 1 M KOH	
$MnCl_2$	1 g
H_2O (deion.)	Up to 100 mL
- Sterile filtered	

10xPBS (Phosphate Buffered Saline)	**1 L**
NaCl	80 g
KCl	2 g
Na_2HPO_4	14.4 g
KH_2PO_4	2.4 g
Adjusted pH to 7.4 with 1N HCl	
H_2O (deion.)	Up to 1 L
- autoclaved for 20 minutes	

2.11.1 Agarose / Polyacrylamide gel electrophoresis

Agarose gel	**100 mL, 1-4%**
Agarose	1-4 g
1xTAE	Up to 100 mL
Ethidium bromide (10 mg/mL stock)	4μL

Polyacrylamide gel	**20 mL, 6%**
10xTBE	2 mL
Polyacrylamide, 60%	3 mL
Ammonium persulfate, 10%	200 μL
TEMED	20 μl
H_2O (deion.)	14.8 mL

6x DNA loading dye	**Fermentas**
Tris-HCl (pH 7.6)	10 mM
Bromophenol blue	0.03%
Xylene cyanol FF	0.03%
Glycerol	60%
EDTA	60 mM

6x orange DNA loading dye	**Fermentas**
Tris-HCl (pH 7.6)	10 mM
Orange G	0.15%
Xylene cyanol FF	0.03%
Glycerol	60%
EDTA	60 mM

50xTAE buffer	**1 L**
Tris base	242 g
Acetic acid, glacial	57.1 mL
$Na_2EDTA \times 2H_2O$	37.2 g
H_2O (deion.)	Up to 1 L
Adjusted pH to 8.3 with acetic acid	

10xTBE buffer	**1 L**
Tris base	108 g
Boric acid	55 g
0.5 M EDTA (pH 8.0)	40 mL
H_2O (deion.)	Up to 1 L

Molecular weight standards used for agarose and polyacrylamide gels:

GeneRuler 50 bp DNA ladder, Fermentas [bp]
1000 / 900 / 800 / 700 / 600 / **500** / 400 / 300 / **250** / 200 / 150 / 100 / 50

GeneRuler 100 bp DNA ladder, Fermentas [bp]
1000 / 900 / 800 / 700 / 600 / **500** / 400 / 300 / 200 / 100

GeneRuler 100 bp Plus DNA Ladder, Fermentas [bp]
3000 / 2000 / 1500 / 1200 / **1000** / 900 / 800 / 700 / 600 / **500** / 400 / 300 / 200 / 100

GeneRuler 1 kb DNA Ladder, Fermentas [kb]
10 / 8 / **6** / 5 / 4 / 3.5 / **3** / 2.5 / 2 / 1.5 / **1** / 0.75 / 0.5 / 0.25

GeneRuler 1 kb Plus DNA Ladder, Fermentas [kb]
20 / 10 / 7 / **5** / 4 / 3 / 2 / **1.5** / 1 / 0.7 / **0.5** / 0.4 / 0.3 / 0.2 / 0.075

MassRuler Low Range DNA Ladder, Fermentas [bp]
1031 / 900 / 800 / 700 / 600 / **500** / 400 / 300 / 200 / 100 / 80

MassRuler High Range DNA Ladder, Fermentas [bp]
48502 / 24508 / 20555 / 17000 / 15258 / 13825 / 12119 / 10171

Lambda DNA / HindIII Marker, 2, Fermentas [bp]
23130 / 9416 / 6557 / 4361 / 2322 / 2027 / 564 / 125

50 bp DNA Ladder, New England BioLabs [bp]
1350 / 916 / 766 / 700 / 650 / 600 / 550 / **500** / 450 / 400 / 350 / 300 / 250 / **200** / 150 / 100 / 50

100 bp DNA Ladder, New England BioLabs [bp]
1517 / 1200 / **1000** / 900 / 800 / 700 / 600 / **500** / 400 / 300 / 200 / 100

1 kb DNA Ladder, New England BioLabs [kb]
10 / 8 / 6 / 5 / 4 / **3** / 2 / 1.5 / 1 / 0.5

Spectra Multicolor Broad Range Protein Ladder, Fermentas [kDa]
225 / 115 / 80 / 65 / 50 / 35 / 30 / 25 / 15 / 10

2.11.2 Western blotting

PEB400	**20 mL**
1 M HEPES-KOH, pH 7.9	1 mL
2 M KCl	4 mL
1 M $MgCl_2$	50 μl
0.5 mM EDTA (pH 8.0)	40 μL
1 M DTT (dithiothreitol)	20 μL
Triton X-100, 100%	20 μL
EDTA-free protease inhibitor tablets (Roche Applied Science)	1/5 tablet
H_2O (deion.)	Up to 20 mL

PEB200	**20 mL**
Same as PEB400 but 2 mL of 2 M KCl instead of 4 mL	
H_2O (deion.)	Up to 20 mL

KCl-free PEB	**20 mL**
Same as PEB400 but without KCl	
H_2O (deion.)	Up to 20 mL

Sample buffer	**20 μL**
Sample	x μL
Invitrogen NuPAGE LDS sample buffer (4x)	5 μL
Invitrogen NuPAGE Reducing agent (10x)	2 μL
H_2O (deion.)	Up to 20 μL

Running buffer	**1 L**
Invitrogen MOPS SDS running buffer	50 mL

Continue on next side

Running buffer	**1 L**
Invitrogen NuPAGE Antioxidant	500 μL
H_2O (deion.)	Up to 1 L

Reduced transfer buffer	**500 mL**
Invitrogen Transfer buffer (20x)	50 mL
Invitrogen NuPAGE Antioxidant	500 μL
Methanol	50 mL
H_2O (deion.)	Up to 500 mL

Blocking solution	**500 mL**
Triton X-100, 0.1%	500 μL
Dry milk, 5%	25 g
1xPBS	Up to 500 mL

PBT	**500 mL**
Triton X-100, 0.1%	500 μL
1xPBS	Up to 500 mL

2.11.3 ELISA

Protamine sulfate solution	**100 mL**
Protamine sulfate, 0.003%	3 mg
H_2O (deion.)	Up to 100 mL

PBS-T	**500 mL**
Tween-20, 0.05%	250 μL
1xPBS	Up to 500 mL

FBS-PBS	**100 mL**
FBS (Fetal Bovine Serum), 2%	2 mL
1xPBS	Up to 100 mL

Citrate phosphate buffer pH 5.0	**1 L**
Citric acid monohydrate	5.1 g
Na_2HPO_4	7.3 g
H_2O (deion.)	Up to 1 L

Substrate solution	**20 mL**
o-Phenylene-diamine-dihydrochloride	10 mg
H_2O_2	2 μL
Citrate phosphate buffer pH 5.0	20 mL

2M H_2SO_4	**100 mL**
H_2SO_4, 96%	7.2 mL
H_2O (deion.)	Up to 100 mL

Chapter 3

Methods

3.1 General methods

3.1.1 Generation of "ultra-competent" *Escherichia coli* DH5α (Slight variation of the Inoue method)

An overnight culture of *Escherichia coli* DH5α was grown in 4 mL LB medium at 37°C. Bacteria were then transferred for further growth into 100 mL of fresh SOB medium at 18°C until an OD600 of 0.6 was reached. At an optical density of 0.6 bacteria were transferred to ice for 10 minutes and then harvested via a 2500 g - 10 min - 4°C centrifugation step. All following steps were carried out on ice or 4°C. After centrifugation, the supernatant was discarded and cells were very gently resuspended in 32 mL of pre-cooled TB. Another centrifugation step was applied after 10 mins and the supernatant was subsequently replaced, again gently, with a fresh amount of 8 mL pre-cooled TB. After addition of DMSO to a final concentration of 7%, cells were distributed in 100 μL aliquots and flash frozen via liquid nitrogen. For long term storage, cells were kept at -80°C [150].

3.1.2 Transformation of *E.coli* DH5α

100 μL aliquots of competent *E.coli* DH5α were first thawed on ice before the pre-cooled ligation mixture was added. After gentle mixing, cells were incubated for approximately 30 minutes on ice. Following the break, a 90 seconds short heat-shock procedure on 42°C was applied, after which 1 mL of fresh LB medium was added. Tubes were gently inverted 1-2 times before the competent bacteria were incubated

for an hour on 37°C accompanied by gentle agitation. After one hour cells were harvested via a 18000 g - 1 min centrifugation step. The majority of the resulting supernatant was discarded and cells were gently resuspended in the remaining LB medium, approximately 50 μL. After this, cells were ready to be distributed on the respective LB-agar dishes in 5 μL and approximately 45 μL aliquots. Depending on the chosen selection method, LB-agar plates were incubated with 60 μl X-Gal (20 mg/mL) and 5 μl IPTG (200 mg/mL) per plate for 30 minutes prior to plating.

3.1.3 Isolation of plasmid DNA

Plasmids were isolated using the Qiaprep Spin Miniprep Kit (Qiagen). The manufacturers' instructions were followed; plasmid elution from the column was done with 50 μL of nuclease-free ddH_2O. The quantity and quality of the isolated plasmids was checked by Nanodrop spectrophotometric measurement as well as agarose gel electrophoresis.

3.1.4 DNA and RNA isolation

The delicate procedures of DNA and RNA isolation were supported by DNeasy and RNeasy Plant Mini Kits (Qiagen). After following the manufacturers' protocols, total DNA and RNA was eluted in 100 μL and 40 μL of nuclease-free ddH_2O, respectively. Quantity and quality of isolated DNA and RNA was determined by Nanodrop spectrophotometric measurements as well as agarose gel electrophoresis in the case of RNA.

3.1.5 Agarose gel elecrophoresis of DNA and RNA

1 μL of sample DNA / RNA was diluted in 4 μL of nuclease-free ddH_2O before 1 μL of 6x loading dye (Fermentas) was added prior to the loading procedure. Gels were prepared, as well as ran, with 1xTAE buffer containing ethidium bromide. Gels were run at 5 V/cm.

3.1.6 DNA fragment purification

Purification of DNA fragments, e.g dissected from a gel, was done by using either the Wizard SV Gel and PCR Clean-Up System (Promega) or the MinElute Gel

Extraction Kit (Qiagen). The manufacturers' instructions were followed along the purification process. DNA was eluted in 20 μL of nuclease-free ddH_2O, quantity and quality control was assessed by spectrophotometric measurements via Nanodrop as well as by agarose gel electrophoresis. Depending on the experiment, purified fragments were either sequenced directly or subcloned via the pGEM-T Easy-Vector System (Promega) into competent *E.coli* bacteria prior to sequencing (VBC Biotech).

3.1.7 Restriction of DNA

Restriction of DNA via enzymes was done according to the recommendations of the respective manufacturer, either Fermentas or New England Biolabs. The table below shows the precise reaction times and temperatures used throughout the respective experiments.

Restriction enzyme	**Buffer**	**Source**	**Time**	**Temperature**
SacI	NEBuffer 1	New England Biolabs	3h	37°C
XbaI	NEBuffer 2	New England Biolabs	3h	37°C
Cfr9I	10x Cfr9I	Fermentas	2h	37°C
BamHI	10x BamHI	Fermentas	2h	37°C
EcoRI	NEBuffer 2	New England Biolabs	1h	37°C
BsrGI	NEBuffer 2 + BSA	New England Biolabs	1h	37°C
NheI	NEBuffer 2 + BSA	New England Biolabs	1h	37°C

3.1.8 TA cloning of DNA fragments produced by Phusion High-Fidelity DNA polymerase

Phusion High-Fidelity DNA Polymerase produces blunt end PCR products. Therefore, procedures which included Promegas pGEM-T Easy Vector System had to undergo the process of a 3'A-overhang addition prior to ligation with the vector. During this process, the Taq DNA-Polymerase (Finnzymes) adds a single dATP-overhang to

the purified DNA fragment, which in turn is then able to bind to the single dTTP-overhang of the pGEM-T vector, thus successfully completing the process of fragment-vector ligation. This procedure was performed according to the table below.

TA cloning	**10 μL**
10x Taq - polymerase buffer	1 μL
10 mM dATP	1 μL
Taq DNA - polymerase	1 μL
DNA fragment	x μL
Nuclease-free ddH_2O	Up to 10 μL

3.1.9 Ligation of DNA fragments

DNA fragments were ligated overnight at 4°C by using a T4 DNA Ligase (Promega). The vector fragment ratio was 1:5. Components were thawed on ice and then combined according to the table below.

DNA ligation	**10 μL**
DNA fragment (usually 250 ng)	x μL
Vector (usually 50 ng)	x μL
10x T4 buffer	1 μL
T4 DNA ligase	1 μL
Nuclease-free ddH_2O	Up to 10 μL

8 μL of the ligation-reaction were used for transformation.

3.1.10 Reverse Transcription - Polymerase Chain Reaction (RT-PCR)

The process of reverse transcription of RNA was performed by using a reverse transcription system (Promega) with following modifications. 0.5-1 μg of isolated RNA was diluted in nuclease-free ddH_2O to a final volume of 10 μL. After 10 minutes at 70°C, RNA was cooled down for 5 minutes on ice before the reverse-transcription mastermix was added (see table below, oligo-dT was used as a reverse primer for cDNA synthesis). After two hours (for *P.patens*) or 30 minutes (for *A.thaliana*) of

reverse transcription, the reaction was stopped by putting the mixture to 95°C for 5 minutes and subsequently 5 minutes on ice for cooling. 80 μL of nuclease-free ddH_2O were added. cDNA was stored at -20°C. The newly synthesized cDNA was used in a control PCR reaction (actin for *P.patens*, ubiquitin for *A.thaliana*), which was further analyzed via agarose gel electrophoresis. The appropriate PCR conditions can be found in the two tables below.

RT (Reverse Transcription)	**100 μL / reaction**
RNA	0.5 - 1 μg
Nuclease-free ddH_2O	Up to 10 μL
70°C	10 min
Ice	5 min
Addition of mastermix	**10 μL**
$MgCl_2$	4 μL
10x Reverse Transcriptase buffer	2 μL
10 mM dNTPs	2 μL
Oligo$(dT)_{15}$ primer	1 μL
RNAsin	0.5 μL
AMV Reverse Transcriptase (HC)	0.5 μL
42°C	120 min (*P.patens* / 30min (*A.thaliana*)
95°C	5 min
Ice	5 min
Nuclease-free ddH_2O	80 μL

PCR (Polymerase Chain Reaction)	**20 μL / reaction**
5x Phusion HF buffer	4 μL
100 μM forward primers	0.1 μL
100 μM reverse primer	0.1 μL
10 mM dNTPs	0.4 μL
Phusion DNA polymerase (0.02 U/μL)	0.2 μL
Nuclease-free ddH_2O	15.2 - 16.2 μL
cDNA template	1 - 2 μL

The table below shows the PCR setup for *A.thaliana* (At) and *P.patens* (Pp) related

primers. For gene specific extension and cycle data, refer to subchapter 2.7.1 and 2.7.2.

Cycling step	Temperature	Duration	Cycles
Denaturation	98°C	3 min	
Denaturation	98°C	10 sec	
Annealing	At: 58°C / Pp: 63°C	10 sec	22-35
Elongation	72°C	15-75 sec	
Final elongation	72°C	5 min	
Final hold	4°C	∞	

3.1.11 UV treatments

If experiments required irradiation of samples with UV-C, a UV stratalinker 4200 (Stratagene) was used. Irradiation was done by using the Energy setting of the respective device. UV-C doses varied among the experiments and are mentioned individually in the respective subchapters. During irradiation, samples were not protected by any kind of materials (e.g. caps of agar dishes etc.).

3.1.12 ELISA (Enzyme-linked immunosorbent assay)

Approximately 100 mg of two weeks old *A.thaliana* seedlings (Col-0) were used for DNA isolation. Nunc MaxiSorp plates were used to perform DNA-ELISAs. For initial coating of the 96 well plates, 50 μL of a 0,003% protamine sulfate solution was added to each well and evaporated overnight at 37°C. To detect cyclobutane-pyrimidine dimers (CPDs), 0.8 μg/mL of DNA was diluted in 1xPBS. This DNA-solution was denatured at 100°C for 10 minutes and subsequently cooled down for 15 minutes on ice. 50 μL of denatured DNA-solution was then added to each protamine-sulfate precoated well (40 ng of DNA in 50 μL 1xPBS). After overnight evaporation at 37°C, plates were washed two times with 150 μL/well of 0.05% Tween-20 in 1xPBS (PBS-T). 150 μL of 2% FBS in 1xPBS was added to each well and incubated for one hour at room temperature to prevent non-specific antibody binding. Plates were washed again, two times, with 150 μL/well of PBS-T before the primary antibody was added. 100 μL of TDM-2 anti-CPD primary antibody (Cosmo Bio Co.) in a 1:1000 dilution in 1xPBS was added to each well for one hour at room temperature. Wells were washed

three times with 150 μL/well PBS-T. The secondary antibody (Biotin-XX F(ab')2 fragment of goat anti mouse IgG (H+L) 2 mg/mL, Invitrogen) was diluted 1:2000 and added in 100 μL/well and incubated for one hour at room temperature. After washing the wells three times with PBS-T, 100 μL/well of Streptavidin-Peroxidase (Invitrogen) in a 1:10000 dilution was added and incubated for one hour at room temperature. Plates were washed three times with PBS-T. 150 μL of citrate phosphate buffer pH 5.0 was added to each well and remained there until the freshly prepared substrate (One tablet of o-Phenylene-diamine-dihydrochloride (10 mg/tablet, Sigma) per 20 mL citrate phosphate buffer pH 5.0, 2 μL 40% H_2O_2 (Sigma)) was ready. After discarding the citrate phosphate buffer, 100 μL/well of substrate was added to each well and the reaction was stopped precisely after 40 minutes on room temperature by adding 50 μL of 2M H_2SO_4 to each well. Wells were analyzed by using light with a wavelength of 492 nm.

3.1.13 Western Blotting

Approximately 100 mg of *A.thaliana* cell culture suspension (HH1, seedling origin, Col-0 ecotype) were resuspended in 200 μL PEB400 and kept on ice for subsequent steps. Cells were subjected to sonication for three times (Bandelin electronic UW200, MS 73/D, 50 cycles, 1 minute pause between six second long strokes). Following sonication, cells were centrifuged at 14.000 rpm for 15 minutes at 4°C to separate insoluble material and unbroken cells from suspended proteins. 150 μL of the resulting supernatant were carefully transferred to a new tube and diluted with 150 μL of KCl-free PEB to adjust the KCl concentration to 200 mM. Protein concentration was determined using Nanodrop and adjusted to 60 μg in 20 μL of sample buffer (see subchapter 2.11.2) and put to 70°C for 10 minutes. After denaturation, Invitrogen NuPAGE Novex 4-12% Bis-Tris precast gels were loaded with 20 μL/well of sample and run in an Invitrogen Xcell SureLock Mini cell system at constant 200 Volts for approximately 30 minutes or until the desired separation had been achieved. Gels were then subjected to blotting at 350 mA for 45 minutes, using Invitrogens Novex Semi dry blotting system and PVDF membranes. The transfer of proteins to the membrane was checked by Ponceau S staining before they were incubated for at least 30 minutes in blocking solution. All following incubation steps were performed at room temperature and slight agitation. Membranes were incubated for one hour with the respective primary antibody (subchapter 2.7.1). After this step, membranes were washed with

blocking solution and incubated for another five minutes, this was repeated five times in summary. Next, the membranes were incubated with the respective secondary antibody (subchapter 2.7.2) for another hour before they were washed with 1xPBS-Triton (0,1%) for two times and another two times with 1xPBS, each time for five minutes. Finally, membranes were covered with GE Healthcares Amersham ECL Western Blotting detection reagents for one minute. For detection, membranes were covered with Kodak films for one and ten minutes as well as overnight. Kodak films were developed using an AGFA Curix 60 developing system.

3.2 Methods used in connection to *A.thaliana*

3.2.1 Description of *A.thaliana* lines

1. Wild type ecotype Col-0
2. At-SR30 overexpression line (overexpression of At-SR30 cDNA under the control of the 35S CaMV promoter) [50].
3. At-RS2Z33 overexpression line (overexpression of At-RS2Z33 genomic clone under the control of the 35S CaMV promoter) [49].
4. At-RS31 overexpression line (overexpression of At-RS31 cDNA under the control of the 35S CaMV promoter) (unpublished).
5. At-RS31 knockout line n1 (SALK_021332, T-DNA insertion in the fifth exon) (unpublished).
6. At-RAD1 knockout line (uvh1, stock CS3819 was obtained from Arabidopsis Biological Resource Center) [151].
7. *A.thaliana* cell suspension culture (HH1, seedling origin, Col-0).

3.2.2 Growth conditions

Wild type plants of *A.thaliana* (Col-0) and overexpression- / mutant-lines were germinated and grown on either ½ GM medium or soil under long day conditions at 23°C. Water was supplied ad libitum.

3.2.3 Cell suspension maintenance

A.thaliana cell suspension cultures (HH1, seedling origin, Col-0 ecotype) were refreshed on a weekly basis in a laminar flow hood. 40 mL of one week old cell suspension cultures were split 1:4. 10 mL of one week old cells were transferred to an autoclaved 250 mL Erlenmeyer flask and resuspended in 30 mL of liquid cell culture medium containing 3% sucrose (subchapter 2.10.2). Capped flasks were sealed with parafilm and incubated in the dark at 23°C with constant shaking for one week.

3.2.4 Seed sterilization

Seed sterilization was carried out in a laminar flow hood by applying 1 mL of 70% EtOH + 0.01% Triton X-100 to dry seeds. After a minute of incubation the solution was replaced with 2 mL of freshly prepared 7.5% sodium hypochlorite + 0.01% Triton X-100 in which the seeds stayed for 10 minutes while being slightly shaked. The solution was removed and replaced with 1 mL of sterile ddH_2O. The following steps were applied to wash seeds until every last trace of sodium-hypochlorite was gone. To do this, 2 mL of ddH_2O was added and a 10 minutes long incubation phase followed, accompanied by slight agitation. This procedure was repeated five times. Sterile seeds were transferred to sterile filter paper for further distribution on ½ GM-agar plates. Sterile seeds were spread across the ½ GM agar plates (approximately 35 seeds per 15 cm diameter plate). The plates were then sealed by using Leukopore and stratified at 4°C for two days. Stratified seeds were transferred to long day conditions, 23°C, and placed nearly upright. After ten days, seedlings were either used or put to pots containing soil for further growth.

3.2.5 Generation of electro-competent *A.tumefaciens* AGL1

A culture of *A.tumefaciens* AGL1 was grown in 4 mL LB + rifampicin (100 μg/mL) at 28°C for two days. Bacteria were then transferred for further growth into 500 mL of LB medium with rifampicin at 28°C until an OD600 of 0.7 was reached. Bacteria were subsequently transferred to 4°C for approximately 20 minutes before they were harvested by a 3000 g - 10 min - 4°C centrifugation step. All following steps were carried out on ice or 4°C. Following centrifugation, the supernatant was discarded and bacteria were gently resuspended in 40 mL of pre-cooled, filter-sterilised, 10% glycerol. This procedure of centrifugation and washing was repeated additional two

times before the final volume of 4 mL 10% glycerol was added. 100 μL aliquots of competent *A.tumefaciens* were first flash frozen in liquid nitrogen and subsequently stored at -80°C.

3.2.6 Electroporation of electro-competent *A.tumefaciens* AGL1 and subsequent verification via colony-PCR

100 μL aliquots of electro-competent *A.tumefaciens* AGL1 were thawed on ice before approximately 250 ng DNA of a specific construct (CSHL_011244, CSHL_078707, CSHL_082339) and 250 ng of the helper plasmid (pSOUP) were added to the cells. After gentle agitation, cells were pulsed for 5 milli-seconds with 15 μF and 2400 Volts (EasyjecT Optima Equibio). Cells were resuspended in 1 mL of fresh LB medium and incubated for 150 minutes at 28°C with slight agitation. Aliquots of 250 μL of electroporated cells were distributed on agar plates containing rifampicin, spectinomycin and tetracyclin (100 μg/mL, 100 μg/mL, 2.5 μg/mL). Cells were incubated for three days at 28°C until colonies were big enough to be tested via colony PCR. A specific set of primers (CaMVPrCon and OCSterm) was used, which is located in the promoter and terminator region, respectively. By this, it was possible to amplify all three respective inserts (artificial microRNAs: CSHL_011244, CSHL_078707, CSHL_082339) with one primer pair. Colony-PCR was performed by subverting a yellow pipette tip in a single colony, which was then subsequently subverted in the PCR-mastermix. The same tip was then used to inoculate an agar plate containing the respective antibiotics (rifampicin 100 μg/mL, spectinomycin 100 μg/mL, tetracycline 2.5 μg/mL) for further growth in case the investigated colony turned out to be positive concerning the transformation.

3.2.7 Transformation of *A.thaliana* (Floral dip)

A.thaliana (Col-0) plants were grown under long-day conditions at 23°C (16h light, 8h dark) on Max-Planck-Soil until a sufficient amount of still closed floral buds emerged. *A.tumefaciens* bacteria, which carried a respective insert, were grown for two days in 500 mL LB medium with 100 μg/mL of rifampicin until they were harvested via a 3000 g - 20 min centrifugation step. The supernatant was discarded and cells were resuspended in 400 mL of a freshly prepared 5% sucrose solution. Immediately before floral dipping, 200 μL of Silwet L-77 (Lehle Seeds) were added to the sucrose - bacteria

mixture. For floral dipping itself, whole plants were simply dipped into the solution of *A.tumefaciens* for approximately one minute and sealed in a plastic bag for one day to keep the appropriate air humidity to ensure bacterial survival. Plants were further cultivated until seed collection [9].

3.2.8 Selection of transformed plants

After collection and subsequent sterilization, seeds were transferred to BASTA- and vancomycin-containing (6 mg/L and 300 mg/L, respectively) ½ GM plates (15 cm in diameter). Approximately 500 seeds were evenly spread across each plate and put to 4°C for two days for stratification. Afterwards, plates were transferred to long day conditions, 23°C. Potentially positive seedlings were relocated from the agar plates to pots containing Max-Planck-Soil where they were further nurtured until screening via leaf-PCR analysis was feasible.

3.2.9 Leaf-PCR

This method was used to analyze potentially transgenic plants without going through the labor of DNA isolations. A single leaf of a respective plant was put on a wet filter paper. Using the sharp end of a Pasteur pipette, a leaf disc was cut out from the leaf and put directly into the PCR-mastermix (18 μL). The number of cycles has to be increased due to a lower DNA yield (See subchapter 2.7.1, Leaf-PCR conditions). PCR products were analyzed via agarose gel electrophoresis.

3.2.10 Experimental setup to subchapter 4.1

The aim of this experiment was to investigate gene expression and alternative splicing events in different genotypes of *A.thaliana* upon UV-C irradiation.

Wild type plants of *A.thaliana* (Col-0), plants overexpressing At-SR30, At-RS31 and At-RS2Z33, as well as At-RS31 mutant plants were germinated and grown on ½ GM medium under long day conditions at 23°C. Seeds were sterilized prior to plating (approximately 35 seeds per 15 cm diameter plate) and ½ GM-agar plates were then sealed by using Leukopore and stratified at 4°C for two days. Stratified seeds were transferred to long day conditions, 23°C, and placed nearly upright. After ten days, half of the plates / seedlings were irradiated with 100 J/m^2 UV-C (Stratalinker). For

irradiation, the lids of the plates were removed to avoid possible shielding effects. After UV-treatment, plates were either returned to the light, 23°C, or kept in the dark at 23°C. After four hours, whole seedlings were harvested and flash frozen in liquid nitrogen. Subsequently, seedlings were processed using pestle, mortar and liquid nitrogen.

Approximately 100 mg of ground seedlings were used to isolate total RNA using the RNeasy Plant Mini Kit, including on-column DNase I treatment (Qiagen). cDNAs of poly-A mRNAs were obtained by reverse transcription, using oligo-dT as a reverse primer (Promega). PCR analysis was performed as described in subchapter 3.1.10; PCR conditions as well as used primers for each gene can be found in subchapter 2.7.1.

3.2.11 Experimental setup to subchapter 4.6

The question behind this experiment was whether *A.thaliana* cell suspension cultures would show differences in gene expression and alternative splicing in response to UV-C irradiation when they are grown in different nutrient conditions.

Therefore we supplied standard growth-media containing either 1% or 0% sucrose (refer to subchapter 2.10.1 for specific media compositions). Two flasks (each 40 mL) of *A.thaliana* cell suspension cultures (HH1, seedling origin, Col-0 ecotype) were split 1:4 (10 mL of one week old cells, 30 mL liquid cell culture medium with 3% sucrose) to result in eight flasks of cell suspension cultures needed for the experiment. These eight flasks were kept in the dark with constant shaking at 23°C. On the fourth day of subculture, the volume of 40 mL cell suspension culture of each flask was transferred to a sterile 50 mL Falcon tube and centrifuged at 800 g for five minutes at room temperature. After removal of the supernatant, the volume of cell suspension cultures per tube was equalized to 10 mL. 30 mL of 1% or 0% sucrose-containing liquid medium was added to four out of eight tubes and cells were gently resuspended. After centrifugation at 800 g for five minutes at room temperature, approximately 40 mL of supernatant was removed and the whole washing procedure was repeated additional two times. After the last centrifugation step and removal of the supernatant, 10 mL of each four Falcon tubes were collected in one. 2 mL of cells were evenly distributed across each cellophane-covered agar plate (10 cm in diameter, 36 plates), containing

either 1% or 0% sucrose. Plates were then transferred to long day conditions at 23°C. After 24 hours, half of the plates were irradiated with 100 J/m^2 UV-C (Stratalinker). For irradiation, the top of the plates was removed to avoid possible shielding effects. After UV-treatment, all the plates were returned to 23°C. Half of the plates were kept under long day conditions while the other half was transferred to the dark (wrapped in aluminium foil). After 0.5, 1, 2, 4, 8 and 24 hours, cells were harvested and flash frozen in liquid nitrogen. Subsequently, cells were processed using pestle, mortar and liquid nitrogen.

Approximately 100 mg of cells were used to isolate total RNA using the RNeasy Plant Mini Kit, including on-column DNase I treatment (Qiagen). cDNAs of poly-A mRNAs were obtained by reverse transcription using Promegas Reverse Transcription System, using oligo-dT as a reverse primer. PCR analysis was performed as described in subchapter 3.1.10; PCR conditions as well as used primers for each gene can be found in subchapter 2.7.1.

3.2.12 Experimental setup to subchapter 4.7.2

The idea behind this experiment was to show the connection between UV-C induced DNA damage and DNA repair in different genotypes of *A.thaliana*.

Wild type plants of *A.thaliana* (Col-0), plants overexpressing At-RS31 as well as At-RS31 and At-RAD1 mutant plants were germinated and grown on ½ GM medium under long day conditions at 23°C. Seeds were sterilized prior to plating (approximately 35 seeds per 15 cm diameter plate) and ½ GM-agar plates were then sealed by using Leukopore and stratified at 4°C for two days. Stratified seeds were transferred to long day conditions, 23°C, and placed nearly upright. After ten days, 40 out of 80 plates were irradiated with 200 J/m^2 UV-C (Stratalinker). For irradiation, the lids of the plates were removed to avoid possible shielding effects. After UV-treatment, plates were either returned to long day conditions, 23°C, or kept in the dark at 23°C. After 0.5, 2, 4, 8 and 24 hours, whole seedlings were harvested and flash frozen in liquid nitrogen. Subsequently, seedlings were processed using pestle, mortar and liquid nitrogen.

Approximately 100 mg of grinded seedlings were used to isolate total DNA using

the DNeasy Plant Mini Kit, including on-column RNase A treatment (Qiagen). The isolated DNA was then used to perform ELISA as described in subchapter 3.1.12. TDM-2 anti-CPD (1:1000) was used as the primary antibody in order to detect cyclobutane-pyrimide dimers (CPDs).

3.2.13 Experimental setup to subchapter 4.7.3

The aim of this experiment was to investigate the effect of UV-C induced DNA damage on the phosphorylation-state of RNA polymerase II and the possible role of non-protein-coding alternative splice isoforms in connection to the stalled RNA polymerase II. For this experiment, each sample was carried out in triplicates to raise a sufficient amount of sample material to be able to perform RT-PCR, ELISA and Western blotting.

Three flasks (each 40 mL) of seven days old *A.thaliana* cell suspension cultures (HH1, seedling origin, Col-0 ecotype) were split 1:4 (10 mL of one week old cells, 30 mL liquid cell culture medium with 3% sucrose) to result in twelve flasks of cell suspension cultures; eight were needed for the experiment. These eight flasks were kept in the dark with constant shaking at 23°C. On the fourth day of subculture, the volume of 40 mL cell suspension culture of each flask was transferred to a sterile 50 mL Falcon tube and centrifuged at 800 g for five minutes at room temperature. After removal of the supernatant, the volume of cell suspension cultures per tube was equalized to 10 mL. Next, 30 mL of 1% sucrose-containing liquid medium was added to each tube before centrifugation at 800 g for five minutes at room temperature. Approximately 40 mL of supernatant was removed from each Falcon tube and the washing procedure was repeated additional two times. After the last centrifugation step and removal of the supernatant, 10 mL of each four tubes were collected in one and the total volume was adjusted to 45 mL, using 1% sucrose-containing liquid medium. 2 mL of cells were evenly distributed across each cellophane-covered agar plate (10 cm in diameter, 42 plates), containing 1% sucrose (refer to subchapter 2.10.2 for specific media compositions). Plates were then transferred to long day conditions at 23°C for 24 hours. Next, 21 of 42 plates were irradiated with 100 J/m^2 UV-C (Stratalinker). For irradiation, the top of the plates was removed to avoid possible shielding effects. After UV-treatment, all the plates were transferred to the dark (wrapped in aluminium foil) at 23°C for 0.25, 0.50, 1, 2, 4, 8 and 24 hours. Cells were harvested and flash

frozen in liquid nitrogen at the aforementioned time points. Subsequently, cells were processed using pestle, mortar and liquid nitrogen.

Approximately 70 mg of cells were used to isolate total RNA using the RNeasy Plant Mini Kit, including on-column DNase I treatment (Qiagen). cDNAs of poly-A mRNAs were obtained by reverse transcription using Promegas Reverse Transcription System, using oligo-dT as a reverse primer. PCR analysis was performed as described in chapter 3.1.10; PCR conditions as well as used primers for each gene can be found in chapter 2.7.1. RT-PCR was primarily performed to control the efficiency of the UV-C treatment.

Approximately 70 mg of cells were used to isolate proteins for Western blotting. The transfer of proteins to the membrane was checked by Ponceau S staining before they were incubated for at least 30 minutes in blocking solution. Membranes were then incubated with the primary antibodies (Pol II aN-15 1:500, anti-α-tubulin 1:5000), which in turn were incubated with their respective secondary antibodies (donkey anti-goat IgG-HRP 1:10000, goat anti-mouse IgG-HRP 1:10000).

3.3 Methods used in connection to *P.patens*

3.3.1 Description of *P.patens* lines

1. *P.patens* (Hedw.) B.S.G. "Gransden" strain [152].
2. Pp-RS27 knockout line (created using targeting vector containing 35S-*nptII*-CaMV-ter selection cassette) (M. Maronova, unpublished).
3. Pp-RS2Z37 knockout line (created using targeting vector containing 35S-*nptII*-CaMV-ter selection cassette) (M. Maronova, unpublished).

3.3.2 Protonemata and gametophytes maintenance

P.patens protonemal tissue was refreshed on a weekly basis in a laminar flow hood. *P.patens* was grown under long day conditions at 24°C. Protonemal tissue was propagated by applying a protocol established by the Cold Spring Harbor Laboraties. Seven days old protonemal tissue was resuspended in 10 mL of sterile ddH_2O in a pre-autoclaved shredder. The moss was then disintegrated by shredding for three

minutes at approximately 10.000 rpm. Afterwards, for simply refreshing protonemal tissue, 3 mL of shredded tissue were evenly distributed on a fresh, cellophane covered BCD-agar plate. If gametophytes were desired, the shredded protonemal tissue was redistributed in a dot-blot-like method. 2 μL dots of material were evenly distributed across the non-cellophane covered agar-plates, which were then sealed with parafilm to avoid excessive evaporation of ddH_2O. Approximately two to four months later, gametophytes were ready for further applications.

3.3.3 Protoplast isolation

Five days old protonemal *P.patens* tissue was incubated in 5 mL of Driselase-mannitol solution for approximately 40 minutes at room temperature. During the process of cell wall digestion, protonemal tissue was checked several times for its integrity via microscopy. After the majority of the sample was displayed as free floating protoplasts, the solution of protonemal tissue and protoplasts was separated by a passage through a 100 μm filter, fixed on a 50 mL falcon tube. Protoplasts were then gently transferred to a 10 mL sterile universal tube and centrifuged at 800 rpm for four minutes at room temperature with the centrifuge-break turned off. The supernatant was then removed and protoplasts were very gently resuspended in 10 mL of a 8% sterile mannitol solution. This procedure of centrifugation and subsequent washing was repeated two additional times before protoplasts were resuspended in 6 mL of PRM-L, which was then equally distributed among three 10 mL sterile universal tubes. Protoplasts were allowed to recover for 24 hours in the dark at 24°C, placed almost horizontally in a rack. Next day, an aliquot of 10 mL PRM-T (stored overnight at 65°C to avoid solidification of agar) was cooled down to 45°C in a water bath, while protoplasts were centrifuged at 800 rpm for three minutes at room temperature. After the supernatant was removed, each 2 mL aliquot of protoplasts was very gently resuspended in 10 mL of 45°C warm PRM-T. The resuspended protoplasts were then gently poured on a cellophane covered PRM-B agar plate and put to long day growth conditions at 24°C.

When protoplasts were used for microscopy, a small gel slide (5x5 mm) was simply cut out by using a sterilized scalpel. The gel piece was then transferred to a glass slide and stained with calcofluor (50 mg/mL in DMSO, 1 μL). Finally, the gel slide was topped by a cover glass, which was then carefully pushed against the gel to ensure a thin layer for efficient microscopy (Zeiss Axioskop microscope, Visitron Systems

SPOT RT3 camera system, wavelength - 365 nm excitation / 435 nm emission).

3.3.4 Experimental setup to subchapter 4.2 - Protonema

This experiment was designed to investigate the effects of UV-C irradiation on different genotypes of *P.patens* protonemal tissues, their gene expression patterns and possible changes in alternative splicing.

P.patens protonemal tissue was propagated by applying a protocol established by the Cold Spring Harbor Laboraties. Six plates of seven days old *P.patens* wild type, Pp-RS27- and Pp-RS2Z37 mutant protonemal tissue were each split 1:3 by resuspension in 10 mL of sterile ddH_2O in a pre-autoclaved shredder. The moss was then disintegrated by shredding for three minutes at approximately 10.000 rpm. Each cellophane covered BCD-agar plate (total 54 plates) was covered with 3 mL shredded tissue of the respective *P.patens* genotype and then transferred to long day conditions at 24°C. At the fifth day of subculture, 27 out of 54 plates were irradiated with 100 J/m^2 UV-C (Stratalinker). For irradiation, the top of the plates was removed to avoid possible shielding effects. After UV-treatment, all the plates were returned to 24°C. Half of the irradiated and non-irradiated plates were kept under long day conditions while the other half was transferred to the dark (wrapped in aluminium foil). After 0.5, 1, 2, 4, 8 and 24 hours, samples were harvested and flash frozen in liquid nitrogen. Subsequently, cells were processed using pestle, mortar and liquid nitrogen.

Approximately 60 mg of protonemal tissue were used to isolate total RNA using the RNeasy Plant Mini Kit, including on-column DNase I treatment (Qiagen). cDNAs of poly-A mRNAs were obtained by reverse transcription using Promegas Reverse Transcription System, using oligo-dT as a reverse primer. PCR analysis was performed as described in chapter 3.1.10; PCR conditions as well as used primers for each gene can be found in chapter 2.7.2.

3.3.5 Experimental setup to subchapter 4.2 - Gametophytes

The idea behind this experiment was to compare the effects of UV-C irradiation on different genotypes of *P.patens* gametophytes, their gene expression patterns and possible changes in alternative splicing with the effects observed in *P.patens* protonemal tissues.

P.patens protonemal tissue was propagated by applying a protocol established by the Cold Spring Harbor Laboraties. Three plates of seven days old *P.patens* wild type, Pp-RS27- and Pp-RS2Z37 mutant protonemal tissue were each split 1:3 by resuspension in 10 mL of sterile ddH_2O in a pre-autoclaved shredder. The moss was then disintegrated by shredding for three minutes at approximately 10.000 rpm. Next, the shredded material of each genotype was applied in a dot-blot-like method (2 μL/dot) to BCD-agar plates (54), which were sealed with parafilm and then transferred to long day conditions at 24°C (see subchapter 3.3.1). After approximately four months, 27 out of 54 plates were irradiated with 100 J/m^2 UV-C (Stratalinker). For irradiation, the top of the plates was removed to avoid possible shielding effects. After UV-treatment, all the plates were returned to 24°C. Half of the plates were kept under long day conditions while the other half was transferred to the dark (wrapped in aluminium foil). After 0.5, 1, 2, 4, 8 and 24 hours, samples were harvested and flash frozen in liquid nitrogen. Subsequently, cells were processed using pestle, mortar and liquid nitrogen.

Approximately 100 mg of gametophytes were used to isolate total RNA using the RNeasy Plant Mini Kit, including on-column DNase I treatment (Qiagen).cDNAs of poly-A mRNAs were obtained by reverse transcription using Promegas Reverse Transcription System, using oligo-dT as a reverse primer. PCR analysis was performed as described in chapter 3.1.10; PCR conditions as well as used primers for each gene can be found in chapter 2.7.2.

3.3.6 Experimental setup to subchapter 4.3

This experiment was conducted to investigate the effects of a 24 hours dark period post UV-C irradiation on wild type *P.patens* protonemal tissue as well as its recovery potential when transferred back to the light.

P.patens protonemal tissue was propagated by applying a protocol established by the Cold Spring Harbor Laboraties. Four plates of seven days old *P.patens* wild type protonemal tissue were each split 1:3 by resuspension in 10 mL of sterile ddH_2O in a pre-autoclaved shredder. The moss was then disintegrated by shredding for three minutes at approximately 10.000 rpm. Each cellophane covered BCD-agar plate (12)

was covered with 3 mL of shredded tissue and then transferred to long day conditions at 24°C. At the fifth day of subculture, 6 out of 12 plates were irradiated with 100 J/m^2 UV-C (Stratalinker). For irradiation, the top of the plates was removed to avoid possible shielding effects. After UV-treatment, all the plates were transferred to the dark (wrapped in aluminium foil) and returned to 24°C. After 24 hours, plates were transferred back to the light for 0.5, 1, 2, 4, 8 and 24 hours. Samples were harvested and flash frozen in liquid nitrogen at the aforementioned time points. Subsequently, cells were processed using pestle, mortar and liquid nitrogen.

Approximately 60 mg of protonemal tissue were used to isolate total RNA using the RNeasy Plant Mini Kit, including on-column DNase I treatment (Qiagen). cDNAs of poly-A mRNAs were obtained by reverse transcription using Promegas Reverse Transcription System, using oligo-dT as a reverse primer. PCR analysis was performed as described in chapter 3.1.10; PCR conditions as well as used primers for each gene can be found in chapter 2.7.2.

Chapter 4

Results

4.1 Analysis of the expression and splicing of SR and DNA repair genes in *A.thaliana* upon UV-C irradiation

Previous studies have revealed that splicing of SR genes is often executed by splicing complexes which contain SR proteins themselves. To add to this intricacy, we wanted to ask the question whether the expression and splicing pattern of SR genes would differ in *A.thaliana* wild-type, SR30-, RS31- and RS2Z33 overexpression as well as RS31 knockout seedlings. Furthermore, we introduced an additional dimension to this experiment by subjecting seedlings to physical stress in form of ultraviolet-C exposure. Since stress is a common trigger of alternative splicing, it was exciting to determine whether different genetic backgrounds of *A.thaliana* would result in different gene expression and splicing patterns of SR genes. Additionally, since UV-C treatment induces the formation of Cyclobutane-pyrimidine-dimers (CPDs / photodimers) and thus causes damage to DNA, we formulated the question whether the expression of DNA repair genes, which are implicated in different repair mechanisms, would be altered as well. Last but not least we wanted to know whether the expression and splicing patterns of DNA repair genes would show differences between the tested genetic backgrounds of *A.thaliana*.

To fully understand the idea behind these experiments, additional background information needs to be considered. Previous studies (M. Kalyna, A. Barta, unpublished)

have shown that the overexpression of At-RS31 affects the splicing patterns of three genes involved in DNA repair, namely At-FPG1, At-RAD1 and At-RAD23. Additionally, plants which overexpress At-RS31 are hypersensitive to UV-C radiation, while At-RS31 knockout plants are more resilient towards UV-C radiation than the wild type. Moreover, At-RS31 overexpression in untreated plants also leads to changes in alternative splicing of SR genes situated within its own subfamily (At-RS31a, At-RS40, At-RS41). Therefore, our interest also focuses on the question whether exposure to UV-C radiation affects the splicing patterns of these genes by At-RS31.

Therefore, ten-days-old *A.thaliana* wild-type, At-SR30oe, At-RS31oe, At-RS31ko_1 and At-RS2Z33oe seedlings were exposed to 100 J/m^2 UV-C and afterwards either kept in the light or dark for four hours (Refer to subchapter 3.2.9 for details). Total RNA was isolated and treated with DNAse. RT-PCR was carried out using oligo-dT for cDNA synthesis and then gene specific primers (Refer to subchapter 2.7.1). Six (At-RS31, RS31a, RS40, RS41, RS2Z32, RS2Z33) out of 18 SR genes were analysed in detail (Figure 17, 18, 19, 20, 21, 22).

4.1.1 At-RS31

At-RS31oe plants were generated by the expression of the fully spliced isoform (IS1) under the control of the strong constitutive CaMV35S promoter (previous unpublished results). The At-RS31 knockout line (SALK_021332) contains a T-DNA insertion in the fifth exon of At-RS31. To proof the effectiveness of the At-RS31ko_1 knockout line, specific primers were designed located in the second and sixth exon. Results obtained from the RT-PCR analysis show a strong overexpression of IS1 in At-RS31oe plants and a lack of products in the At-RS31ko_1 line, which confirms the nature of these lines (see below).

Exon 2 - Exon 6

A specific primer located in the second exon was designed to further analyse alternative splicing, as well as to proof the knockout effectiveness of the At-RS31ko_1 line. Besides the obvious lack of At-RS31 expression in the At-RS31ko_1 background, the patterns of expression and alternative splicing in untreated and treated samples are in agreement with the results obtained in the analysis of At-RS31 Exon 2 - Exon 4 (Figure 17).

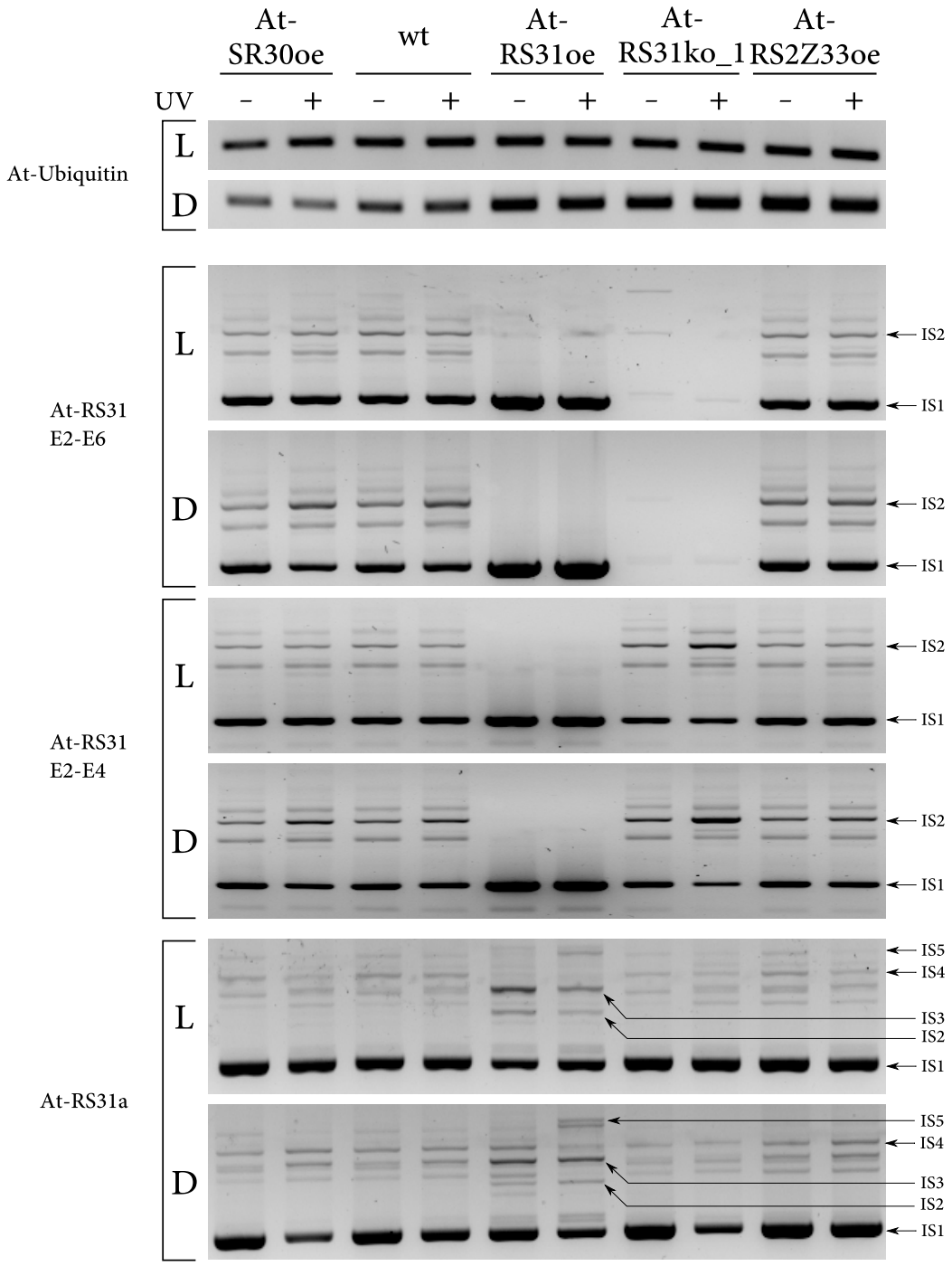

Figure 17: **Expression and splicing of At-Ubiquitin, At-RS31 and At-RS31a in *A.thaliana* upon UV-C irradiation.** Ten-days-old *A.thaliana* wild-type, At-SR30oe, At-RS31oe, At-RS31ko_1 and At-RS2Z33oe seedlings were irradiated with 100 J/m^2 UV-C. After irradiation, seedlings were either exposed to light or kept in the dark for additional 4 hours before total RNA was isolated and analysed via RT-PCR. For each treated sample, an untreated control sample was included. At-Ubiquitin served as a RT-PCR loading control. Genetic backgrounds are depicted on top of the figure, each represented by two lanes. UV-C treatment is represented by minus (-, untreated) and plus (+, treated). Gene names are on the left side of the figure. Every gene is represented by two agarose-gel pictures, differentiated by L (exposed to the light) and D (kept in the dark). Relevant splice isoforms are highlighted by black arrows and numbered IS 1-5. If not stated elsewhere, IS1 refers to the "correctly" spliced isoform, which generates the full-length protein. Abbreviations: (-) - untreated sample; (+) - treated sample; At - *Arabidopsis thaliana*; D - Dark; E - Exon; I - Intron; IS - Isoform; ko - knockout; L - Light; oe - overexpression; UV - Ultraviolet-C; wt - wild type (Col-0)

Exon 2 - Exon 4

As mentioned before, At-RS31 regulates the splicing patterns of genes situated in its own subfamily (unpublished). However, unlike At-RS2Z33, At-RS31 does not seem to regulate splicing of its own pre-mRNA, as was checked in HeLa splicing extracts and also in transient expression experiments conducted in *A.thaliana* protoplasts [75]. To share some more light on the autoregulation (or its absence) of At-RS31, RT-PCRs with primers to the second and fourth exons were performed. Result analysis shows that alternative splicing in the second intron of At-RS31 is not affected by a T-DNA-insertion mediated gene disruption in the fifth exon (Figure 17, compare untreated wild type and At-RS31ko_1 lanes). These findings point to the conclusion that the gene region upstream of the insertion contains all necessary *cis* signals, which are required to facilitate alternative splicing. Furthermore, the At-RS31 protein is not needed to regulate its own splicing.

Addtionally, when kept in the light, the expression and splicing pattern of At-RS31 shows no differences between non-irradiated and UV-C irradiated samples among wt (wild type), At-SR30oe and At-RS2Z33oe lines (Figure 17). However, when kept in the dark, irradiated samples among these genotypes show reduced expression of IS1 and an increase in IS2, proving that UV-C treatment was indeed effective. Interestingly, in the background of At-RS31ko_1, the effects of UV-C irradiation are more obvious since the ratio-change between IS1 and IS2 towards IS2 can already be observed in samples kept in the light and is even easier to observe within samples kept in the dark, which is in agreement with previous findings (Kalyna et al., unpublished).

Taken together, these results conclusively demonstrate the nature of the At-RS31 knockout- and overexpression lines. Moreover, the presented findings do not reflect autoregulation of At-RS31. Furthermore, regulation of At-RS31 by At-SR30 and At-RS2Z33 overexpression can not be observed, even though previous studies show that overexpression of At-SR30 [50] and At-RS2Z33 [75] affects splicing of At-RS31. Since these regulatory interactions could not be observed, the question on the effects of UV-C irradiation on this interplay is rendered mute.

4.1.2 At-RS31a

Untreated and treated samples of wt, At-SR30oe, AtRS31ko_1 and At-RS2Z33oe lines show no significant differences in the expression and splicing pattern of At-RS31a when kept in the light (Figure 17). Minor differences in alternative splicing of At-RS31a can be observed between plants overexpressing At-RS2Z33 and wild type plants. Also, At-RS31ko_1 plants show slight differences in the abundance of At-RS31a alternative splice variants in comparison to the wild type. On the contrary, when kept in the dark, UV-C treated samples show various results. In the wt background, IS1 is slightly reduced and IS3 mildly increased in the treated sample in comparison to the untreated one. The irradiated sample in the background of At-SR30oe shows a stronger ratio change from IS1 towards IS3 and IS4. The expression of IS1 is also reduced in the background At-RS31ko_1, however, there is no increase of any other alternative transcript evident, pointing to a reduced overall expression of At-RS31a rather than a change of transcript ratios. In the background of At-RS2Z33oe, no reduction of IS1 or increase of other alternative transcripts can be observed in UV-C treated samples when compared to untreated samples.

Untreated, as well as treated samples of At-RS31oe seedlings show significant changes when compared to other lines. When kept in the light, the untreated sample shows a reduced amount of IS1 and IS4 and an increased expression of IS2 and IS3 in comparison to the wt sample. When irradiated with UV-C, this splicing pattern changes towards an increase of IS1, as well as IS5 and a reduction of IS2 and IS3. When kept in the dark, the untreated sample shows a higher amount of IS1 and IS4 and a reduced amount of IS2 and IS3 in comparison to the light exposed sample. The treated sample expresses less IS1 and IS3 but elevated amounts of IS5 in comparison to the untreated sample kept in the dark. When compared to the treated sample kept in the light, the expression of IS1 is lower while the expression of IS3 and IS5 is higher.

Taken together, these results suggest that At-RS31a, the closest paralog to At-RS31 in this subfamily, behaves similiar to At-RS31 in respect to the reactions observed in the light and dark after UV-C irradiation. Furthermore, since the splicing patterns of At-RS31a appear to be basically identical between wild type and At-SR30oe plants, the conclusion can be drawn that At-SR30 does not affect splicing of At-RS31a. Additionally, splicing patterns of At-RS31a remain unchanged in plants overexpressing

At-RS2Z33 when treated with UV-C radiation, since treated and untreated samples behave similiar. The most obvious regulation of At-RS31a is executed by At-RS31. Moreover, this regulation is dependent on both light and dark conditions as well as UV-C treatment.

4.1.3 At-RS40 & At-RS41

Light exposed samples in wt, At-SR30oe, At-RS31ko_1 and At-RS2Z33oe background show no significant differences in the expression and alternative splicing pattern of At-RS40 between UV-C untreated and treated samples (Figure 18). When kept in the dark, untreated samples show a slight increase in IS2 and IS3, while treated samples show a small reduction in IS1, except for the treated sample in the background of At-RS2Z33oe.

Samples of the At-RS31oe line show dramatic changes in the expression and splicnig of At-RS40 in comparison to other genetic backgrounds. When kept in the light, the non-irradiated sample expresses IS1 on a very low level, while IS3, IS4 and IS5 show elevated amounts of transcripts. The irradiated sample shows an overall slightly decreased expression. The untreated sample, which was kept in the dark, shows an increased amount of IS1, IS2, IS3 and a reduced expression of IS4 and IS5 in comparison to the light exposed untreated sample. The treated sample kept in the dark shows a decreased amount of IS1 and IS2, but an increased amount of IS4.

UV-C non-irradiated, as well as irradiated samples with the genetic backgrounds of wt, At-SR30oe, At-RS31ko_1 and At-RS2Z33oe show no significant differences in expression or alternative splicing of At-RS41, regardless of the exposure to light or dark (Figure 18).

However, samples with the genetic background of At-RS31oe show differences. The light exposed untreated sample shows a decreased expression of IS1 and an increased expression of IS2, IS3 and IS4. When treated with UV-C, these splicing isoforms are slightly reduced in total. When the untreated sample is kept in the dark, the amount of IS1 transcripts is slightly elevated, while IS2, IS3 and IS4 transcripts are less prominent. When compared to this untreated sample, the UV-C irradiated sample kept in the dark shows a decrease of IS1 and an increase of IS2, IS3 and IS4. The

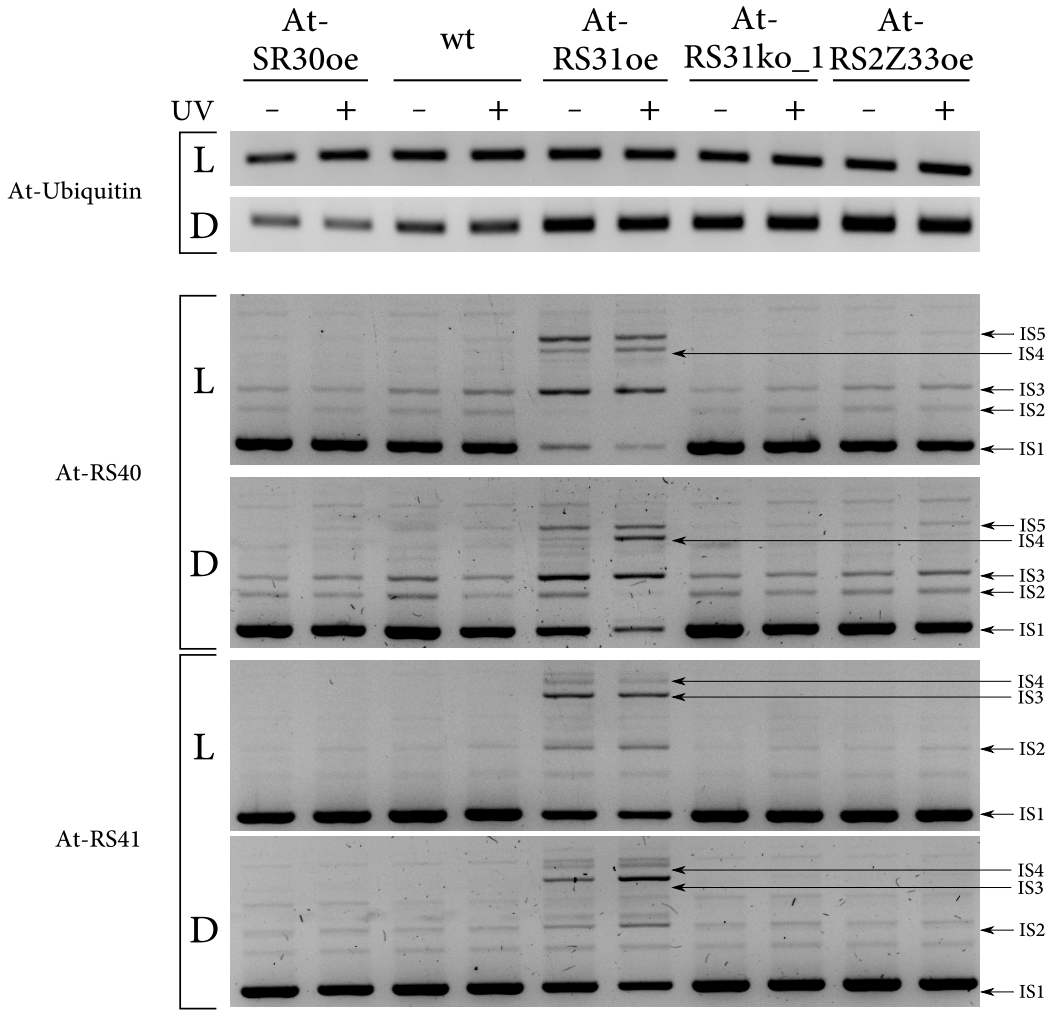

Figure 18: **Expression and splicing of At-Ubiquitin, At-RS40 and At-RS41 in *A.thaliana* upon UV-C irradiation.** For each treated sample, an untreated control sample was included. At-Ubiquitin served as a RT-PCR loading control. Genetic backgrounds are depicted on top of the figure, each represented by two lanes. UV-C treatment is represented by minus (-, untreated) and plus (+, treated). Gene names are on the left side of the figure. Every gene is represented by two agarose-gel pictures, differentiated by L (exposed to the light) and D (kept in the dark). Relevant splice isoforms are highlighted by black arrows and numbered IS 1-5. If not stated elsewhere, IS1 refers to the "correctly" spliced isoform, which generates the full-length protein. Abbreviations: (-) - untreated sample; (+) - treated sample; At - *Arabidopsis thaliana*; D - Dark; E - Exon; I - Intron; IS - Isoform; ko - knockout; L - Light; oe - overexpression; UV - Ultraviolet-C; wt - wild type (Col-0)

overall expression of this samples transcripts is higher in comparison to the treated sample exposed to light.

In conclusion, alternative splicing of At-RS40 and At-RS41 is not significantly affected by UV-C radiation in ten-days-old *A.thaliana* seedlings. Moreover, At-RS31 regulates splicing of both these genes. Also, this regulation is modulated in response to UV-C irradiation when kept in the dark, but not when exposed to the light.

4.1.4 At-RS2Z32 & At-RS2Z33

At-RS2Z32 and At-RS2Z33 are two paralogs, situated in the RS2Z subfamily. The At-RS2Z33oe line was generated by overexpression of the genomic clone (which contains all introns) under the control of the strong constitutive CaMV35S promoter. This line was shown to autoregulate splicing of both the endogenous and the transgenic version of At-RS2Z33 [49].

The expression and splicing pattern of At-RS2Z32 shows no significant differences when kept in the light or dark among the lines of At-SR30oe, wt, At-RS31oe and At-RS31ko_1 (Figure 19). Furthermore, there is no UV-C induced reduction of expression or changes in splicing observable.

However, in the background of At-RS2Z33oe, alternatively spliced transcript ratios change. The untreated sample exposed to the light shows a near 1:1 ratio between IS1 and IS2, while the treated sample shows an elevated amount of IS1 and a reduced amount of IS2. The non-irradiated and irradiated sample kept in the dark show an equal ratio between IS1 and IS2, with IS1 being more prominently expressed than IS2. When compared to the rest of the samples kept in the dark, IS1 seems to be lower expressed, while IS2, IS3 and IS4 show a slightly increased amount of transcripts.

The expression and splicing pattern of At-RS2Z33 is greatly affected in the background of At-RS2Z33oe (Figure 19). The untreated sample exposed to light shows very low amounts of IS1, while IS2, IS5, IS6 and especially IS3 and IS4 expression is increased in comparison to At-RS2Z33 expression in the remaining backgrounds. When irradiated with UV-C, the amount of IS1 is increased, while all other transcripts are being expressed less. The untreated sample kept in the dark shows a

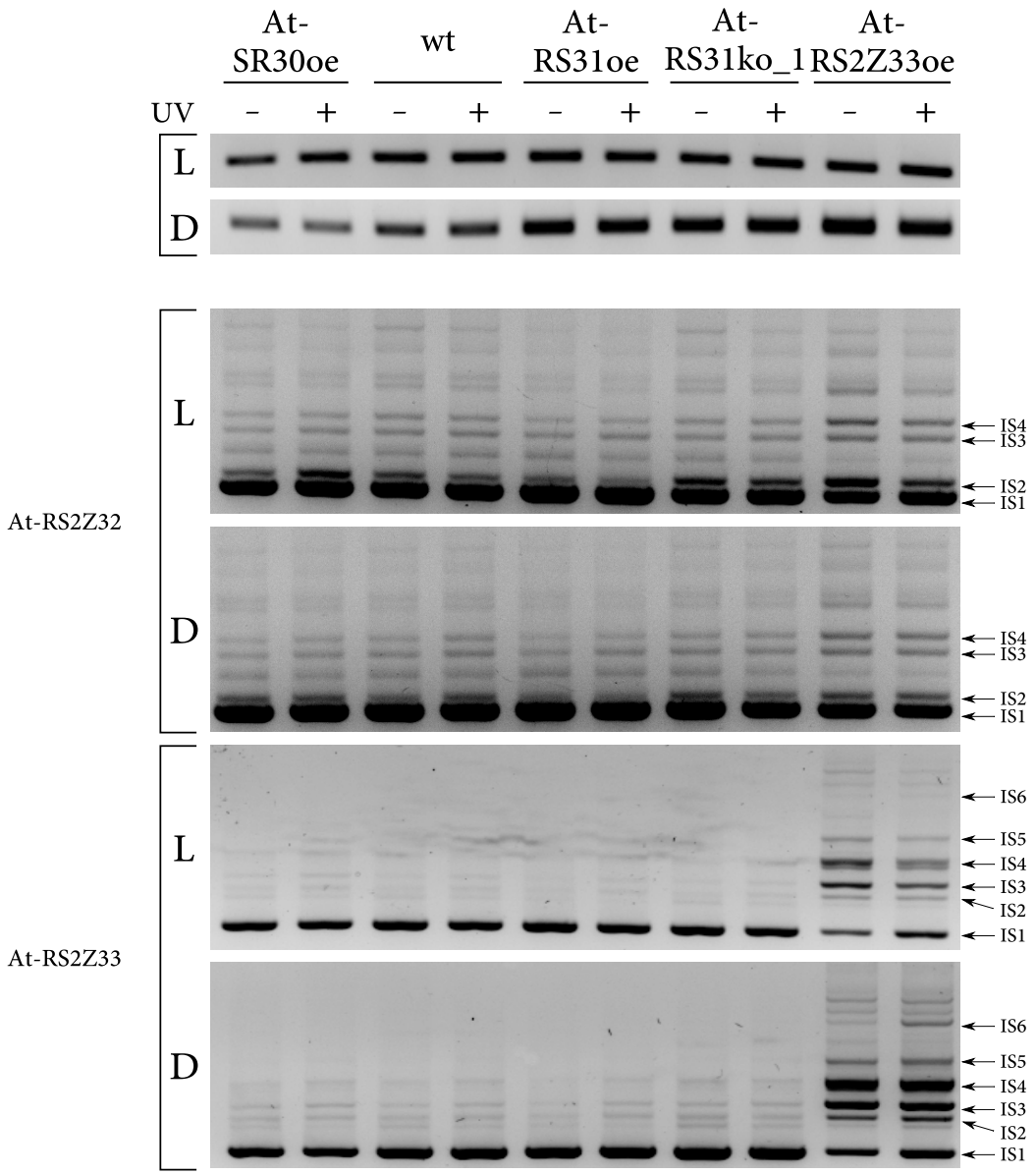

Figure 19: **Expression and splicing of At-Ubiquitin, At-RS2Z32 and At-RS2Z33 in *A.thaliana* upon UV-C irradiation.** For each treated sample, an untreated control sample was included. At-Ubiquitin served as a RT-PCR loading control. Genetic backgrounds are depicted on top of the figure, each represented by two lanes. UV-C treatment is represented by minus (-, untreated) and plus (+, treated). Gene names are on the left side of the figure. Every gene is represented by two agarose-gel pictures, differentiated by L (exposed to the light) and D (kept in the dark). Relevant splice isoforms are highlighted by black arrows and numbered IS 1-6. If not stated elsewhere, IS1 refers to the "correctly" spliced isoform, which generates the full-length protein. Abbreviations: (-) - untreated sample; (+) - treated sample; At - *Arabidopsis thaliana*; D - Dark; E - Exon; I - Intron; IS - Isoform; ko - knockout; L - Light; oe - overexpression; UV - Ultraviolet-C; wt - wild type (Col-0)

decreased amount of IS1 compared to other backgrounds, but at the same time IS1 is more prominently expressed than the untreated sample exposed to light. Further, IS2, IS3, IS4, IS5 and IS6 amounts are elevated compared to other backgrounds, as well as to the light exposed equivalent. When treated with UV-C, the levels of all mentioned transcripts even slightly increases.

In summary, splicing of At-RS2Z32 appears to be slightly changed towards alterantive transcripts in the background of At-RS2Z33oe, however UV-C irradiation does not affect these patterns, neither when exposed to light or when kept in the dark. At-RS2Z33 autoregulation is evident, as the expression and splicing pattern of this gene is significantly influenced in the At-RS2Z33oe line. Furthermore, UV-C radiation differentially influences autoregulation of At-RS2Z33 when exposed to the light or kept in the dark.

4.1.5 At-FPG1

At-FPG1 is a specific DNA glycosylase, which is implicated in the base excision repair process. DNA glycosylases typically scan the minor groove of the DNA for damage, which is subsequently removed upon detection. To date, at least six splice variants of At-FPG1 have been identified. Using alternative splicing RT-PCR panels [153], previous studies have shown that an overexpression of At-RS31 changes alternative splicing of At-FPG1 (unpublished).

Indeed, significant changes in the expression and splicing pattern of At-FPG1 can be observed with samples originating from the At-RS31oe background. The untreated sample, which was exposed to light, shows a decrease in IS1 and IS2 and an increase in IS3 and IS4. The UV-C treated sample shows a similar pattern, however its IS3 to IS4 ratio is inverted respective to the untreated sample. The untreated sample kept in the dark shows a similar expression of IS1 in comparison to other lines, but the amount of IS2 is slightly reduced while levels of IS3 and IS4 are elevated. The irradiated sample expresses a significant amount of IS3, while IS1 and IS4 amounts are lower when compared to its untreated pendant. Untreated, as well as treated samples of At-SR30oe, wt, At-RS31ko_1 and At-RS2Z33oe show no significant change in their expression of IS1 when kept in the dark or exposed to light (Figure 20). However, UV-C treated samples of these respective lines, which were kept in the dark, show a

slight increase in IS3 when compared to their untreated pendants. Interestingly, the RT-PCR product of approximately 370 bp (marked as IS3) did not match by size to any of the six described splice variants of At-FPG1. We were able to identify that this product originates from the transcript antisense to At-FPG1.

Taken together, these results show that expression and splicing of At-FPG1 is indeed changed in the presence of overexpressed At-RS31 protein. Moreover, these changes are even more prominent when UV-C treatment is applied.

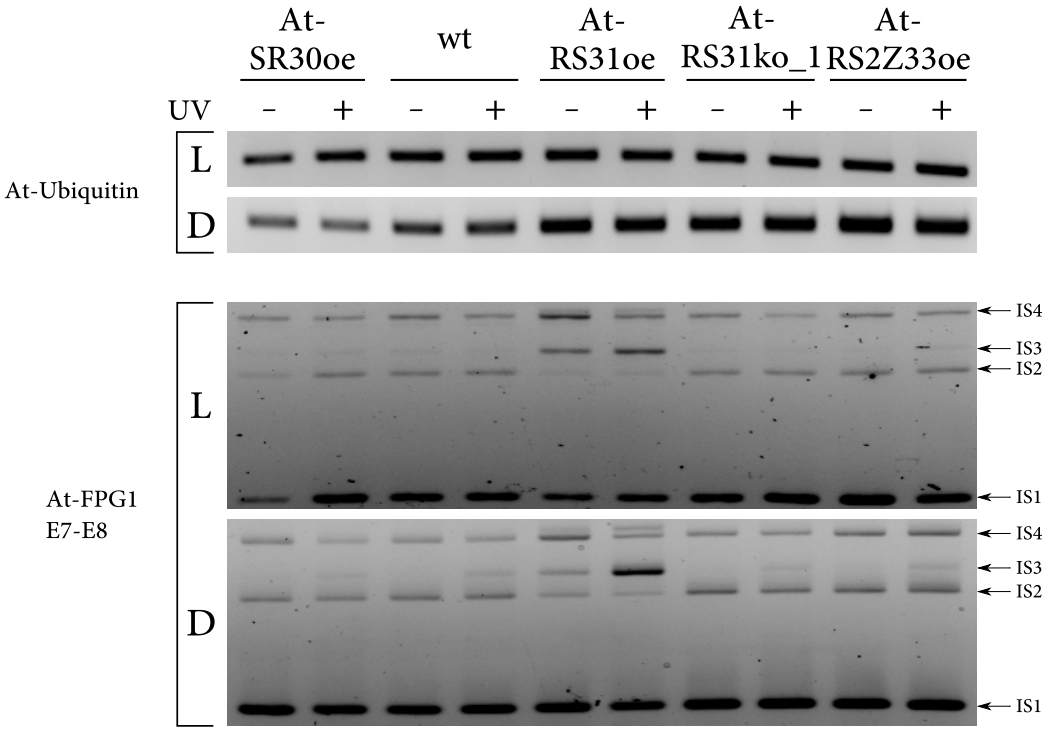

Figure 20: **Expression and splicing of At-Ubiquitin and At-FPG1 in *A.thaliana* upon UV-C irradiation.** For each treated sample, an untreated control sample was included. At-Ubiquitin served as a RT-PCR loading control. Genetic backgrounds are depicted on top of the figure, each represented by two lanes. UV-C treatment is represented by minus (-, untreated) and plus (+, treated). Gene names are on the left side of the figure. Every gene is represented by two agarose-gel pictures, differentiated by L (exposed to the light) and D (kept in the dark). Relevant splice isoforms are highlighted by black arrows and numbered IS 1-4. If not stated elsewhere, IS1 refers to the "correctly" spliced isoform, which generates the full-length protein. Abbreviations: (-) - untreated sample; (+) - treated sample; At - *Arabidopsis thaliana*; D - Dark; E - Exon; I - Intron; IS - Isoform; ko - knockout; L - Light; oe - overexpression; UV - Ultraviolet-C; wt - wild type (Col-0)

4.1.6 At-RAD1

At-RAD1 (also known as UVH1), a homolog of yeast RAD1 and human XPF, is a DNA repair exonuclease, which plays an integral part during the nucleotide excision repair mechanism. At-RAD1 is recruited to the site of damage with additional interacting proteins, like ERCC1 and XPG. Alternative splicing of At-RAD1 removes its ERCC1 interaction domain, which significantly influences the functional integrity of the protein isoform. Furthermore, a uvh1 mutant was identified in *A.thaliana*, which introduces a premature in-frame stop codon in the At-RAD1 gene, leading to the production of a protein isoform, which also lacks the ERCC1 interaction domain. Such mutant plants are unable to repair DNA damage in the dark [136]. In fact, the uvh1 mutant behaves almost identical, both on the molecular and phenotypical level, as plants overexpressing At-RS31 (Kalyna et al., unpublished).

Exon 5 - Exon 6

Non-irradiated and irradiated At-RS31oe samples express IS1 and IS2 in a 1:1 ratio while all other samples have an increased amount of IS1 in comparison to IS2. When kept in the dark, the untreated sample shows a decrease in IS2 while the UV-C treated one shows an enhanced amount of IS2 over IS1. Interestingly, treated samples of At-RS31ko_1 and At-RS2Z33oe overexpress At-RAD1 in comparison to the rest of the samples. Light exposed At-SR30oe, wt, At-RS31ko_1 and At-RS2Z33oe samples show no significant changes in the expression and splicing patterns of At-RAD1 (Figure 21).

In conclusion, At-RAD1 expression and splicing patterns do indeed differ in the background of an At-RS31 overexpression. Moreover, UV-C irradiation triggers a more prominent shift towards the alternative splice isoform (IS2) when kept in the dark in comparison to the light exposed samples, where the effects of UV-C treatment can not be observed. Additionally, At-RAD1 is clearly overexpressed in the plant lines At-RS31ko_1 and At-RS2Z33oe, however only when kept in the dark after UV-C irradiation.

Exon 7 - Exon 8

Expression and splicing patterns of At-RAD1 are alike along different genetic backgrounds (Figure 21). However, untreated At-RS31ko_1 and At-RS2Z33oe samples, which were kept in the dark show an increase in overall expression compared to other

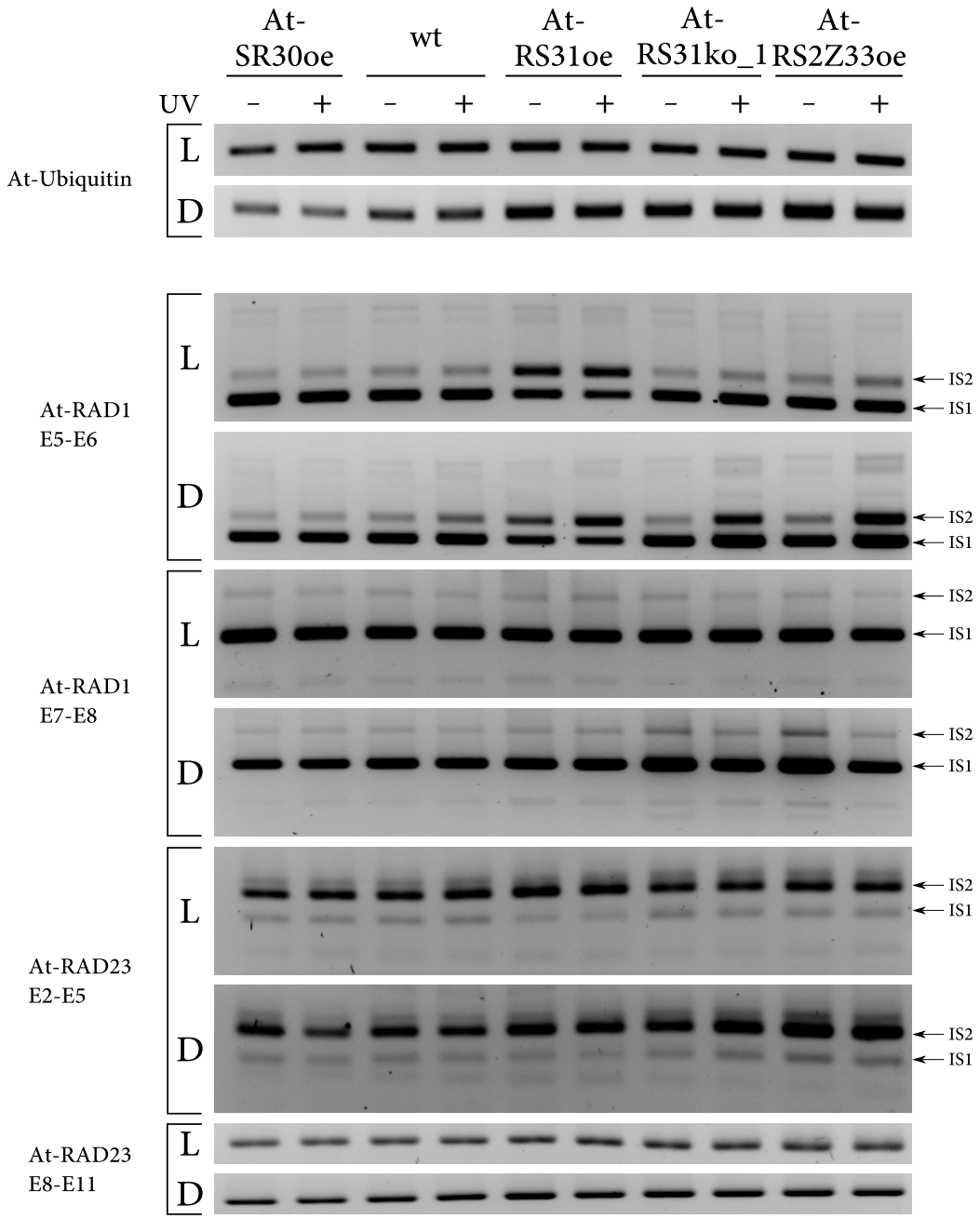

Figure 21: **Expression and splicing of At-Ubiquitin, At-RAD1 and At-RAD23 in *A.thaliana* upon UV-C irradiation.** For each treated sample, an untreated control sample was included. At-Ubiquitin served as a RT-PCR loading control. Genetic backgrounds are depicted on top of the figure, each represented by two lanes. UV-C treatment is represented by minus (-, untreated) and plus (+, treated). Gene names are on the left side of the figure. Every gene is represented by two agarose-gel pictures, differentiated by L (exposed to the light) and D (kept in the dark). Relevant splice isoforms are highlighted by black arrows and numbered IS 1-2. If not stated elsewhere, IS1 refers to the "correctly" spliced isoform, which generates the full-length protein. Abbreviations: (-) - untreated sample; (+) - treated sample; At - *Arabidopsis thaliana*; D - Dark; E - Exon; I - Intron; IS - Isoform; ko - knockout; L - Light; oe - overexpression; UV - Ultraviolet-C; wt - wild type (Col-0)

untreated samples. This expression is directly opposite to the pattern seen from the fifth to the sixth exon.

4.1.7 At-RAD23

At-RAD23 is a homolog of the hHR23b protein (see fig. 15), which is recruited during the nucleotide excision repair mechanism. It is a constituent of the Rad23B-XPC complex responsible for damage recognition in the global genome NER subpathway. Our previous studies, using the alternative splicing RT-PCR panel, have shown that an overexpression of At-RS31 slightly changes alternative splicing of this DNA repair gene (unpublished). The idea was to check whether UV treatment (as well as light and dark conditions) would enhance this effect.

Exon 2 - Exon 5

When exposed to light, untreated and treated At-RS31oe samples show a slightly higher amount of IS2 and lower amount of IS1 compared to other samples (Figure 21). None of the treated samples appear to show a lower expression of At-RAD23 due to UV-C. When kept in the dark, treated At-SR30oe, wt and At-RS31oe samples show a lower amount of IS2 compared to At-RS31ko_1 and At-RS2Z33oe. The latter samples appear to be overexpressed in comparison to the remaining samples and their light exposed pendants. The treated At-RS31ko_1 sample shows an elevated expression compared to the untreated sample and also compared to its expression in the light.

In short, slight changes in splicing towards the alternative transcript (IS2) can be observed in plants overexpressing At-RS31, both during light exposure and when kept in the dark. Additionally, alternative transcript levels are clearly elevated in the At-RS2Z33oe background.

Exon 8 - Exon 11

The expression and splicing pattern for At-RAD23 from the eighth to elenvth exon shows no significant differences between different samples or light/dark exposure (Figure 21).

4.1.8 Photolyases

We were interested in the expression levels of photolyases, since they are known to effectively repair UV induced DNA damage using photons, which are naturally only abundant during light conditions. At-PHR2, At-UVR2 and At-UVR3 are photolyases, which deal with differentially induced DNA damage through photoreactivation.

At-PHR2

UV-C treated, light exposed samples show a slightly diminished expression of At-PHR2 compared to untreated samples (Figure 22). When kept in the dark, expression levels are lower compared to light exposed samples, however no difference between irradiated and non-irradiated samples is evident.

At-UVR2

At-UVR2 expression is elevated in light exposed samples compared to dark exposed ones (Figure 22). UV-C treated samples show no reduction in expression compared to untreated samples, neither when exposed to light nor when kept in the dark.

At-UVR3

Expression of At-UVR3 is equivalent between light exposed and dark exposed samples (Figure 22). UV-C treated samples show a slight reduction of expression in comparison to untreated samples.

In short, no aberrant expression of these three different photolyase genes could be observed, neither in the light, nor in the dark (Figure 22).

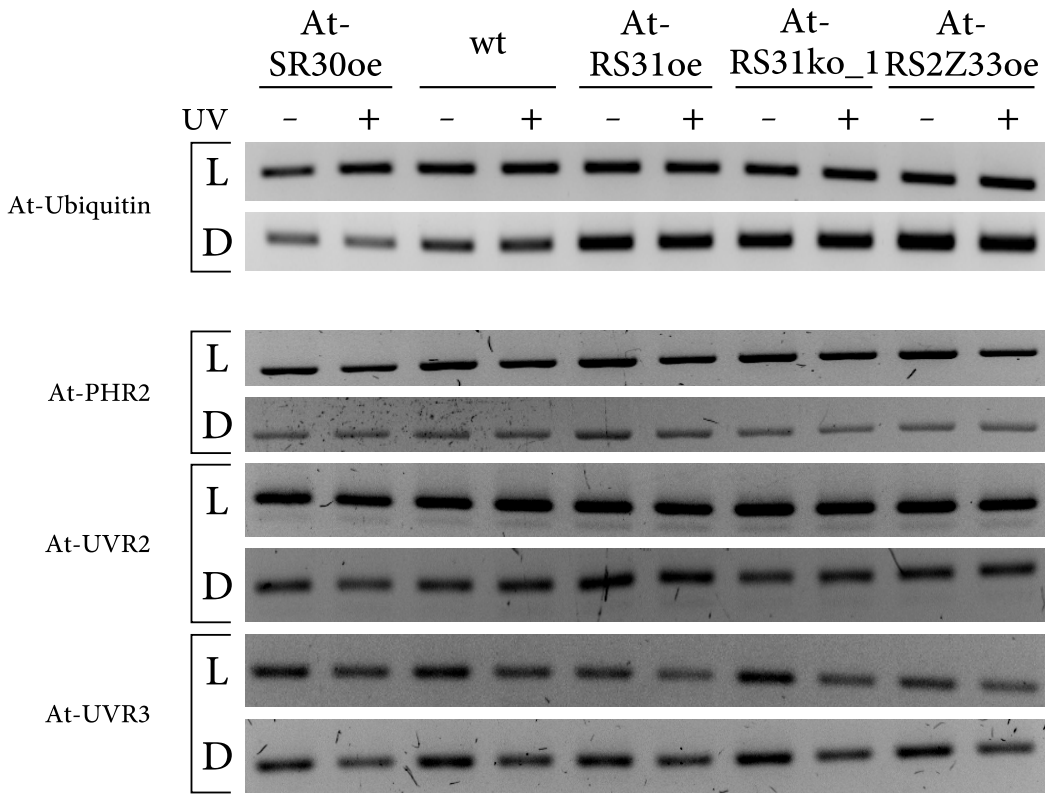

Figure 22: **Expression of At-Ubiquitin, At-PHR2, At-UVR2 and At-UVR3 in *A.thaliana* upon UV-C irradiation.** For each treated sample, an untreated control sample was included. At-Ubiquitin served as a RT-PCR loading control. Genetic backgrounds are depicted on top of the figure, each represented by two lanes. UV-C treatment is represented by minus (-, untreated) and plus (+, treated). Gene names are on the left side of the figure. Every gene is represented by two agarose-gel pictures, differentiated by L (exposed to the light) and D (kept in the dark). Abbreviations: (-) - untreated sample; (+) - treated sample; At - *Arabidopsis thaliana*; D - Dark; ko - knockout; L - Light; oe - overexpression; UV - Ultraviolet-C; wt - wild type (Col-0)

4.2 Analysis of the expression and splicing of SR- and DNA-repair genes in *P.patens* protonemal and gametophytal tissue upon UV-C irradiation

Previous studies have identified SR orthologs of the *A.thaliana* RS and RS2Z subfamilies in *Physcomitrella patens* and have been able to show that they indeed inherit highly conserved alternative splicing patterns [75]. After observing the impact of UV-C exposure on *A.thaliana*, we were eager to find out whether the regulation of gene expression and alternative splicing of SR and DNA repair genes differs in *Physcomitrella patens*. Therefore, two SR genes of *P.patens* were analysed; Pp-RS27 is orthologous to At-RS31, At-RS31a, At-RS40 and At-RS41 while Pp-RS2Z37 is orthologous to At-RS2Z32 and At-RS2Z33. Screening for orthologs of At-FPG1 and At-RAD1 revealed two RAD1-like and three FPG1-like genes in *P.patens*. After analysis of sequence and gene structure similarities, we termed the gene NW_001865259.1 Pp-RAD1 and NW_001865590.1 Pp-FPG1.

Five-days-old protonemal and four-months-old gametophytal wild-type tissues were exposed to 100 J/m^2 UV-C. Light exposed samples were collected after 0.5, one, two and four hours post treatment. Samples kept in the dark were collected after 0.5, two, four, eight and 24 hours post treatment. Total RNA was isolated and treated with DNase. RT-PCR analysis was carried out using oligo-dT for cDNA synthesis and then gene specific primers (Refer to subchapter 2.7.2).

4.2.1 Pp-RS27

In Pp-RS27, fifteen splice variants, all involving the second intron, have been identified (Maronova et al., unpublished). The expression and splicing pattern of Pp-RS27 shows significant differences both between protonemal and gametophytal tissues, non-irradiated and irradiated protonemal samples and between light exposed and dark kept samples (Figure 23). Untreated protonemal as well as gametophytal samples, which were transfered from light to dark conditions, show a splice isoform switch from the fully spliced IS1 towards the alternative IS2 transcript along 24 hours. This very same effect mediated by dark conditions on this alternative splicing pattern was

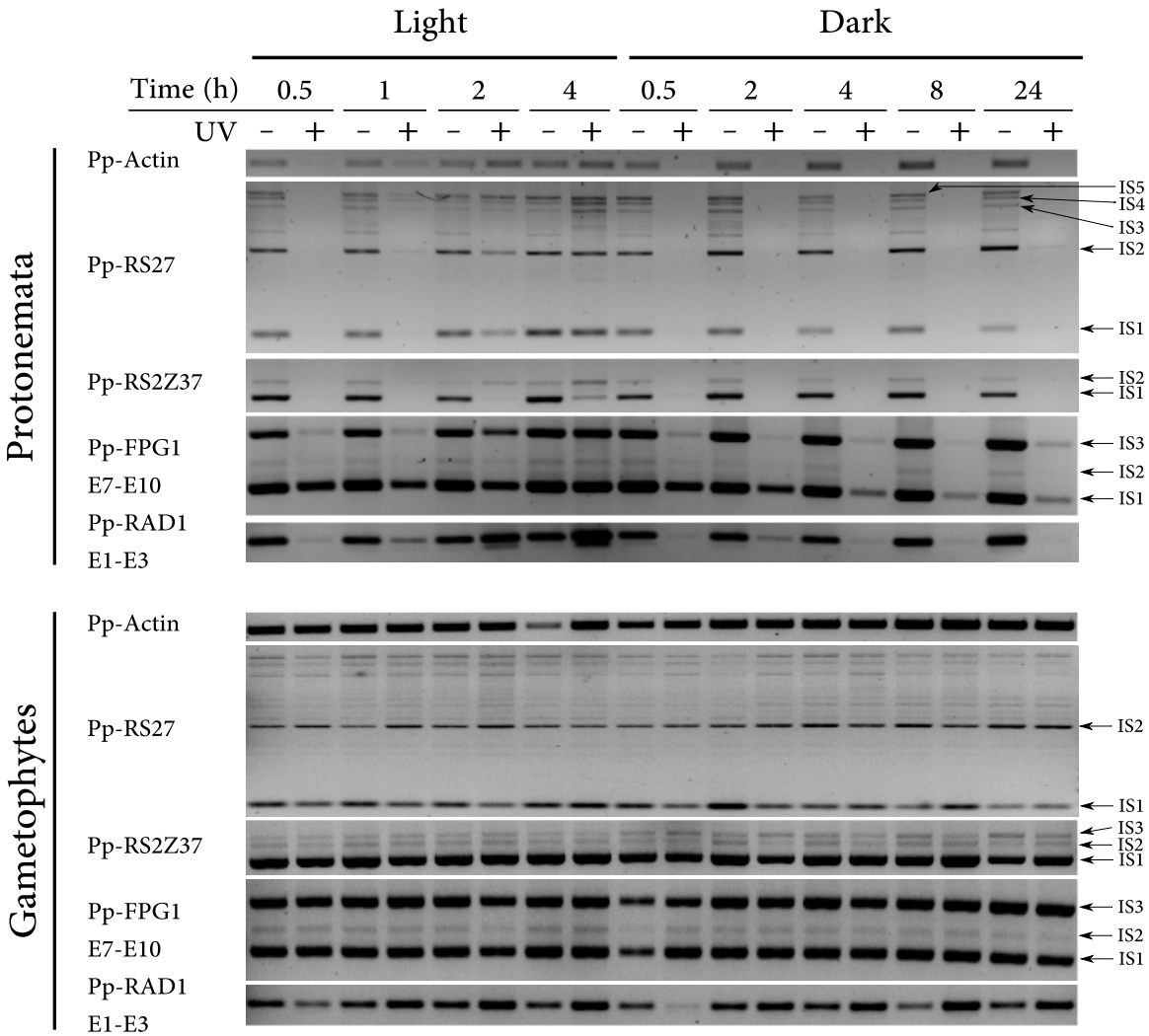

Figure 23: **Expression and splicing of SR and DNA repair genes in *P.patens* protonemal and gametophytal tissue upon UV-C irradiation.** Five-days-old *P.patens* wild-type protonemal and four-months-old *P.patens* wild type gametophytal tissues were irradiated with 100 J/m^2 UV-C. After irradiation, tissues were either exposed to light for 0.5, 1, 2, and 4 hours or kept in the dark for 0.5, 2, 4, 8 and 24 hours before total RNA was isolated and analysed via RT-PCR. For each treated sample, an untreated control sample was included. Pp-Actin served as a RT-PCR loading control. The phrase "Light" depicted on top of the figure enfolds the first eight, light exposed samples. The phrase "Dark" enfolds samples 9 to 18, which were kept in the dark. The elapsed time after UV-C exposure is given in hours and can be found beneath the previously mentioned phrases. UV-C treatment is represented by minus (-, untreated) and plus (+, treated). Gene names are on the left side of the figure, as are the tissue differentiations (Protonemata, Gametophytes). Every gene is represented by two agarose-gel pictures, directed to their respective tissues. Relevant splice isoforms are highlighted by black arrows and numbered IS 1-5. If not stated elsewhere, IS1 refers to the "correctly" spliced isoform, which generates the full-length protein. Abbreviations: (-) - untreated sample; (+) - treated sample; E - Exon; IS - Isoform; Pp - *Physcomitrella patens*; (h) - Time in hours; UV - Ultraviolet-C

observed in the *A.thaliana* ortholog of Pp-RS27, namely At-RS31 (Kalyna et al., unpublished). In contrast to the effect observed in *A.thaliana* seedlings, exposure of protonemal tissue to UV-C led almost to a complete shut down of Pp-RS27 expression. However, light exposed samples nearly recover to untreated levels after four hours, with slightly decreased IS1 and IS2 and increased IS3, IS4 and IS5 levels. Unexpectedly, expression of protonomal Pp-RS27 is not restored when samples are kept in the dark even for a longer period of time (24 hours).

However, exactly the same expression and splicing pattern of Pp-RS27 can not be observed in gametophytal tissue. The effects of UV-C treatment were rather mild and resembled the ones observed in *A.thaliana* seedlings. The treated, light exposed sample only shows a slight ratio change from IS1 towards IS2 after 0.5 hours, which slowly switches back to the ratio of the untreated sample as time reaches four hours. UV-treated samples, which were kept in the dark show similar mild dynamics of changes, while treated protonemal samples completely lack any sign of Pp-RS27 expression in these very conditions.

4.2.2 Pp-RS2Z37

Pp-RS2Z37 expression and alternative splicing properties in protonemal and gametophytal samples strongly resemble the patterns observed with Pp-RS27 (Figure 23). Protonemal samples kept in the dark completely lack expression of Pp-RS2Z37, while light exposed samples show a partial recovery four hours post UV-C exposure. At this time point, a 1:1 ratio between IS1 and IS2 can be observed while the untreated sample maintains a significantly higher level of IS1 compared to IS2.

On the contrary, gametophytal samples show no significant difference in expression and splicing of Pp-RS2Z37 between non-irradiated and irradiated samples. Interestingly though, gametophytes express an additional splice isoform of Pp-RS2Z37, which can only be vaguely recognized in the treated protonemal sample at four hours post treatment between IS1 and IS2.

4.2.3 Pp-FPG1

Pp-FPG1 is a DNA repair gene, therefore it is very interesting to note that it actually is expressed in treated protonemal tissue, whether it was kept in the dark or

exposed to light (Figure 23). 0.5 hours after UV-C treatment, the light exposed sample shows a significant decrease of splice isoform IS3 and IS1, which slowly recover to untreated levels four hours post treatment. Oddly enough, expression of Pp-FPG1 decreases over time in treated, dark exposed protonemal samples, but not in gametophytes. This said, it should be noted that UV-C treatment hardly shows any effect on expression and splicing of Pp-FPG1 at all in gametophytal samples.

4.2.4 Pp-RAD1

Pp-FPG1 and Pp-RAD1, both DNA-repair genes, are involved in different DNA-repair mechanisms. Thus it is very exciting to note that the expression of Pp-RAD1 differs from Pp-FPG1 (Figure 23). 0.5 hours after UV-C exposure, the protonemal sample exposed to light hardly shows any detectable levels of Pp-RAD1. However, one hour after treatment, recovery slowly starts and already reaches overexpression-levels two hours post UV-C irradiation. Additional two hours later, the amount of Pp-RAD1 has approximately doubled compared to the untreated sample. Following these events, it is intriguing to observe that Pp-RAD1 expression can hardly be detected in treated protonemal samples which were kept in the dark, while treated gametophytal samples show an overexpression of Pp-RAD1 already two hours post UV-C irradiation. Furthermore, in light exposed samples, Pp-RAD1 overexpression can be detected already one hour after UV-C treatment in comparison to two hours for protonemal samples.

In conclusion, these findings indicate that gametophytal *P.patens* tissues are significantly more robust and sturdier towards UV-C radiation than protonemal tissues. While expression levels dramatically drop in the latter tissues and only recover over a copious amount of time, expression levels remain almost unchanged in gametophytal tissues. Furthermore, the occurrence of alternative splicing events in UV-C treated samples is significantly higher in protonemal than in gametophytal tissues. While a transcriptional shutdown of Pp-RS27 and Pp-RS2Z37 can be observed in protonemal tissues, expression of the DNA-repair genes Pp-FPG1 and Pp-RAD1 prevails and even reaches overexpression-levels after four hours in light exposed conditions, which is in logical agreement to their roles in DNA damage response mechanisms. Interestingly, while Pp-FPG1 levels remain approximately the same in non-treated and treated samples in gametophytal tissues, Pp-RAD1 transcripts are already overex-

pressed after two hours, both in light and dark exposed conditions, most probably to cope with DNA damage inflicted by UV-C radiation.

4.3 UV-C mediated transcriptional shutdown in *P.patens* protonemal tissue kept in the dark is revertible through light exposure

We were curious to know whether UV-C exposed protonemal tissue, which was kept in the dark, could be rescued and returned to normal transcription levels through light exposure. Therefore, five-days-old protonemal wild type tissues were irradiated with 100 J/m^2 UV-C and kept in the dark for 24 hours. Afterwards, samples were returned to long-day conditions for 0.5, one, two, four, eight and 24 hours before collection. Total RNA was isolated and treated with DNase. RT-PCR analysis was carried out using oligo-dT for cDNA synthesis and then gene specific primers (Refer to subchapter 2.7.2).

Already 0.5 hours of light exposure are sufficient for treated protonemal tissue to restore transcription of Pp-RS27, Pp-RS2Z37 and Pp-RAD1 (Figure 24). Expression of these genes continues to increase after one and two hours before levels drop again after four and eight hours. However, 24 hours after the transfer to long-day conditions, treated samples even show an overexpression of Pp-RS27, Pp-RS2Z37 and Pp-RAD1 in comparison to untreated samples. However, it should be noted that, due to technical difficulties, this experiment was only done once and still awaits repetition for the sakes of a definite confirmation of the observed dynamic events.

4.4 Regulation of alternative splicing by SR proteins in *P.patens* protonemal and gametophytal tissues

Physcomitrella patens is one of few plant model organisms, which can be manipulated by gene targeting. Our lab was able to establish stable Pp-RS27 and Pp-RS2Z37

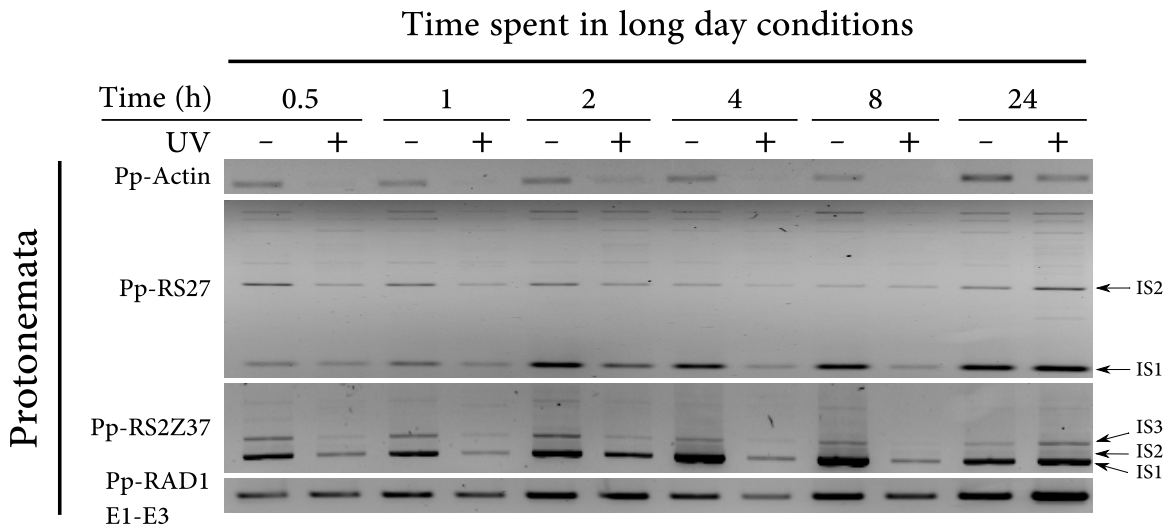

Figure 24: **Transcription recovery of UV-C exposed *P.patens* protonemal tissues through transfer to long-day conditions.** Five-days-old *P.patens* wild type protonemal tissues were irradiated with 100 J/m^2 UV-C. After irradiation, tissues were kept in the dark for 24 hours before transfer to long-day conditions for 0.5, 1, 2, 4, 8, and 24 hours. After sample collection, total RNA was isolated and analysed via RT-PCR. For each treated sample, an untreated control sample was included. Pp-Actin served as a RT-PCR loading control. The elapsed time after the transfer to long-day conditions is given in hours. UV-C treatment is represented by minus (-, untreated) and plus (+, treated). Gene names are on the left side of the figure, as is the tissue information (Protonemata). Every gene is represented by an agarose-gel picture. Relevant splice isoforms are highlighted by black arrows and numbered IS 1-3. If not stated elsewhere, IS1 refers to the "correctly" spliced isoform, which generates the full-length protein. Abbreviations: (-) - untreated sample; (+) - treated sample; E - Exon; IS - Isoform; Pp - *Physcomitrella patens*; (h) - Time in hours; UV - Ultraviolet-C

knockout-lines (Maronova, unpublished PhD Thesis). Thus, we were curious to find out whether the absence of these proteins would affect splicing of SR- and DNA-repair genes, since we have already shown above that modulating levels of At-RS31 (ortholog of Pp-RS27) in *A.thaliana* plants affects splicing patterns of DNA repair genes as well as of other SR genes.

Five-days-old protonemal and four-months-old gametophytal wild type, Pp-RS27ko and Pp-RS2Z37ko tissues were exposed to 100 J/m^2 UV-C. Light exposed samples were collected after 0.5, one, two and four hours post treatment. Samples kept in the dark were collected after 0.5, two, four, eight and 24 hours post treatment. Total RNA was isolated and treated with DNase. RT-PCR analysis was carried out using oligo-dT for cDNA synthesis and then gene specific primers (Refer to subchapter 2.7.2).

4.4.1 Analysis of protonemal tissues

Pp-RS27

Pp-RS27 expression and splicing patterns behave quite similar in the background of Pp-RS2Z37ko in comparison to the wild type control. However, IS3, IS4 and IS5 levels seem to be slightly elevated within knockout tissues (Figure 25).

Pp-RS2Z37

Expression and splicing patterns of Pp-RS2Z37 are almost identical between wild type control and Pp-RS27ko tissues (Figure 25). Again, visible differences are due to handling mistakes.

Pp-FPG1

The DNA repair gene Pp-FPG1 shows significant differences in expression and splicing patterns along wild type control, Pp-RS27ko and Pp-RS2Z37ko tissues (Figure 25). The overall expression of Pp-FPG1 is lowest in Pp-RS27ko-, intermediate in wild type control- and highest in Pp-RS2Z37ko-tissues. Non-irradiated samples of the wild type control show a higher amount of IS1 compared to IS3. This ratio seems to be even in both knockout backgrounds. Furthermore, IS2 levels are almost undetectable in Pp-RS27ko samples, while this splice isoform is clearly visible in untreated samples

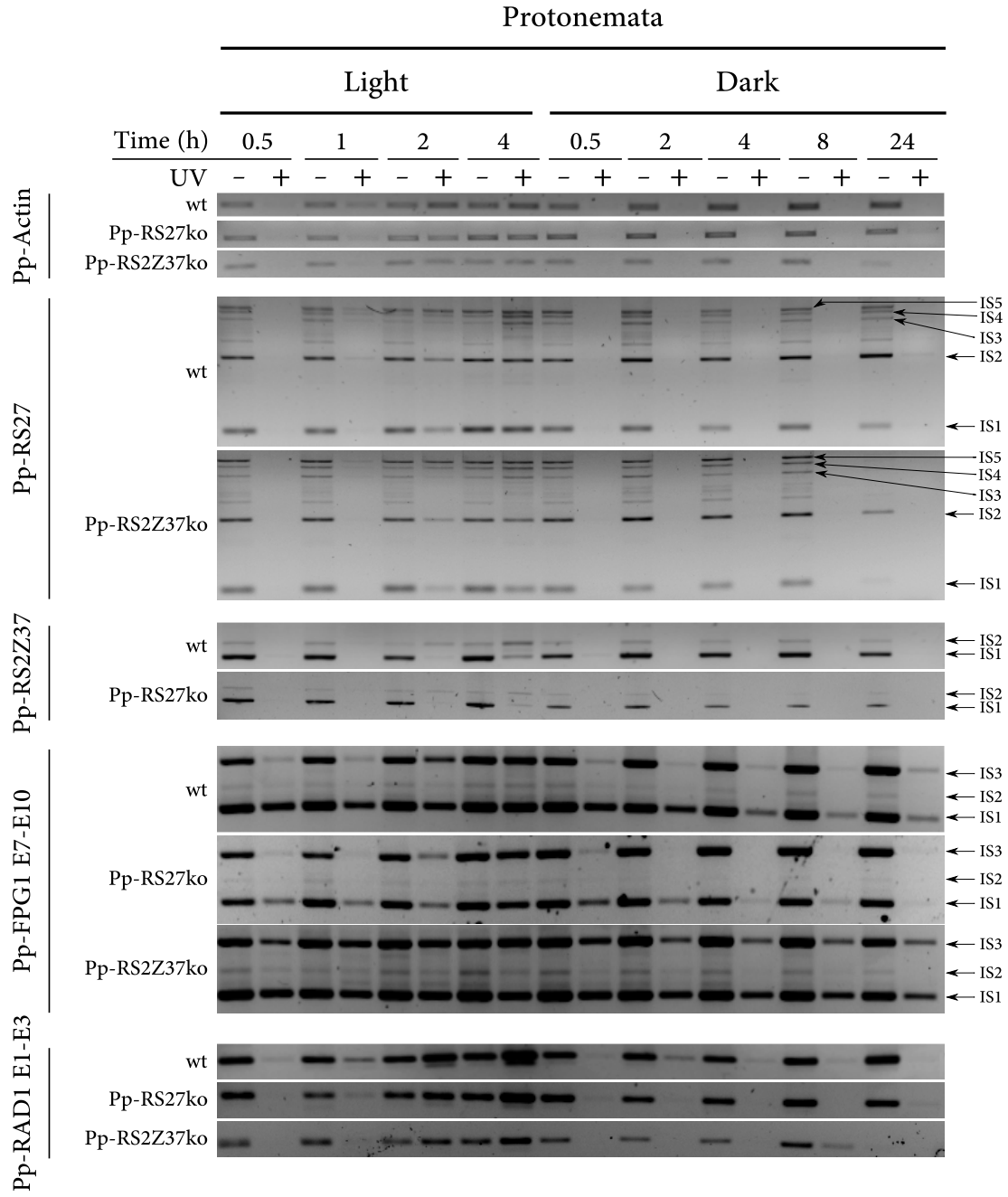

Figure 25: **Expression and splicing of SR and DNA repair genes in *P.patens* protonemal wild type, Pp-RS27ko and Pp-RS2Z37ko tissues upon UV-C irradiation.** For each treated sample, an untreated control sample was included. Pp-Actin served as a RT-PCR loading control. The phrase "Light" depicted on top of the figure enfolds the first eight, light exposed samples. The phrase "Dark" enfolds samples 9 to 18, which were kept in the dark. The elapsed time after UV-C exposure is given in hours and can be found beneath the previously mentioned phrases. UV-C treatment is represented by minus (-, untreated) and plus (+, treated). Gene names are positioned vertically on the far left side of the figure. Different genetic backgrounds of *P.patens* are positioned to the left of the agarose gel pictures. Relevant splice isoforms are highlighted by black arrows and numbered IS 1-5. If not stated elsewhere, IS1 refers to the "correctly" spliced isoform, which generates the full-length protein. Abbreviations: (-) - untreated sample; (+) - treated sample; E - Exon; IS - Isoform; ko - knockout; Pp - *Physcomitrella patens*; (h) - Time in hours; UV - Ultraviolet-C; wt - wild type

in both the wild type control and Pp-RS2Z37ko samples.

UV-C exposed samples, which were kept in the light, show recovery of expression from 0.5 hours to four hours post treatment. However, splice isoform levels differ greatly between these genetically different tissues. 0.5 hours after UV-C irradiation, IS1 and IS3 levels remain highest in Pp-RS2Z37 samples and decline along wild-type and Pp-RS27ko samples. As described before (Refer to subchapter 4.3.3), Pp-FPG1 expression steadily drops in samples kept in the dark along 24 hours post treatment while they remain even in untreated samples. At this time point however, splice isoforms are almost undetectable in Pp-RS27ko samples, while they are clearly present in wild type and especially in Pp-RS2Z37ko specimen.

Pp-RAD1

No significant differences in the expression and splicing of Pp-RAD1 are noteworthy between wild type and Pp-RS27ko samples (Figure 25). What should be noted are the low levels of Pp-RAD1 expression in Pp-RS2Z37ko specimen, since the expression of Pp-FPG1 was significantly enhanced among these samples.

Taken together, the data presented here indicates that Pp-RS27 and Pp-RS2Z37 are not connected in a regulatory way, which is in agreement to the events observed with the SR orthologs in ten-days-old *A.thaliana* seedlings. However, Pp-FPG1 shows obvious changes in expression and alternative splicing in the Pp-RS27ko and Pp-RS2Z37ko backgrounds in protonemal tissues. While changes in splicing of At-FPG1 were observed in *A.thaliana* plants overexpressing At-RS31, no changes were observed in At-RS31 knockout plants. Furthermore, plants overexpressing At-RS2Z33 did not show altered expression and splicing levels of At-FPG1. Therefore, it would be interesting to work on *P.patens* lines, which overexpress Pp-RS27 and Pp-RS2Z37 to analyse whether the regulatory interactions between SR and DNA repair genes significantly differ between *A.thaliana* and *P.patens*, at least in protonemal tissues.

4.4.2 Analysis of gametophytal tissues

Pp-RS27

As in protonemal tissues, the levels of the splice isoforms IS3, IS4 and IS5 are elevated in Pp-RS2Z37ko samples compared to the wild type controls (Figure 26). Additionally, the expression of IS2 is higher than IS1 along untreated as well as treated Pp-RS2Z37ko samples, which is a clear difference to wild type specimen.

Pp-RS2Z37

Expression and splicing patterns of Pp-RS2Z37 appear to be similar between wild type and Pp-RS27ko samples (Figure 26). There are no noteworthy differences to be mentioned.

Pp-FPG1

Pp-FPG1 expression and splicing differs greatly among the different genetic backgrounds tested (Figure 26). While the splice isoform IS2 is still visible in wild type tissues, it is hardly detectable in Pp-RS27ko samples and elusive in Pp-RS2Z37ko samples (indicated by grey arrow). Furthermore, the ratio of IS1 to IS3 is roughly 1:1 in wild-type samples. However, this ratio starts to slightly shift towards IS3 in Pp-RS27ko samples and is completely biased towards IS3 in Pp-RS2Z37ko samples.

Pp-RAD1

Expression of Pp-RAD1 is lowest in Pp-RS2Z37ko samples and equal among wild type and Pp-RS27ko tissues (Figure 26).

In conclusion, the regulatory interactions between Pp-RS27 and Pp-RS2Z37 appear to be similar in gametophytal tissues, no significant changes can be observed in comparison to protonemal samples. However, as in protonemal tissues, the expression and splicing pattern of Pp-FPG1 is significantly different between wild type, Pp-RS27ko and Pp-RS2Z37ko samples, which is yet another reason to work on overexpression lines in *P.patens* to unravel the regulatory mechanisms behind these events.

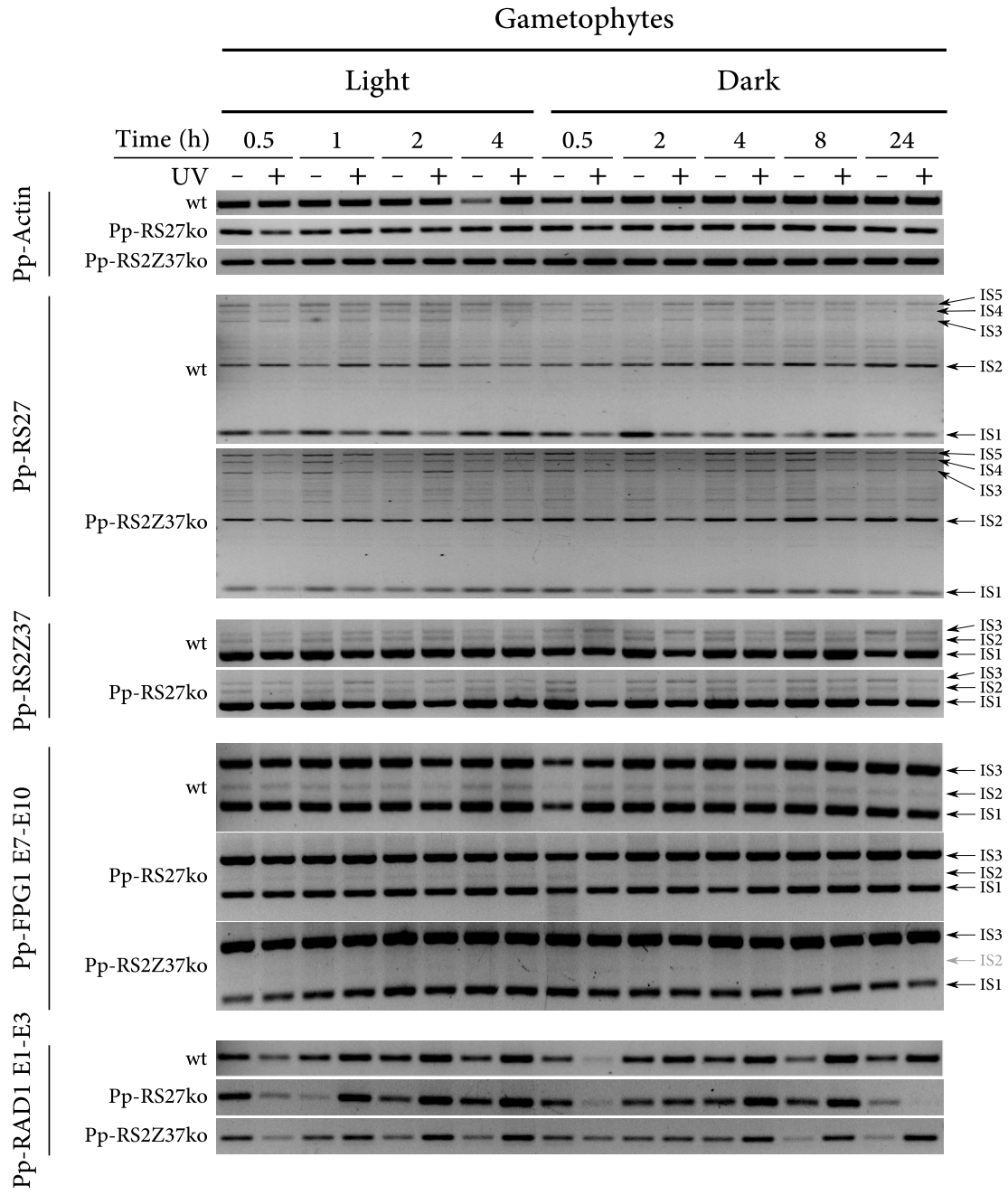

Figure 26: **Expression and splicing of SR and DNA repair genes in *P.patens* gametophytal wild type, Pp-RS27ko and Pp-RS2Z37ko tissues upon UV-C irradiation.** For each treated sample, an untreated control sample was included. Pp-Actin served as a RT-PCR loading control. The phrase "Light" depicted on top of the figure enfolds the first eight, light exposed samples. The phrase "Dark" enfolds samples 9 to 18, which were kept in the dark. The elapsed time after UV-C exposure is given in hours and can be found beneath the previously mentioned phrases. UV-C treatment is represented by minus (-, untreated) and plus (+, treated). Gene names are positioned vertically on the far left side of the figure. Different genetic backgrounds of *P.patens* are positioned to the left of the agarose gel pictures. Relevant splice isoforms are highlighted by black arrows and numbered IS 1-5. If not stated elsewhere, IS1 refers to the "correctly" spliced isoform, which generates the full-length protein. Abbreviations: (-) - untreated sample; (+) - treated sample; E - Exon; IS - Isoform; ko - knockout; Pp - *Physcomitrella patens*; (h) - Time in hours; UV - Ultraviolet-C; wt - wild type

4.5 A combination of UV-C exposure and sucrose-starvation further increases alternative splicing events in *A.thaliana* cell suspension cultures

After observing the effects of UV-C irradiation on *P.patens* protonemal tissues (e.g. transcriptional shutdown), we were eager to find out whether *A.thaliana* behaves in a similar way. Since protonemal tissue is merely a cell layer, we could not compare the data to seedlings or fully grown plants. Thus we needed to analyse *A.thaliana* cells on an analogue level; cell suspension cultures. Unlike *P.patens* cultures, which grow on sucrose-free media, *A.thaliana* cell culture medium contains sucrose. Therefore, we added sucrose depletion as an additional stress factor to analyse possible accumulating effects on alternative splicing events.

Therefore, five-days-old *A.thaliana* wild type cell suspension culture (HH1, originated from seedlings, Col-0 ecotype), incubated in either sucrose containing or sucrose free medium (refer to subchapter 3.2.10), were exposed to 100 J/m^2 UV-C. Light exposed samples were collected after 0.5, one, two and four hours post treatment. Samples kept in the dark were collected after 0.5, two, four, eight and 24 hours post treatment. Total RNA was isolated and treated with DNase. RT-PCR analysis was carried out using oligo-dT for cDNA synthesis and then gene specific primers (Refer to subchapter 2.7.1).

Observations have shown that the general level of gene expression is reduced in sucrose depleted *A.thaliana* cell suspension cultures. Thus, this analysis will solely focus on significant differences in alternative splicing caused by the combined stress factors of UV-C exposure and sucrose depletion.

Before the analysis of each gene follows, it should be mentioned that no similar effect to the transcriptional shutdown observed in *P.patens* was detected in this experimental setup with *A.thaliana* cell suspension cultures.

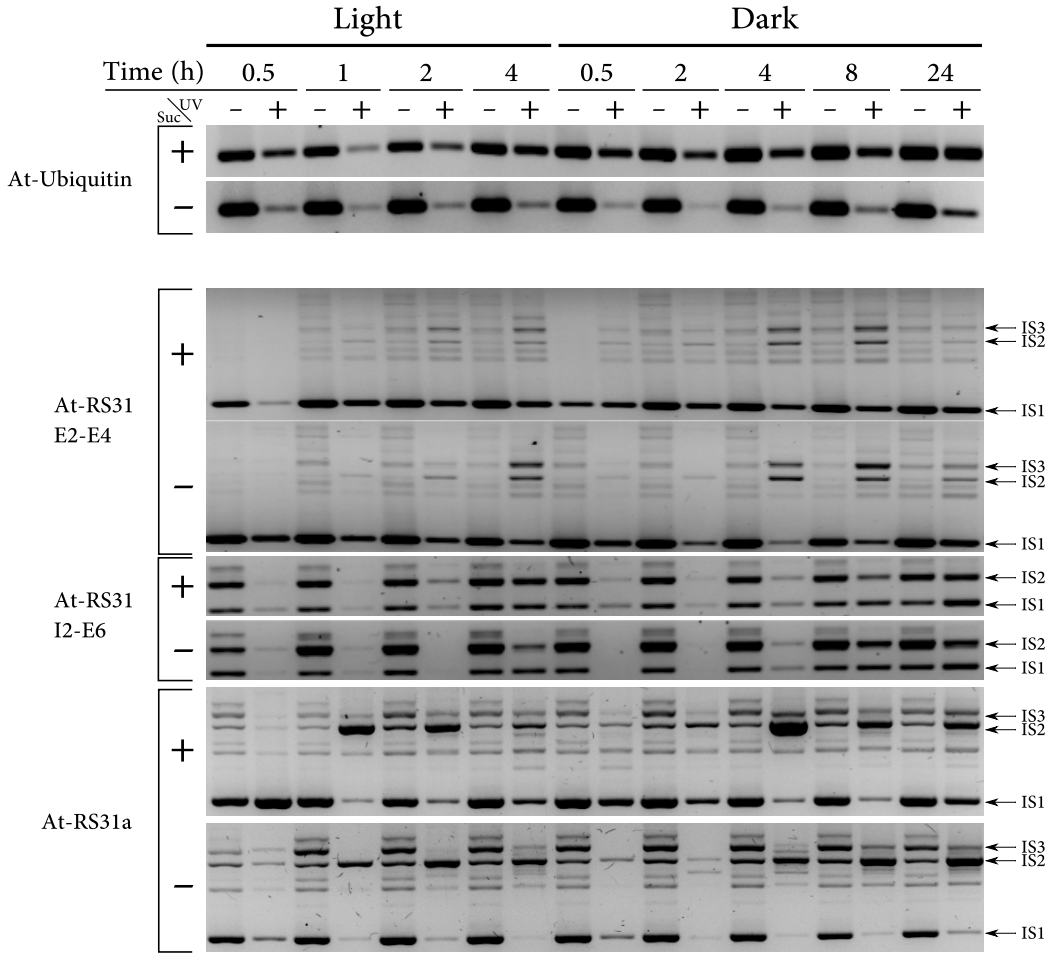

Figure 27: **Expression and splicing of At-RS31 and At-RS31a in *A.thaliana* cell suspension cultures upon UV-C irradiation.** Five-days-old *A.thaliana* wild type cell suspension cultures (HH1, seedling origin, Col-0 ecotype) were incubated for additional 24 hours in either 1% or 0% sucrose containing media before exposure to 100 J/m^2 UV-C. After irradiation, cells were either exposed to light for 0.5, 1, 2, and 4 hours or kept in the dark for 0.5, 2, 4, 8 and 24 hours before total RNA was isolated and analysed via RT-PCR. For each treated sample, an untreated control sample was included. At-Ubiquitin served as a RT-PCR loading control. The phrase "Light" depicted on top of the figure enfolds the first eight, light exposed samples. The phrase "Dark" enfolds samples 9 to 18, which were kept in the dark. The elapsed time after UV-C exposure is given in hours and can be found beneath the previously mentioned phrases. UV-C treatment is represented by horizontally arranged minus (-, untreated) and plus (+, treated) symbols. Whether the final media contained sucrose or not is depicted by vertically arranged minus (-, no sucrose) and plus (+, sucrose) symbols. Gene names can be found on the left side of the figure. Every gene is represented by two agarose-gel pictures, one for sucrose supplemented and one for sucrose free samples. Relevant splice isoforms are highlighted by black arrows and numbered IS 1-3. If not stated elsewhere, IS1 refers to the "correctly" spliced isoform, which generates the full-length protein. Abbreviations: (-) - untreated sample; (+) - treated sample; At - *A.thaliana*; E - Exon; IS - Isoform; (h) - Time in hours; I - Intron; Suc - Sucrose; UV - Ultraviolet-C

4.5.1 At-RS31

Exon 2 - Exon 4

Two hours after UV-C irradiation, the sucrose supplemented sample, which was kept in the light, shows a higher level of IS1, IS2 and IS3 than the sucrose depleted one (Figure 27). However, four hours after treatment, while the ratios stay quite similar in the sucrose supplied sample, IS2 and IS3 are significantly increased in the sucrose free sample. The same principle can be converted to samples kept in the dark. While the expression of IS1 remains more prominent in sucrose supplemented, irradiated samples, IS2 and IS3 levels are elevated in sucrose depleted samples. Handling mistakes are responsible for reduced signals in the second and ninth lane of sucrose supplemented samples.

Intron 2 - Exon 6

Untreated, sucrose depleted samples show a significantly higher level of IS2 splice isoforms than sucrose supplemented samples, regardless of light or dark exposure (Figure 27). Apart from this observation, no obvious changes in splicing patterns are occurring, other than the reduced levels of gene expression in sucrose depleted samples.

Taken together, these results show that the effect of UV-C irradiation on alternative splicing of At-RS31 is significantly stronger in *A.thaliana* cell suspension cultures in comparison to ten-days-old seedlings. Furthermore, these findings indicate that alternative splicing levels are further elevated due to sucrose depletion mediated stress. Moreover, sucrose depleted samples seem to recover at slower rates compared to sucrose supplemented ones.

4.5.2 At-RS31a

In general, sucrose depleted, untreated samples show elevated levels of IS2 and IS3 and decreased amounts of IS1 transcripts in comparison to sucrose supplemented samples (Figure 27). An interesting phenomenon can be observed in UV-C irradiated, sucrose supplemented samples kept in the light. 0.5 hours after treatment, IS1 levels are significantly elevated in comparison to its untreated pendant, while the sucrose free sample shows a lower expression of IS1 when compared to its untreated control.

However, one hour post irradiation, IS1 is rapidly degraded while IS2 expression is significantly increased in the sucrose supplemented sample. Along two and four hours after treatment, IS2 levels decrease while at the same time IS1 levels start to recover. In sucrose depleted samples, this recovery process is not taking place, IS2 levels stay approximately the same even four hours after irradiation. Sucrose supplemented samples, which were irradiated and kept in the dark, show a degradation-to-recovery scheme from 0.5 to 24 hours after treatment. IS1 expression drops until eight hours after irradiation and recovers slightly after 24 hours. Simultaneously, IS2 levels first increase after four hours and then steadily drop until 24 hours post irradiation. Sucrose depleted samples show only a very slow recovery process with slightly enhancing IS1 levels along time, while IS2 and IS3 levels basically remain constant.

The expression and splicing patterns of At-RS31a clearly demonstrate a dynamic process of generation and degradation of splice variants along the recovery process from UV-C treatment and sucrose depletion. As with the expression of At-RS31, sucrose depleted samples recover slower than sucrose supplemented ones.

4.5.3 At-RS40 & At-RS41

Untreated, sucrose free samples show decreased At-RS40 IS1 and increased IS2 and IS3 levels compared to sucrose supplemented specimen (Figure 28). When UV-C irradiated, recovery is almost non-existent in sucrose depleted samples, no matter if they were exposed to light or kept in the dark while sucrose supplemented samples show steady recovery along time. Other than that, no significant changes in splicing occur when sucrose depletion stressed samples are exposed to UV-C in comparison to sucrose supplemented samples.

Expression and splicing patterns of At-RS41 appear to be fairly equal between sucrose supplemented and depleted samples, besides afore mentioned decreases in overall gene expression (Figure 28). Though it should be noted that four hours after UV-C exposure, the ratio between IS1 and IS2 in light exposed, sucrose supplemented samples is approximately 2:1 while it is 1:1 in sucrose depleted samples.

In summary, the recovery rates of sucrose supplemented and depleted samples post UV-C irradiation are in agreement with the previously mentioned results. Interest-

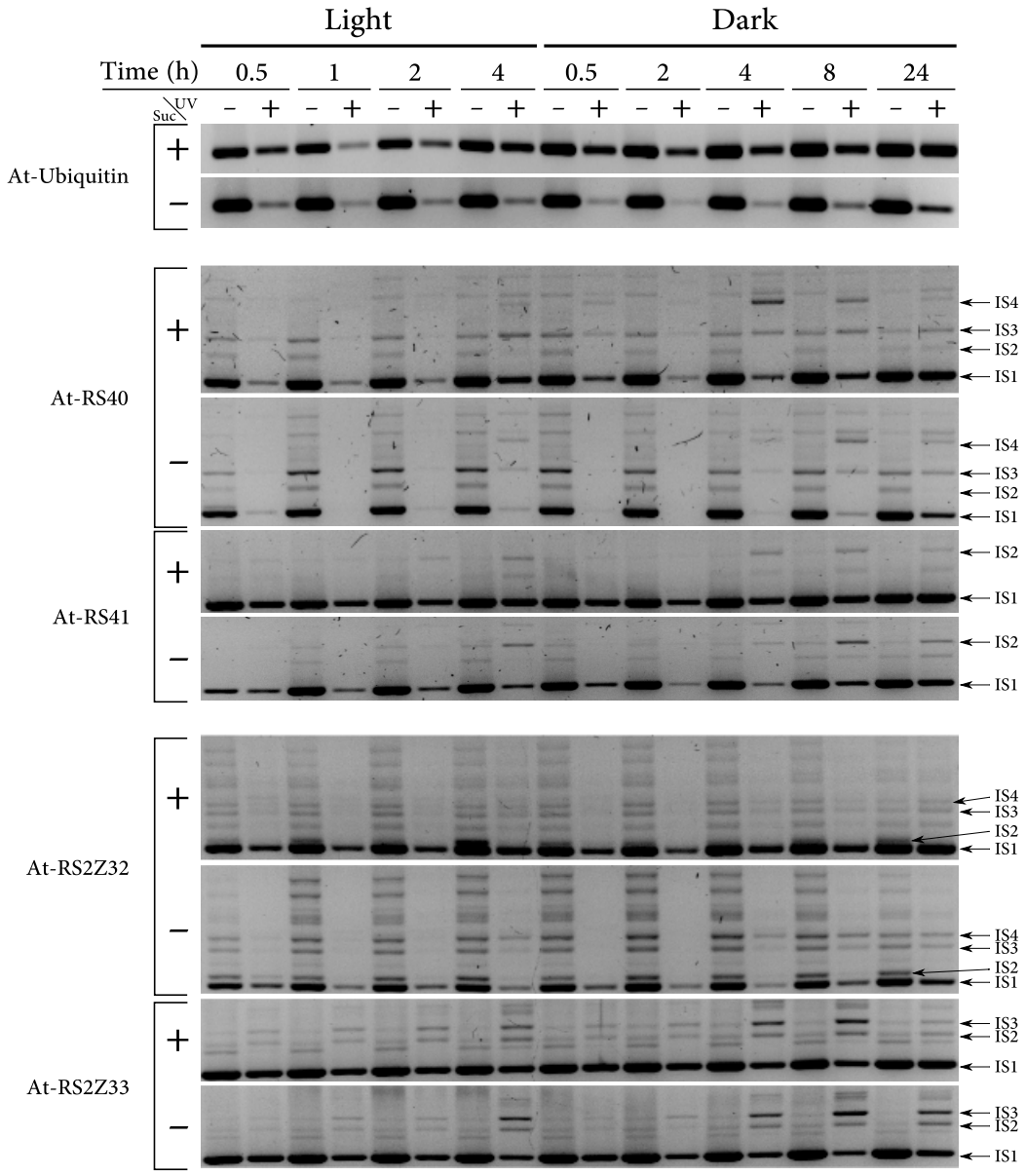

Figure 28: **Expression and splicing of At-RS40, At-RS41, At-RS2Z32 and At-RS2Z33 in *A.thaliana* cell suspension cultures upon UV-C irradiation.** At-Ubiquitin served as a RT-PCR loaiding control. The phrase "Light" depicted on top of the figure enfolds the first eight, light exposed samples. The phrase "Dark" enfolds samples 9 to 18, which were kept in the dark. The elapsed time after UV-C exposure is given in hours and can be found beneath the previously mentioned phrases. UV-C treatment is represented by horizontally arranged minus (-, untreated) and plus (+, treated) symbols. Whether the final media contained sucrose or not is depicted by vertically arranged minus (-, no sucrose) and plus (+, sucrose) symbols. Gene names can be found on the left side of the figure. Every gene is represented by two agarose-gel pictures, one for sucrose supplemented and one for sucrose free samples. Relevant splice isoforms are highlighted by black arrows and numbered IS 1-4. If not stated elsewhere, IS1 refers to the "correctly" spliced isoform, which generates the full-length protein. Abbreviations: (-) - untreated sample; (+) - treated sample; At - *A.thaliana*; E - Exon; IS - Isoform; (h) - Time in hours; I - Intron; Suc - Sucrose; UV - Ultraviolet-C

ingly, the expression of At-RS41 seems to be more resilient towards UV-C treatment than the expression of At-RS40. Furthermore, untreated and sucrose depleted samples show an almost identical expression of At-RS41 compared to sucrose supplemented, untreated samples while At-RS40 expression is shifted towards alternative splice isoforms in similar samples.

4.5.4 At-RS2Z32 & At-RS2Z33

Sucrose supplemented, untreated samples show a higher expression of At-RS2Z32 IS1 and reduced levels of IS2, IS3 and IS4 compared to sucrose depleted samples (Figure 28). Upon UV-C treatment, a depletion of splice isoforms IS2, IS3 and IS4 occurs in both sucrose supplemented and depleted samples. Additionally, recovery of IS1 is slowed down in sucrose free samples.

Expression of the At-RS2Z33 splice isoforms IS1, IS2 and IS3 is slightly enhanced in untreated, sucrose supplement samples (Figure 28). When exposed to UV-C, IS2 and IS3 levels are up- and IS1 levels down-regulated in sucrose free samples when compared to sucrose supplemented samples.

In conclusion, alternative splicing is clearly more prominent in untreated sucrose depleted samples in comparison to sucrose supplemented ones, both for the expression of At-RS2Z32 and At-RS2Z33. Unlike in ten-days-old seedlings, UV-C treatment leads to a clearly elevated level of At-RS2Z33 alternative splice isoforms.

4.5.5 At-SR30 & At-SR34

Untreated, sucrose supplemented samples show a higher expression of At-SR30 IS1 and lower expression of IS2 and IS3 than sucrose free ones (Figure 29). Additionally, as described before, recovery rates of IS1 are lower in sucrose depleted samples upon UV-C irradiation in comparison to sucrose supplemented specimen. Besides that, splicing patterns do not show significantly aberrant changes.

Interestingly, expression of At-SR34 is higher in sucrose free samples than in sucrose supplemented samples, regardless of UV-C treatment (Figure 29).

Taken together, these findings are slightly opposing. While the expression and splicing

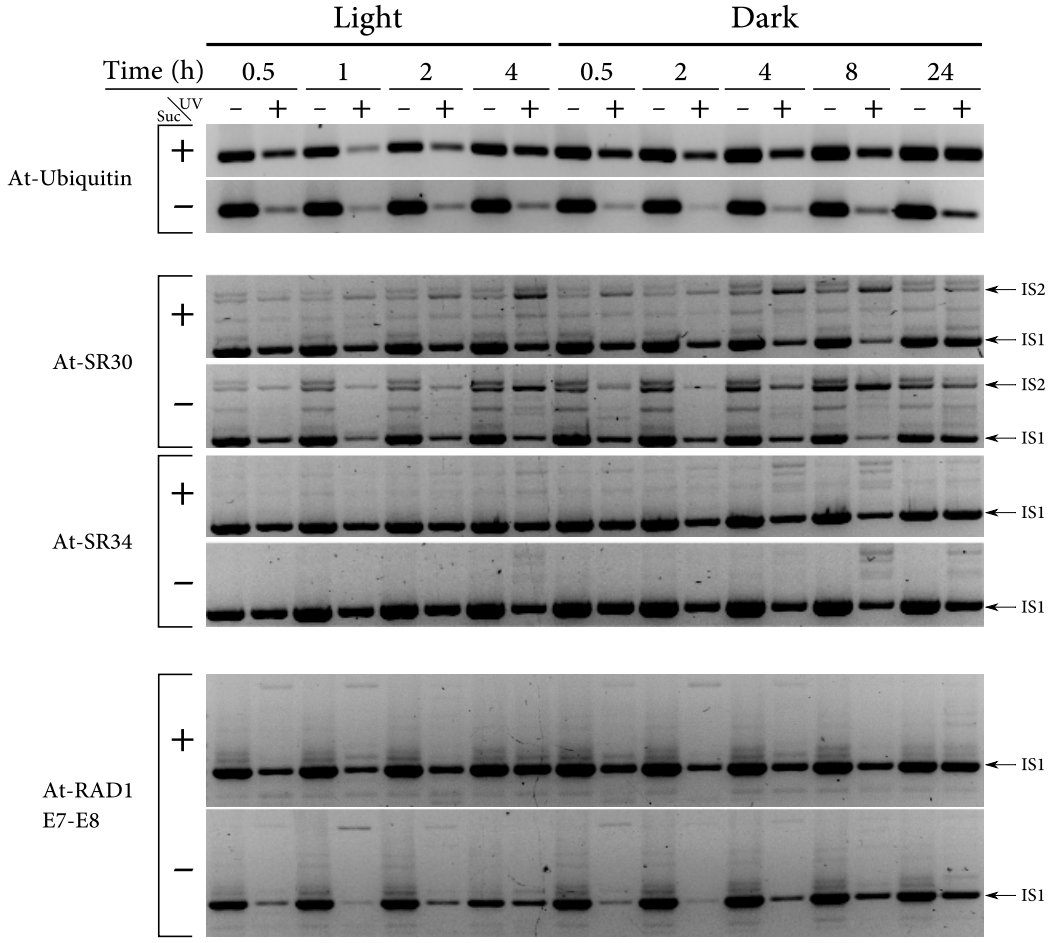

Figure 29: **Expression and splicing of At-SR30, At-SR34 and At-RAD1 in *A.thaliana* cell suspension cultures upon UV-C irradiation.** At-Ubiquitin served as a RT-PCR loading control. The phrase "Light" depicted on top of the figure enfolds the first eight, light exposed samples. The phrase "Dark" enfolds samples 9 to 18, which were kept in the dark. The elapsed time after UV-C exposure is given in hours and can be found beneath the previously mentioned phrases. UV-C treatment is represented by horizontally arranged minus (-, untreated) and plus (+, treated) symbols. Whether the final media contained sucrose or not is depicted by vertically arranged minus (-, no sucrose) and plus (+, sucrose) symbols. Gene names can be found on the left side of the figure. Every gene is represented by two agarose-gel pictures, one for sucrose supplemented and one for sucrose free samples. Relevant splice isoforms are highlighted by black arrows and numbered IS 1-2. If not stated elsewhere, IS1 refers to the "correctly" spliced isoform, which generates the full-length protein. Abbreviations: (-) - untreated sample; (+) - treated sample; At - *A.thaliana*; E - Exon; IS - Isoform; (h) - Time in hours; I - Intron; Suc - Sucrose; UV - Ultraviolet-C

patterns of At-SR30 are in agreement to the previously analysed genes in regard to recovery rates, both in sucrose depleted and supplemented samples, the expression of At-SR34 is inverse to these findings. At-SR34 is the only gene analysed that shows an increased expression in sucrose depleted samples after UV-C treatment. Furthermore, expression of At-SR34 is also higher in untreated, sucrose depleted samples than in supplemented ones.

4.5.6 At-RAD1

Expression of At-RAD1 is elevated in sucrose supplemented samples compared to depleted ones (Figure 29). Interestingly, upon UV-C treatment, no overexpression of At-RAD1 appears, neither in light nor in dark exposed samples. Furthermore, recovery of UV-C treated samples never reaches the level of untreated ones, which is quite odd given that At-RAD1 is involved in the repair mechanisms of DNA damage.

4.6 Analysis of alternatively spliced transcripts in *A.thaliana* during DNA damage and a possible interaction with the RNA polymerase II

Since we have previously shown that UV-C is a potent trigger for alternative splicing, we wanted to analyse a possible interplay between non-protein coding transcripts and the RNA polymerase II during DNA damage.

4.6.1 Shifting splicing patterns emerge

Our theory first popped into existence when we analysed the expression and splicing patterns of SR genes in UV-C irradiated (100 J/m^2) *A.thaliana* cell suspension cultures (refer to subchapter 4.6) over a period of 24 hours via RT-PCR. Fully and alternatively spliced transcripts show a clear dynamic along 24 hours. As time progresses, the amount of fully spliced transcripts increases while alternatively spliced transcripts decrease, indicating DNA integrity restoration. Figure 30 shows the expression and splicing patterns of At-RS31a, At-RS40 and At-SR30 of untreated and treated samples, which were kept in the dark for up to 24 hours after UV-C treatment.

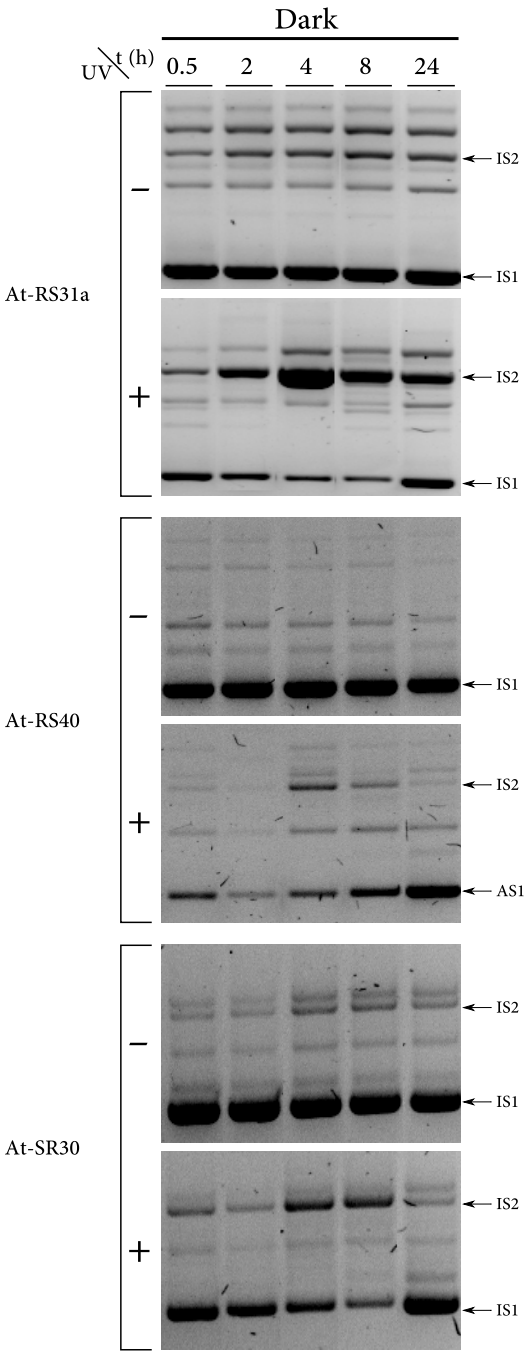

Figure 30: **Expression and splicing of SR genes upon UV-C irradiation.** Five-days-old *A.thaliana* cell suspension cultures (HH-1, seedling origin, Col-0 ecotype) were irradiated with 100 J/m^2 UV-C. After irradiation, samples were kept in the dark for 0.5, 2, 4, 8 and 24 hours before total RNA was isolated and analysed via RT-PCR. For each treated sample, an untreated control sample was included. The phrase "dark" on top of the figure emphasizes that all shown samples were kept in the dark after UV-C irradiation. Distinct time points are listed to the right of "t (h)". UV-C treatment is represented by minus (-, untreated) and plus (+, treated). Gene names are on the left side of the figure. Every gene is represented by two agarose-gel pictures, differentiated by - (untreated) and + (treated). Relevant splice isoforms are highlighted by black arrows and numbered IS1-2. If not stated elsewhere, IS1 refers to the "correctly" spliced isoform, which generates the full-length protein. Abbrevations: (-) - untreated sample; (+) - treated sample; At - *Arabidopsis thaliana*; IS - Isoform; t (h) - Time in hours; UV - Ultraviolet-C

At-RS31a

While non-irradiated samples show no significant changes in expression or alternative splicing of At-RS31a along 24 hours, irradiated specimen indeed show prominent alterations (Figure 30). 0.5 hours after UV-C treatment, overall gene expression is decreased while IS2 remains slightly increased. Two hours after irradiation, IS1 levels are even lower while the expression of IS2 is clearly increased, reaching its height at four hours post UV-C treatment. Eight hours after irradiation, IS2 expression is declining and the amount of IS1 is reaching its lowest point. However, 24 hours after treatment, IS2 declines further while IS1 shows its highest expression along the measured period. A clear switch from IS1 to IS2 and from IS2 to IS1 can be observed along 24 hours.

At-RS40

The expression and splicing pattern of At-RS40 remains unchanged in untreated samples while obvious changes occur in UV-C irradiated samples (Figure 30). 0.5 hours post treatment, the overall expression is lower than in the untreated sample and further drops at two hours after irradiation. An additional two hours later, expression is partially restored and a 1:1 ratio between IS1 and IS2 can be observed. Eight hours after UV-C treatment, expression shifts from IS2 towards IS1 and reaches almost untreated levels after 24 hours, in general resembling the pattern observed with At-RS31a.

At-SR30

The expression and splicing pattern of At-SR30 in treated samples strongly resembles the emerging pattern observed in At-RS40 and especially At-RS31a (Figure 30). Until eight hours after UV-C irradiation, expression is shifted away from IS1 towards IS2. However, 24 hours post treatment, a clear shift from IS2 towards IS1 can be observed.

Taken together, these findings depict an interesting dynamic in the alternative splicing patterns of At-RS31a, At-RS40 and At-SR30 (and has also been observed for additional SR genes). The increase in alternative splice isoforms seems to nicely coincide with the infliction of DNA damage through UV-C treatment. As a next step, we wanted to adress the question whether DNA damage is fully repaired after 24 hours, when splicing switches back to the fully spliced isoform IS1.

4.6.2 Identification of UV-C induced DNA damage

After the identification of distinct splicing patterns, we tried to analyse the severity and recovery of UV-C inflicted DNA damage over a period of 24 hours by targeting Cyclobutane-pyrimide-dimers (CPDs) via ELISA. Wild type plants of *A.thaliana* (Col-0), plants overexpressing At-RS31 as well as At-RS31 and At-RAD1 mutant plants were grown for ten days under long day conditions before they were irradiated with 200 J/m^2 UV-C. DNA was isolated after four and 24 hours and subjected to ELISA using an antibody (TDM-2 anti-CPD, [154]) which is able to bind CPDs. We used 200 instead of 100 J/m^2 UV-C due to questionable antibody sensitivity connected to low-yield plant DNA isolation complications.

Detection of CPDs via ELISA

Refer to subchapter 3.2.11 for a detailed description of the working protocol regarding ELISA.

Four hours post UV-C treatment, the average density of detected CPDs among samples with different genetic backgrounds results in an absorption of approximately 0.08 (Figure 31). However, 24 hours after irradiation, absorption drops to approximately 0.05, indicating a reduction of detectable CPDs and thus recovery from DNA damage. When focusing on light exposed samples four hours post treatment, wild type plants show the lowest amount of CPDs, followed by At-RS31ko_1, At-RS31oe and At-RAD1ko. 24 hours after UV-C irradiation, this scheme remains approximately the same with At-RAD1ko still showing the highest CPD level. Interestingly, samples kept in the dark show a clearly increased level of detected CPDs four hours post irradiation resulting in an absorption of up to 0,12 when compared to their light exposed pendants. Furthermore, differences between genetic backgrounds are more pronounced. Again, wild type plants show the lowest absorption, followed by At-RS31ko_1. A clear difference can be seen between light and dark exposed At-RS31oe and At-RAD1ko samples. Exposed to light, At-RAD1ko shows the highest amount of detectable CPDs followed by At-RS31oe. However, when kept in the dark, this finding is inverted, with At-RS31oe samples showing the highest amount of CPDs. 24 hours after UV-C irradiation samples kept in the dark show almost no reduction in CPDs when compared to absorption values four hours after treatment. This is a clear difference to light exposed samples, which show a CPD reduction of roughly 50%.

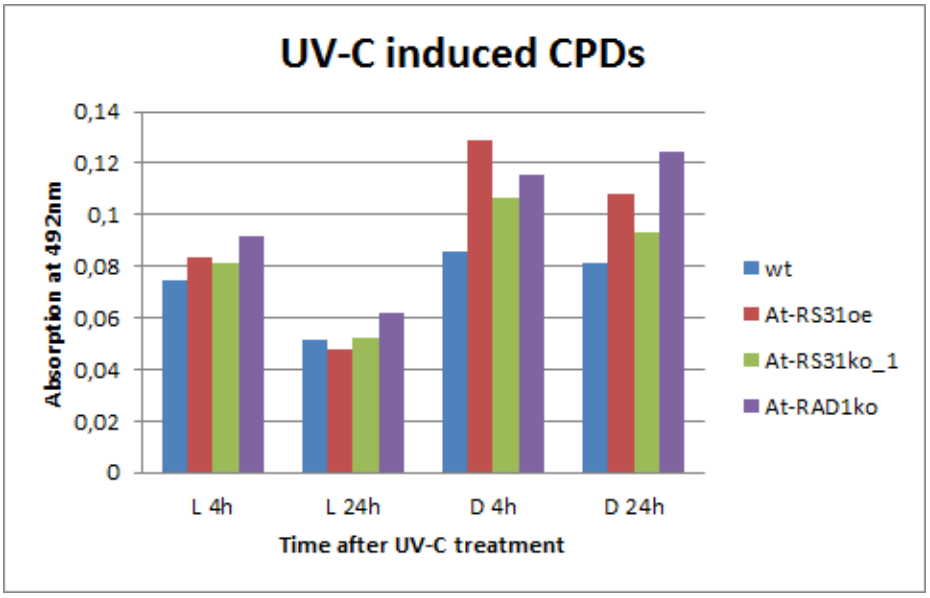

Figure 31: **Induction of CPDs in wild-type (Col-0), At-RS31oe, At-RS31ko_1 and At-RAD1ko (uvh1 mutant) seedlings after UV-C exposure.** Ten-days-old seedlings were irradiated with 200 J/m^2 UV-C and afterwards transferred to light or dark conditions for four and 24 hours before DNA isolation. Absorption data for each sample are given as the mean value derived from triplicates. The mean absorption values derived from untreated control samples were subtracted from UV-C exposed samples to correct for default DNA damage, which is not connected to UV-C irradiation. Shown data represents two technical replications (Standard deviations for technical replicates are not included in the figure. Standard deviation values are: wt (L4h - 0,002; L24h - 0,006; D4h - 0,0003; D24h - 0,008), At-RS31oe (L4h - 0,008; L24h - 0,005; D4h - 0,006; D24h - 0,01), At-RS31ko_1 (L4h - 0,003; L24h - 0,0006; D4h - 0,006; D24h - 0,0008), At-RAD1ko (L4h - 0,006; L24h - 0,005; D4h - 0,018; D24h - 0,006). Abbreviations: CPDs - Cyclobutane-pyrimidine-dimers; D - Dark; h - hours; ko - knockout; L - Light; oe - overexpression; UV-C - ultraviolet-C; wt - wild type

Interestingly, 24 hours after UV-C treatment, dark kept samples still show high levels of CPDs, which indicates slow progress in DNA repair. However, at this time point, observed splicing patterns resemble almost untreated levels.

4.6.3 Mapping of the RNA polymerase II phosphorylation status during UV-C induced DNA damage

Finally, we tried to find out whether the status of the RNA polymerase II (Pol II) coincides with changes in alternative splicing and the repair process of damaged DNA. The Pol II is extensively phosphorylated along the different stages of transcription. Furthermore, these phosphorylation events have previously been connected to the

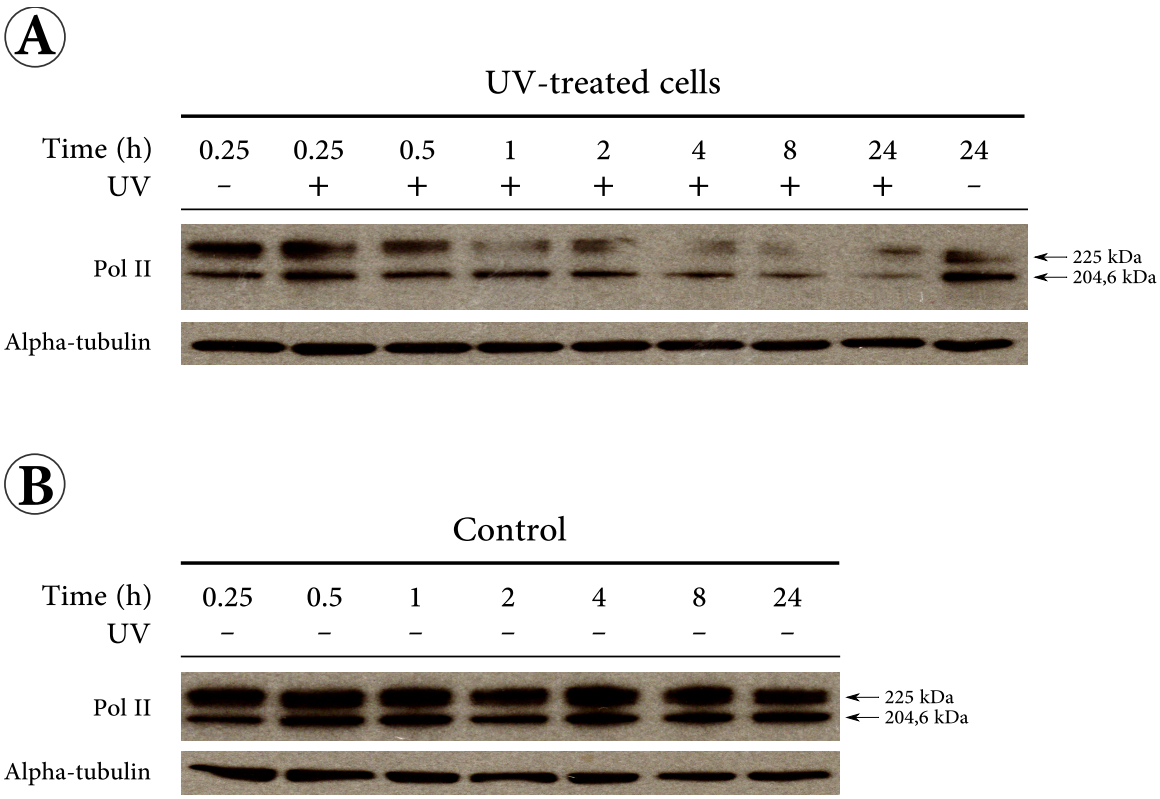

Figure 32: **Detection of the phosphorylation status of the RPB1 subunit of the RNA polymerase II.** Five-days-old *A.thaliana* cell suspension cultures (HH1, seedling origin, Col-0 ecotype) were irradiated with 100 J/m^2 UV-C. Samples were isolated after 0.25, 0.5, 1, 2, 4, 8 and 24 hours. Proteins were isolated and resuspended in protease inhibitor (Roche) to prevent degradation. 30 μg of protein were loaded per lane on a 4-12% Bis-TrisMOPS NuPAGE gel (Invitrogen). Spectra Broad Range Protein Ladder was used as a marker (Fermentas). Pol II (aN-15, sc-34092, 1:500, Santa Cruz Biotechnology, Inc.) was used as the primary antibody to detect RPB1. Donkey anti-goat IgG-HRP (sc-2020, 1:10000, Santa Cruz Biotechnology, Inc.) was used as the corresponding secondary antibody. Anti-α-tubulin (DM1A, T9026, 1:5000, Sigma) was used as the primary antibody to detect α-tubulin. Goat anti-mouse IgG-HRP (CatN 170-6516, 1:10000, Bio-Rad) was used as the corresponding secondary antibody. **A)** UV-C treated samples. The upper panel shows the detection of RPB1, while the lower panel serves as a loading control, showing the detection of α-tubulin. Untreated control samples were included on the far left and right of the gel for direct comparison between irradiated and non-irradiated samples. **B)** Non-irradiated control samples. The upper panel shows the detection of RPB1, while the lower panel serves as a loading control, showing the detection of α-tubulin. Abbrevations: (-) - untreated sample; (+) - treated sample; (h) - Time in hours; UV - Ultraviolet-C

occurence of alternative splicing. It has been conclusively demonstrated that the Pol II CTD is hyperphosphorylated both at the second and fifth serin (Ser2, Ser5) after UV irradiation. These phosphorylation events affect the elongation process of the Pol II and thus subsequently alternative splicing of currently transcribed genes [96]. Furthermore, DNA damage has been shown to cause ubiquitination of the Pol II, which might result in its degradation, however this is currently debated.

To identify the status of the Pol II and its abundance after UV treatment, we used the primary antibody Pol II (aN-15), which binds to the N-terminus of the largest subunit of the Pol II, namely RPB1. RPB1 comprises all the key features of the Pol II, such as its catalytic activity as well as the C-terminal domain, which is subjected to extensive phosphorylation events. Thus it is possible to distinguish between an unmodified and modified RPB1 due to differences in the molecular weight, which is the consequence of different modification events, such as phosphorylation or ubiquitinilation. An unmodified RPB1 subunit has a mass of 204.6 kDa, while an elevated molecular weight represents a modified Pol II. We used five-days-old *A.thaliana* cell suspension cultures (HH1, seedling origin, Col-0 ecotype), which were exposed to 100 J/m^2 UV-C before samples were isolated after 0.25, 0.5, one, two, four, eight and 24 hours. After protein isolation, samples were subjected to western blotting using the respective primary and secondary antibodies (Refer to subchapters 2.6 and 3.2.12 for methodical details).

Figure 32 shows the obtained results. Western blots were performed with UV-C treated, as well as untreated control samples and the expression of α-tubulin was mapped as a loading control. In conclusion, the detection of total RPB1 levels gradually declines along time in UV-C treated cells, which is not the case in the control samples. Additionally, our observations indicate that 24 hours post UV-C treatment is not sufficient to restore RPB1 levels.

4.7 Generation and phenotypic analysis of SR mutant lines in *P.patens* and *A.thaliana*

Besides analysing splicing and expression patterns of SR genes, our lab devotes considerable efforts towards manipulating SR genes, either by overexpression or knock-

out/down approaches. Subsequently, phenotypic characterisation of these lines is an integral part towards understanding the full scale of interactions and roles that SR genes inherit.

Previous studies in *A.thaliana* At-RS2Z33 overexpression lines have shown aberrant cell divisions and irregular structures forming on the surface of leaves [49]. Thus, it was interesting to find out whether *P.patens* Pp-RS2Z37ko lines would exhibit similar phenotypic effects. Additionally, we included the Pp-RS27ko line since its phenotype has not been studied in detail before. Protoplasts were isolated from five-days-old protonemal wild type, Pp-RS27ko and Pp-RS2Z37ko tissues. Protoplasts were subsequently embedded in a low density agarose-gel-matrix (refer to subchapter 3.3.3). Samples were taken after one and seven days, stained with Calcofluor (cell wall) and finally visualised via fluorescent microscopy.

Figure 33 shows dividing protoplasts (A), as well as the initial growth stages of forming protonemata (B). Already one day after isolation, protoplasts are able to recover from the procedure and start to divide. Alas, we were not able to observe significant differences during cell division. The asymmetric position of the constricting cell wall suggests a budding-like division of protoplasts, which behaves the same among wild type, Pp-RS27ko and Pp-RS2Z37ko samples. What appears to be a difference in the Pp-RS27ko protoplast shown in Figure 33A is most probably simply a slightly advanced state during cell division.

Possibly of more interest is the state of cells seven days after isolation. At this stage, protoplasts have long since recovered and are now forming protonemata, spreading tissues to locate nutrition resources. While the wild type protonema already forms two side branches, none are formed in the Pp-RS27ko sample and Pp-RS2Z37ko protonema only just started formation of a side branch. Also notable is the roundish structure of Pp-RS2Z37ko cells compared to Pp-RS27ko and wild type cells. Pp-RSZ37ko cells are slightly larger and more expanded crosswise than wild type and Pp-RS27ko cells and thus are probably impaired in elongation. This observation would correlate to the events observed in *A.thaliana* upon overexpression of the genomic clone of At-RS2Z33, which leads to autoregulation and thus a decrease in the levels of the At-RS2Z33 protein.

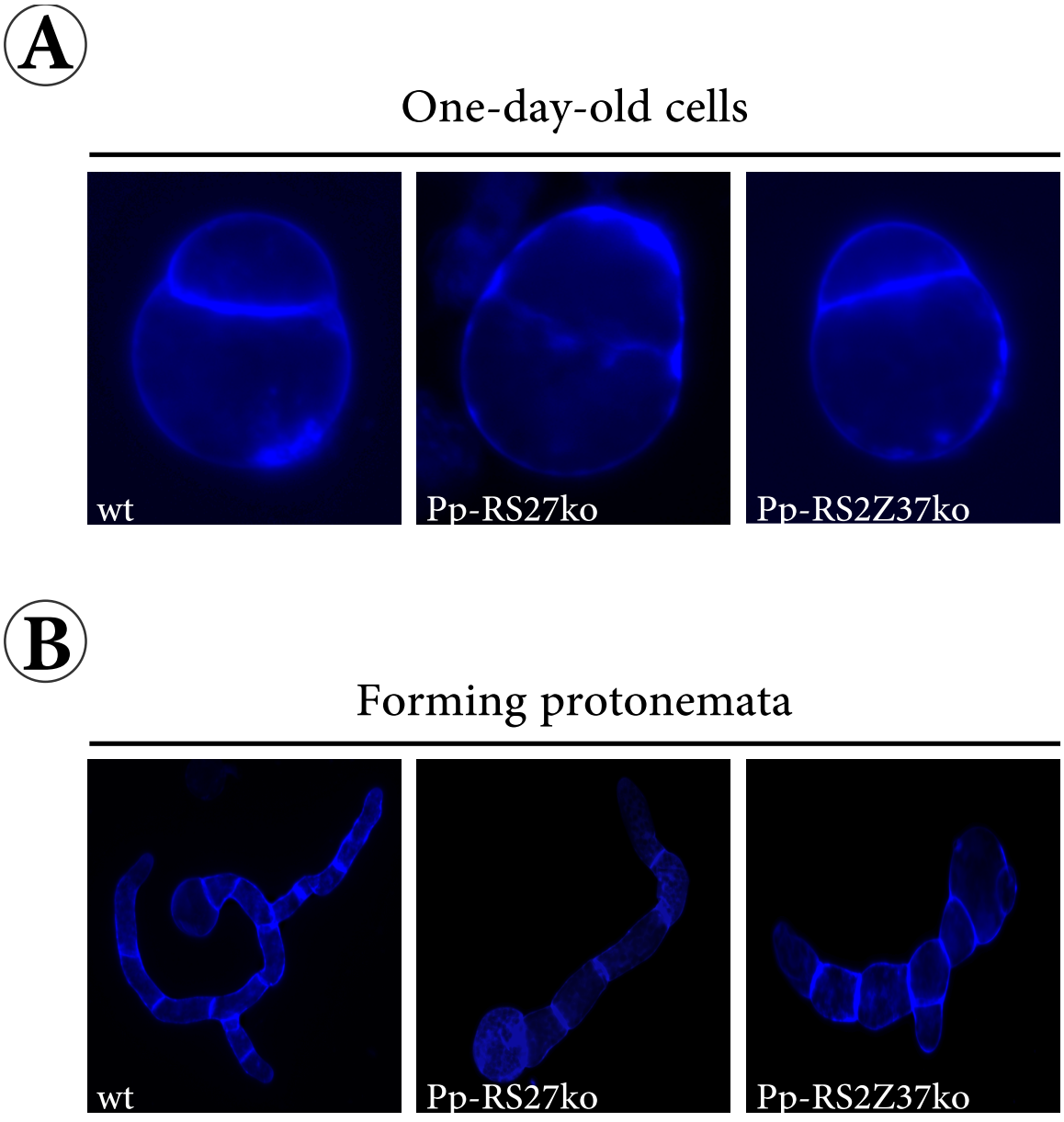

Figure 33: **Calcofluor staining of *P.patens* cell walls, visualized by fluorescent microscopy.** Samples were prepared after one (A) and seven days (B) after protoplast isolation. Cells in (A) are of the same size as the initial cells in (B), from which the protonemata starts to spread. Thus, magnification differs between (A, 1000x) and (B, 200x). Refer to text for a detailed description.

Unfortunately, with *A.thaliana*, manipulation of SR genes is not quite as easy as it is with other organisms, since this plant lacks the genetic prerequisites which are necessary to make use of gene targeting. The most popular way to manipulate *A.thaliana* is by *A.tumefaciens* mediated T-DNA insertions. Alas, this method does not provide targeted gene disruption but rather is based on random insertions, thus screening of random T-DNA insertion lines does not always provide a line for the desired gene. However, this time we chose a fancier approach; artificial microRNAs.

In addition to designing our very own amiRNAs to At-RS31a and to the whole RS subfamily in *A.thaliana* (data not shown), we also implemented available amiRNA constructs from the Cold Spring Harbor Laboratories (CSHL): CSHL_078707 to knock At-RS41 down, which is a member of the RS subfamily. In addition, we used two other available constructs, which target *A.thaliana* SR proteins At-SR30 and At-SC35, CSHL_011244 and CSHL_082339, respectively.

The amiRNA construct CSHL_011244 targets the seventh exon of At-SR30, which encodes the proteins second RRM domain. Both the amiRNA constructs CSHL_078707 and CSHL_082339 target the 3'UTR (untranslated region) of their respective target genes, At-RS41 and At-SC35.

These amiRNA constructs are fused with the vector pAmiR, which is able to replicate within *E.coli* as well as *A.tumefaciens*, thus rendering it perfect for *A.thaliana* transformations. Furthermore, it contains a BASTA-resistance cassette for efficient selection of positively transformed seeds.

To start, the respective plasmids were isolated from *E.coli*, transformed into *A.tumefaciens* via electroporation and then incubated for three days at 28°C (refer to subchapter 3.2.5). To verify the successful transformation of the respective plasmids, besides rifampicin / spectinomycin / tetracycline selection on agar-plates, colony-PCRs were performed using specific primers (refer to subchapter 2.7.1) that were located on the promoter and terminator region flanking the individual amiRNA-sequences. Simultaneously, *A.thaliana* wild type plants were grown on soil for approximately three weeks. Initial emerging flower buds were cut to trick the plants into forming multiple additional buds, thus effectively enhancing *A.tumefaciens* transformation efficiency.

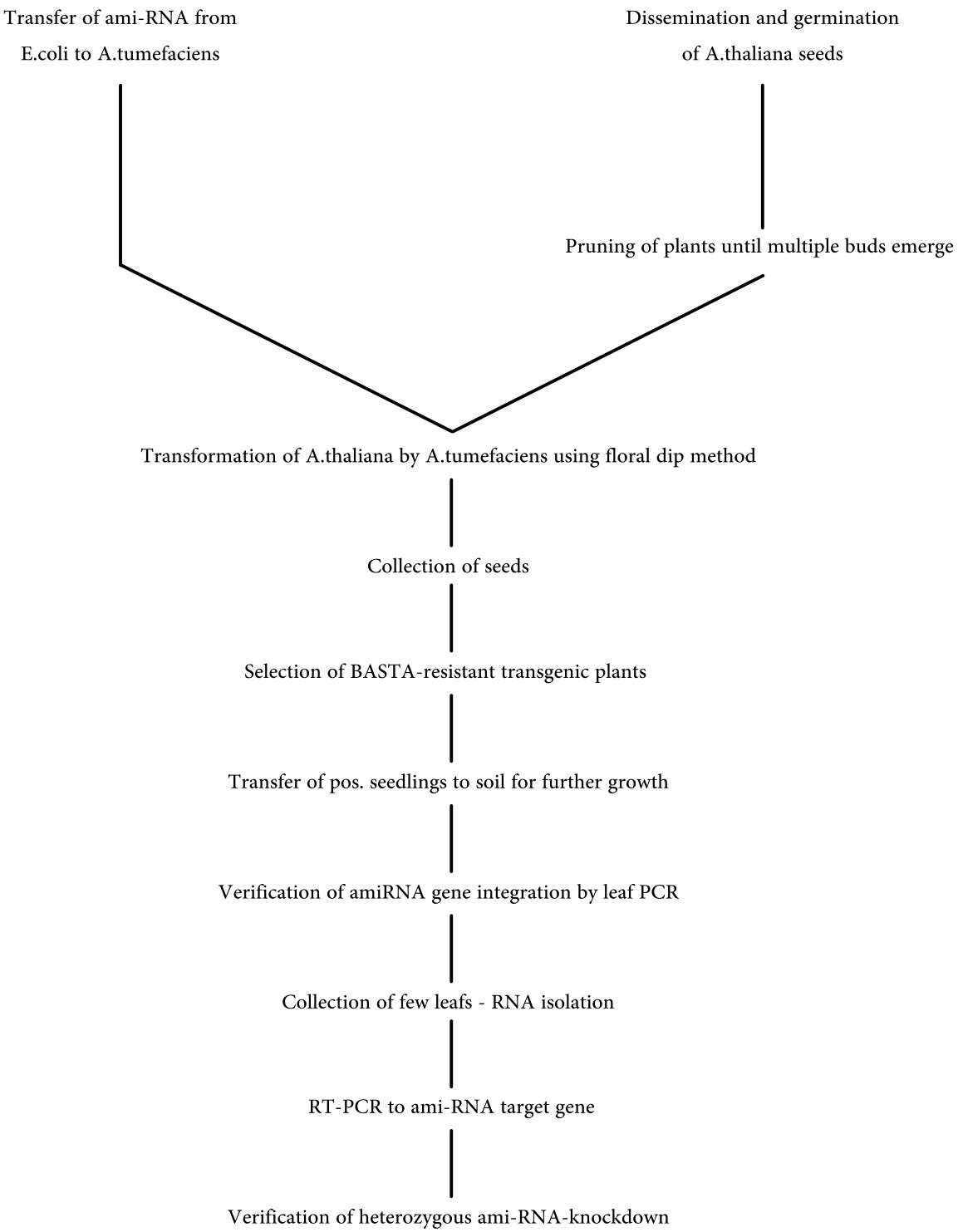

Figure 34: **Summary of the actions performed to achieve amiRNA mediated knockdowns.** Refer to text for further details.

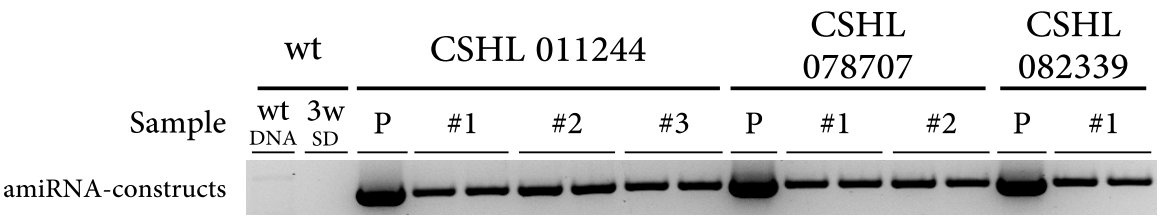

Figure 35: **Confirmation of the successful integration of the respective amiRNA constructs in *A.thaliana*.** A single leaf was detached from individual two-week-old plants to perform leaf-PCR using primers to the CaMV35S promoter and octopine synthase terminator sequences, which surround the individual amiRNA sequences. Wild type plants as well as wild type DNA were used for the negative controls, while the original plasmids were used for the positive controls. Every leaf-PCR was carried out in duplicate for each plant. Three, two and one plants were checked for CSHL_011244, CSHL_078707 and CSHL_082339, respectively. Every plant checked carries the respective amiRNA construct. Abbrevations: #1, 2, 3 - Individual plant number; 3w-SD - 3 weeks old plant, grown in short day conditions; P - Plasmid; wt - wild type

When plants were ready to be transformed, indicated by multiple emerging, yet still closed flowering buds, *A.tumefaciens* cultures, carrying the pAmiR vector containing the respective amiRNA, were grown for two days at 28°C in one litre of LB supplemented with rifampicin. Transformation of *A.thaliana* was done via the floral dipping method (refer to subchapter 3.2.6); each plant was transformed two times in an interval of one week to further increase transformation efficiency. Approximately three weeks later, seeds were collected. After desiccation, seeds were sterilized (refer to subchapter 3.2.3) and transferred to ½ GM agar plates containing 6 mg/l BASTA. Growing seedlings were transferred to soil containing pots once they seemed viable enough to survive this critical intervention. Seedlings growing on the borders of agar-plates were not considered for transfer since BASTA-concentrations are known to significantly vary in this location.

Once plants seemed stable enough, a single leaf was detached from individual plants to perform leaf-PCRs using the same specific primer pair as mentioned above to check the successful integration of the respective amiRNA sequences into the genome of *A.thaliana* (Figure 35). On a side note, it should be mentioned that the targeted genes are known to be expressed in leaves. False-positive plants were discarded while truly positive plants were further nurtured until a few leafs could be removed. Following RNA isolation, the expression of the gene targeted by the respective amiRNA was analysed via RT-PCR using gene specific primers (refer to subchapter 2.7.1). Each PCR reaction was carried out in duplicates.

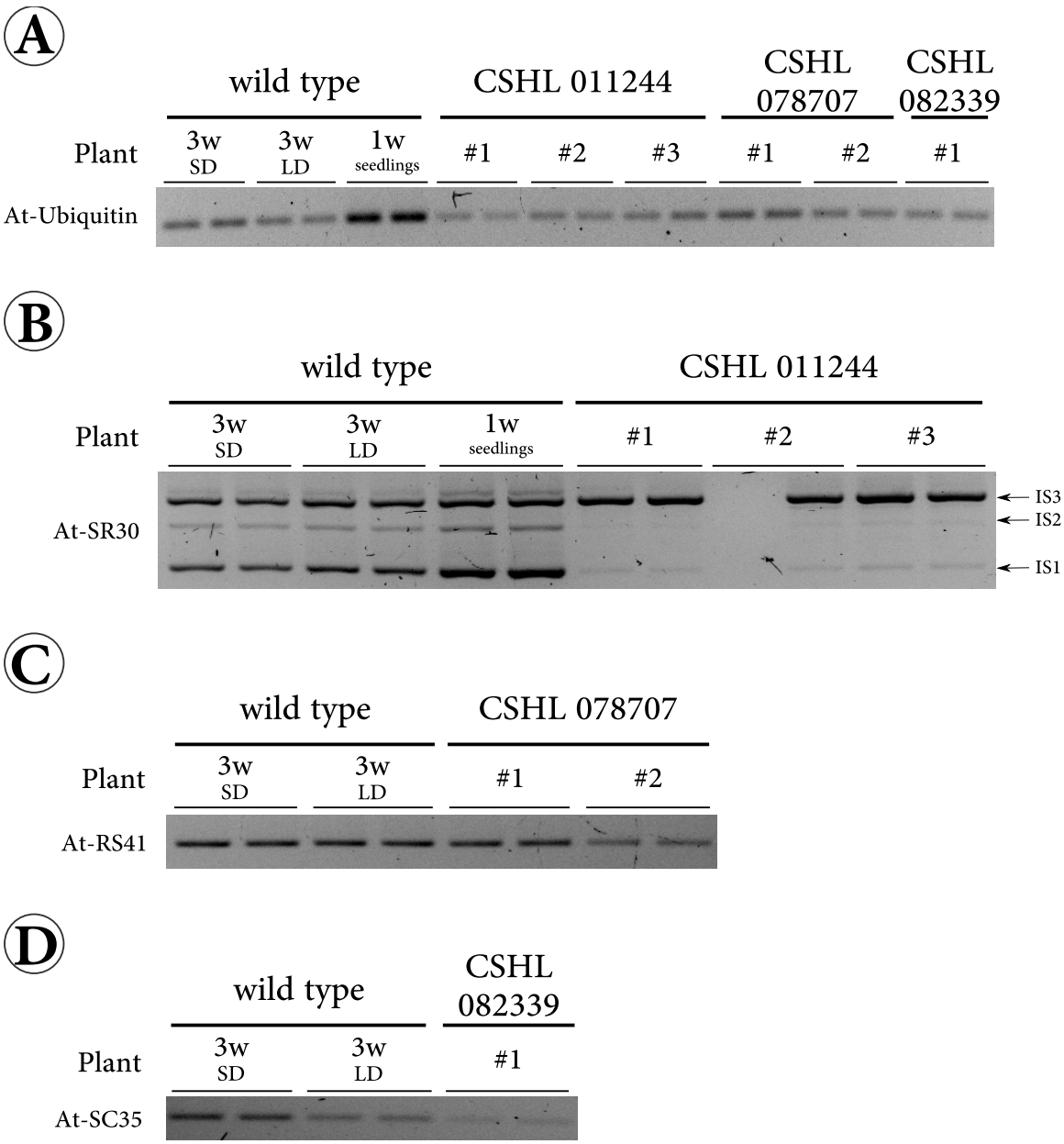

Figure 36: **Expression of amiRNA target genes.** Two-week-old plants were bereft of several leafs for RNA isolation, followed up by RT-PCR to check the expression of At-SR30, At-RS41 and At-SC35 and At-Ubiquitin as an expression control. Refer to subchapter 2.7.1 for detailed information on the primers used. **A)** shows the expression of At-Ubiquitin in three control and six transgenic plants. The expression of At-Ubiquitin serves as a control to normalize for general expression-differences between individual plants. **B)** shows the expression of At-SR30, the target gene of the amiRNA construct CSHL_011244, in three control and three transgenic plants. **C)** shows the expression of At-RS41, the target gene of the amiRNA construct CSHL_078707, in two control and two transgenic plants. **D)** shows the expression of At-SC35, the target gene of the amiRNA construct CSHL_082339, in two control and one transgenic plants. Abbrevations: #1, 2, 3 - Individual plant number; 3w-SD - Three-weeks-old plant, grown in short day conditions; 3w-LD - Three-weeks-old plant, grown in long day conditions; 1w seedlings - One-week-old seedlings, grown on agar-plates; IS - Isoform; P - Plasmid; wt - wild type

Figure 36A shows the expression of At-Ubiquitin in different control as well as in the transgenic samples. The expression of At-Ubiquitin was checked to normalize for eventual markedly differences in the overall gene expression between samples due to various stress sources, such as the transfer from agar plates to soil. Such differences could falsify the results for the respective target genes if they went unchecked. In any case, the expression patterns are equal throughout most of the samples, only the one-week-old seedlings control shows a slightly elevated expression of At-Ubiquitin.

Figure 36B shows the expression of At-SR30, the target gene of the amiRNA construct CSHL_011244. Three controls were included, which show similar expression patterns of IS1, IS2 and IS3. One-week-old seedlings shows a slightly elevated expression of At-SR30, which fits nicely to the elevated expression of At-Ubiquitin. However, the expression pattern of At-SR30 looks significantly different in amiRNA transgenic plants. IS1 and IS2 are hardly detectable while IS3 is overexpressed when compared to the control samples.

Figure 36C shows the expression of At-RS41, the target gene of the amiRNA construct CSHL_078707. Two controls were included, which show a similar expression of At-RS41. Two transgenic samples were checked for the expression of At-RS41. The first plant shows similar expression intensity to the control samples while the second plant shows a reduced amount of At-RS41 transcripts.

Figure 36D shows the expression of At-SC35, the target gene of the amiRNA construct CSHL_082339. Again, two controls were included, which do not show a similar expression of At-SC35. Nevertheless, the expression of At-SC35 is hardly detectable in the transgenic sample in comparison to the controls.

In conclusion, the results presented here demonstrate that the amiRNA mediated approach indeed knocked the expression of At-SR30, At-RS41 and At-SC35 down. However, these findings are derived from heterozygous plants, which means that knock down efficiency should be even more prominent in homozygous plant. Thus, amiRNA mediated knockdown approaches prove to be a valuable alternative to random T-DNA insertion lines in *A.thaliana*.

Chapter 5

Discussion

When alternative splicing was discovered more than 30 years ago, it was considered the exception rather than the rule. Today it is known that more than 95% of human genes are alternatively spliced [155, 156, 157]. The fact that a plenitude of human diseases, such as cystic fibrosis, Parkinsonism, spinal muscular atrophy, etc., are the result of mutations in either cis-acting RNA elements or trans-acting protein splicing factors further stresses the importance of alternative splicing [43, 158, 159]. Although alternative splicing is widely conserved across eukaryotes, with the prominent exception of yeast, significant differences emerge between animal and plant systems.

The average gene in *A.thaliana* is roughly 2.4 kb short and is usually subdivided into 5 exons and 4 introns. A human gene is on average larger by tenfold with 28 kb, which, surprisingly, only yields around 8 exons and 7 introns [160]. This discrepancy may be explained by the much shorter size of plant introns compared to human ones, which are by themselves on average larger than a whole gene in *A.thaliana*. Besides marked differences in gene sizes, also subtle alterations in splice site consensus sequences can be found. While the core of these sequences is equally conserved among animals and plants, with the GU dinucleotide at the 5' splice site and the AG dinucleotide at the 3' splice site, modifications are eminent in the close vicinity to these sequences, which most likely explains the differences in splice site recognition between these organisms [31].

Subsequently, these differing characteristics most likely account for the dissimilarities in the prevalence of alternative splicing events. Intron retention accounts for the most- and exon skipping for the least prominent splicing events in *A.thaliana*, which

behaves exactly vice versa in humans [31, 38]. Furthermore, the family of SR proteins, which act as crucial trans-acting factors during splicing, is significantly expanded in *A.thaliana* with 18 members in comparison to the human genome, which harbours only 12 SR genes [62]. Although eight out of 18 plant SR genes are clear orthologs of mammalian ones, the remaining ten SR genes are plant-specific and thus very likely play distinct parts in the process of alternative splicing in plants. Interestingly, it has been shown that SR pre-mRNAs themselves undergo extensive alternative splicing and that SR proteins regulate splicing within their own family, which illuminates a tightly controlled and highly complex regulation network, which needs to be elucidated step by step [70, 50, 77, 69, 71, 46].

A.thaliana is a flowering plant and thus represents a rather advanced level in land plant evolution. The moss *Physcomitrella patens* on the other hand belongs to bryophytes, an ancient lineage of land plants [20]. Orthologs of plant-specific SR genes found in *A.thaliana* have also been identified in *P.patens*, therefore posing a very interesting opportunity to analyse the possible fine-tuning of the functions of SR proteins from *P.patens* to *A.thaliana* during evolution [75].

Additionally, numerous studies have shown that *P.patens* is very resilient towards environmental stress due to effective DNA repair mechanisms [20, 15, 14]. Thus the question arises whether DNA-repair genes are differently regulated and spliced in *P.patens* and *A.thaliana*.

5.1 UV-C irradiation triggers alternative splicing

To investigate the functions of SR proteins, we first had to identify a potent trigger of alternative splicing. UV-C radiation is highly energetic, hence lethal, but is effectively absorbed by the atmosphere, thus earthly organisms seldom have to cope with UV-C. However, UV-C is absorbed by DNA and induces mutagenic photoproducts similar to the types of damage caused by UV-B. Furthermore, UV-C radiation is easier to apply and also to quantify in regular laboratory conditions. Last but not least, artificial UV-C irradiation caused damage is still an issue, e.g. when using UV-C sterilization equipment. Therefore, we irradiated *A.thaliana* seedlings with UV-C and extensively analysed the expression and splicing patterns of SR and DNA repair genes via RT-

PCR.

Figures 17 - 21 show that alternative splicing of At-RS31, At-RS31a, At-RS40, At-RS41, At-RS2Z32, At-RS2Z33, At-FPG1 and At-RAD1 pre-mRNAs is indeed triggered by UV-C irradiation. In detail, our analysis shows that UV-C induced stress leads to a shift from the correctly spliced isoform (IS1) towards alternative splice isoforms. These alternative splice isoforms have a potential to code for heavily truncated proteins, however due to the introduction of premature termination codons, in many cases they are subjected to nonsense mediated decay, as has been shown for various SR proteins before [161]. Furthermore, previous studies have shown that alternative splicing of At-FPG1 and At-RAD1 gives rise to functional modifications of subsequently translated proteins, e.g. the loss of the ERCC1 interaction domain in At-RAD1 or the loss of the nuclear localisation signal in At-FPG1 [146, 136].

Interestingly, this shift is even more prevalent when plants are kept in the dark after UV-C treatment, which might indicate more efficient DNA repair mechanisms during light exposure. However, we did not detect an increase in the gene expression of photolyases four hours after UV-C treatment in light exposed samples (Figure 22). This said, it should be noted that *A.thaliana* encodes multiple photolyase genes. Additionally, it may also be the case that the up- and following down-regulation of photolyases is completed within four hours. Besides the expression of photolyases, we also checked the expression of At-FPG1 and At-RAD1, which are part of the base excision- and nucleotide excision repair pathway, respectively. These repair mechanisms are active during light as well as dark conditions. However, we were not able to detect any aberrant expression of At-FPG1 or At-RAD1 four hours after UV-C treatment, neither when samples were kept in the light, nor in the dark.

Therefore this might indicate that the observed shift in alternative splicing of pre-mRNAs in the dark after UV-C treatment is caused by a differential expression of splicing regulators. In fact, plants overexpressing At-RS31 clearly show changes in alternative splicing of At-RS31a, At-RS40, At-RS41, At-FPG1 and At-RAD1 pre-mRNAs. These findings are in agreement to previous observations (Kalyna et al., unpublished) and suggest that splicing regulators are differentially expressed during day- and night conditions and thus influence alternative splicing of target pre-mRNAs, especially during stress conditions.

5.1.1 At-RS31 regulates alternative splicing of At-RS31a, At-RS40, At-RS41, At-FPG1 and At-RAD1

Alternative splicing is not equally triggered across all tested mutant backgrounds. In fact, the most obvious changes in alternative splicing patterns emerge in plants which overexpress At-RS31 (Figure 17 - 21).

At-RS31 overexpressing plants exhibit increased alternative splicing of At-RS31a, At-RS40, At-RS41, At-FPG1 and At-RAD1 pre-mRNAs in comparison to splicing patterns seen in the wild type background. This strongly implicates that splicing of these pre-mRNAs is, at least partially, regulated by At-RS31. Additionally, the effects of UV-C radiation on alternative splicing are more prevalent with pre-mRNAs regulated by At-RS31. These findings strongly indicate that At-RS31 plays a critical role during alternative splicing of SR and DNA repair genes, which is in agreement to previously conducted studies (Kalyna et al., unpublished).

5.1.2 At-RS2Z33 regulates splicing of At-RS2Z32 and of its own pre-mRNA

Kalyna et al. have previously reported that At-RS2Z33 regulates splicing of its own pre-mRNA [49]. Here we present results which acknowledge these findings and additionally show that At-RS2Z33 also regulates pre-mRNA splicing of its close paralogue, At-RS2Z32 (Figure 19). This outcome goes hand in hand with the observation that At-RS31 too regulates pre-mRNA splicing of its paralogous gene, At-RS31a. However, these findings confirm previous indications by Kalyna et al. [49, 75], which state that At-RS31 does not regulate splicing of its own pre-mRNA, as At-RS2Z33 does. These regulatory and autoregulatory feedback loops implicate tight control mechanisms behind the expression and splicing of SR genes.

5.2 UV-C radiation severly effects alternative splicing and gene expression in *P.patens* protonemata, but not in gametophytes

Since we identified UV-C as a potent trigger of alternative splicing and observed regulative interactions between SR proteins and SR pre-mRNAs in *A.thaliana*, we wanted to address the question whether similar effects could be seen in *P.patens*, as has previously been suggested by Kalyna et al. [75]. Therefore we irradiated *P.patens* protonemal and gametophytal tissues and extensively analysed the expression and alternative splicing patterns of two SR and two DNA repair pre-mRNAs via RT-PCR. Pp-RS27 and Pp-RS2Z37 are ortholog to At-RS31 and At-RS2Z33, respectively. The orthologous genes to Pp-FPG1 and Pp-RAD1 in *A.thaliana* should be fairly obvious.

UV-C treatment of protonemal tissue resulted in either a temporal or even complete shutdown of Pp-Actin, Pp-RS27 and Pp-RS2Z37 transcription during light exposed and dark kept conditions, respectively (Figure 23). Transcription of Pp-RS27 recovers over four hours, however splicing is shifted towards the alternative splice isoforms IS2, IS3 and IS4. Interestingly, splicing is shifted towards IS2 in control samples which were kept in the dark, which is in agreement with our previous results regarding the differential expression of At-RS31 in light and dark conditions. This might indicate that the day-night expression pattern of Pp-RS27/At-RS31 is conserved from *P.patens* to *A.thaliana*. Transcription of Pp-RS2Z37 behaves similar to Pp-RS27. Expression recovers along four hours in light kept samples, yet splicing is shifted towards the alternative splice isoform IS2.

In contrast, the DNA repair genes Pp-FPG1 and Pp-RAD1 are expressed during UV-C induced stress conditions. However, expression of Pp-FPG1 is significantly altered in UV-C treated samples when compared to the non-irradiated controls. 30 minutes after treatment, transcription of IS3 disappears almost completely, while transcription of IS1 is only slightly reduced. Light exposed tissues show a full recovery of Pp-FPG1 transcription while exactly the opposite can be observed in dark kept samples. Interestingly, transcription of IS1 steadily drops from 30 minutes to 24 hours in UV-C treated samples. This discrepancy between light exposed and dark kept samples is quite peculiar and could not be observed for At-FPG in *A.thaliana*. Pre-

vious studies have shown that at least seven different splice isoforms of At-FPG exist [145, 146, 147, 148]. While not all of these alternative transcripts could be linked to actual translated proteins, the ones which are produced inherit functional modifications due to splicing related sequence alterations. These protein isoforms mainly differ in their nuclear localisation, e.g. through the loss of a nuclear localisation signal. Considering these findings, it would be interesting to thoroughly identify and analyse FPG splice isoforms and proteins in *P.patens* for the sakes of evolutionary conservation.

Pp-RAD1 is part of the nucleotide excision repair pathway, which has been implicated in the repair of UV-C induced DNA damage. We observed an overexpression of Pp-RAD1 four hours after UV-C treatment in light exposed samples, which is in line with the functions of the NER pathway. However, when samples were kept in the dark, Pp-RAD1 transcription does not recover. Considering that the NER pathway is primarily regarded as the dark repair pathway in plants, this certainly is defying logic. This may be an indication of a differential regulation of Pp-RAD1 in *P.patens* and *A.thaliana*. Furthermore, previous studies in *A.thaliana* have shown that alternative splicing affects the functional range of At-RAD1, e.g. through the loss of interaction domains, such as the ERCC1 binding domain (Kalyna et al., unpublished). Similar to Pp-FPG1, it would be interesting to further identify and analyse Pp-RAD1 splice variants.

The observed phenomenon of a transcriptional shutdown may serve as a protective mechanism when severe damage is inflicted, since the production of aberrant proteins might potentially hold detrimental effects for a cell. Therefore, transcription of non-essential proteins may be shut down until DNA repair proteins, such as Pp-FPG1 and Pp-RAD1, deal with the inflicted damage.

The peculiar strategy of a transcriptional shutdown of certain genes in protonemal tissue fuelled our interest to find out whether the same would be true in *P.patens* gametophytal tissue. Our results clearly show that this is not the case (Figure 23). Gametophytes appear to be far sturdier and robust than the protonemata. Additionally, while protonemal tissue turned yellowish after UV-C treatment, gametophytes stood unchanged and unimpressed after the same radiation dose. As observed in protonemata, splicing of Pp-RS27 shifts towards the alternative splice isoform IS2

when samples are kept in the dark for a prolonged period of time. Furthermore, transcription of Pp-RAD1 in gametophytes is equal to protonemal tissue when samples were exposed to light. However, in contrast to protonemata, transcription of Pp-RAD1 continues and even overshoots in dark kept, UV-C treated samples. The lack of visible and persistent UV-C induced damage of *P.patens* gametophytes might be explained by an increased expression of DNA-repair proteins. In the life cycle of *P.patens*, the gametophytic phase is crucial in regards of reproduction, therefore the faithful transmission of genetic material needs to be ensured. However, the lack of visible damage or hampered gene expression may also be due to the enhanced appearance of UV-absorbing compounds, such as flavonoids, which effectively prevent any DNA damage or cellular stress responses from happening by directly nullifying the detrimental effects of UV-C on the surface of the organism. Wolf et al. [15] have previously shown that UV-B radiation induces the biosynthesis of flavonoids, thus rendering *P.patens* gametophytes sturdier towards UV radiation. Furthermore, the authors conclude that a possible avoidance response is triggered through UV-B irradiation. This reaction implies a reduction of the surface area to effectively shield underlying tissues. Given that the findings presented here show a high degree of UV-C resistance in *P.patens* gametophytes, this conclusion is definitely worth considering.

In any case, protonemal and gametophytal *P.patens* tissues show significant differences in their responses to UV-C radiation.

5.2.1 Transcription shutdown is reversible through light-exposure

In addition to our proposed theories regarding the functions and benefits of a transcriptional shutdown, one might simply argue that protonemal cells are overwhelmed by the UV-C treatment and are instead slowly dying one by one. Therefore, we irradiated another set of *P.patens* protonemata samples, kept them in the dark for 24 hours and then transferred them back to light exposed conditions. In fact, transcription prevails (Figure 24). Already 30 minutes worth of photons is enough for *P.patens* to restore transcription of Pp-RS27, Pp-RS2Z37 and Pp-RAD1. However, probably the most fascinating detail is that these genes, except Pp-Actin, are even overexpressed 24 hours after their escape from the dark. These findings indicate that protonemal cells reduce unnecessary expression to a minimum until the inflicted damage is repaired, as was shown before in the initial UV-C treatment experiments on protonemal

tissues.

5.2.2 Pp-RS27 and Pp-RS2Z37 pre-mRNA targets

P.patens is one out of few plant model organisms which is equipped with the genetic prerequisites required to carry out gene targeting and thus effective knockout-approaches. Our lab was able to establish stable knockout lines of the genes Pp-RS27 and Pp-RS2Z37 (Maronova et al., unpublished). Hence we tried to identify potential target pre-mRNAs of these proteins in protonemal and gametophytal tissues by analysing possible shifts in alternative splicing patterns.

Upon knockout of Pp-RS2Z37, alternative splicing of Pp-RS27 appears to shift towards the alternative splice isoforms IS2, IS3, IS4 and IS5, both in protonemata and gametophytes (Figure 25, 26). This might indicate that Pp-RS2Z37 is, to some extent, involved in the splicing process of Pp-RS27, which would stand in line with their orthologous genes At-RS2Z33 and At-RS31 in *A.thaliana*, respectively, as has been shown previously [75].

We also observed shifts in alternative splicing of Pp-FPG1 in Pp-RS2Z37 knockout samples. However, these differences were limited to gametophytal tissues and could not be seen in protonemal cells. Alternative splicing of Pp-FPG1 is clearly shifted towards IS3 with the complete disappearance of IS2 in gametophytes devoid of Pp-RS2Z37. This may imply a differential regulation of Pp-FPG1 across different phases in the life cycle of *P.patens*.

5.3 Knockout of Pp-RS27 or Pp-RS2Z37 does not impact cell or protonema development

In addition to the analysis of alternative splicing of potential target pre-mRNAs of Pp-RS27 and Pp-RS2Z37, we addressed the question whether these knockout-lines show differences in cell division or protonemata development, since Kalyna et al. [49] have conclusively shown that an overexpression of the genomic clone of At-RS2Z33, which is ortholog to Pp-RS2Z37, results in a plenitude of phenotypical defects in *A.thaliana* (Figure 33). Therefore we generated *P.patens* protoplasts via cell wall digestion and

analysed their development over a one-week period. For fluorescence microscopy analysis we stained protoplasts undergoing the first cell division and forming protonemata with Calcifluor (cell wall). We were not able to observe any significant differences between wild type and knockout lines during cell division. However, Pp-RS2Z37 cells of the forming protonema appear to be hindered in elongation, as they are larger in a crosswise way. This finding would be in agreement with previous studies conducted by Kalyna et al. [49], in which they were able to show that changed levels of At-RS2Z33 protein (ortholog to Pp-RS2Z37) lead to impairments in cell expansion and elongation. To confirm this suspicion, additional repetitions will be needed. Even more so since initial analysis revealed differences in the development of gametophytes in the Pp-RS2Z37 knockout line (our own observation, data not shown).

5.4 Multiple stress sources further increase alternative splicing rates in *A.thaliana*

In addition to UV-C radiation as a potent stress source, we included nutrition deprivation as an additional stress factor and analysed changes in gene expression and pre-mRNA splicing via RT-PCR in *A.thaliana* wild type cell suspension cultures (HH1, originated from seedlings, Col-0 ecotype). Besides the idea of an additional stress factor, we also tried to generate more comparable growth conditions, since *P.patens* grows on media without sucrose while *A.thaliana* medium includes sucrose. Another aspect worthy of consideration is the phenomenon of calorie restriction, which has been linked to DNA repair processes. Simply put, caloric restriction describes an extension of the lifespan through a decrease in the calorie uptake. While the underlying mechanisms are as of yet unclear, studies have shown that genes involved in DNA repair processes are expressed differentially [162].

Previous studies have shown that alternative splicing is triggered by a wide range of stress factors, therefore an overlay of multiple factors might provide further insights into the specific regulation of alternative splicing events [46]. In our case, nutrition deprivation is defined by the lack of sucrose in the medium, which serves *A.thaliana* as a nutrition source.

We were able to identify two specific effects due to our experimental conditions.

First, when cultures are subjected to UV-C radiation and nutrition deprivation simultaneously, the general level of gene expression drops. Figures 27 - 29 clearly show that expression rates of almost all alternative splice isoforms are reduced in stressed samples compared to the non-irradiated controls. The second effect is limited to non-irradiated control samples, which still lack sucrose as a nutrition source. Nutrition deprivation itself leads to an increase in alternative splice isoforms other than the correctly spliced IS1 isoform.

Interestingly, we observed an overshoot in the expression of splice isoform IS1 for At-RS31a 30 minutes after UV-C radiation in sucrose supplemented samples. This cellular response is quite peculiar, especially so since an additional 30 minutes later, alternative splicing completely shifts away from IS1 towards IS2 in a 1:1 ratio. Therefore, in a time window of one hour, splicing of At-RS31a pre-mRNAs is completely inverted from an overexpressed, correctly spliced isoform IS1 towards the alternative splice isoform IS2. This effect was not observed in sucrose depleted samples and may be a specific cellular response to UV radiation. However, currently we can only speculate about strategic values of this abrupt shift in alternative splicing and temporal overexpression of IS1.

We were able to identify another interesting pattern of alternative splicing, which was already mentioned before in the experiment regarding DNA damage and the RNA polymerase II (Figure 30). Samples which were kept in dark show a distinct pattern in alternative splicing over a time period of 24 hours. Immediately after UV-C treatment, alternative splicing drifts away from the correctly spliced isoform IS1 towards alternative isoforms. Four to eight hours post irradiation, this shift is reversed towards IS1 once again, which arguably coincides with a progress in DNA repair. We observed this pattern for At-RS31, At-RS31a, At-RS40, At-RS41, At-RS2Z33, At-SR30 and At-SR34.

Our findings show that a lack of sucrose leads to an increase in alternative splicing and a combination of UV-C radiation and nutrition deprivation lowers the general level of gene expression in *A.thaliana* cell suspension cultures. As a result, recovery to control-like expression and splicing patterns is delayed in comparison to sucrose supplemented, UV-C irradiated samples, especially in dark exposed samples. As a possible interpretation of our findings, one might regard increased alternative splicing

rates and lowered levels of gene expression as a "defence" mechanism to prevent the production of proteins from erroneous templates till DNA damage is repaired. Interestingly, we conducted a series of experiments in *P.patens*, which included sucrose containing media. UV-C treated samples, which grew on sucrose supplemented media died faster than samples that grew on non-sucrose containing media (data not shown). These observations might hint towards a possible defence mechanism and, maybe, towards the phenomenon of calorie restriction.

5.5 Looking for a connection between alternative splicing, DNA damage repair and the status of the RNA polymerase II

Numerous studies have shown that splicing occurs cotranscriptional and is tightly connected to the activity of the RNA polymerase II [84, 96, 43]. The C-terminal domain of the Pol II acts as a binding site for splicing regulators, such as SR proteins, which directly bind to the emerging transcript. If the DNA is damaged due to various stress sources, the Pol II is stalled at the site of transcription until the damage has been repaired. In addition, as a result of the systemic response to DNA damage, the CTD is hyperphosphorylated, thus Pol II works slower, which in turn leads to a drop in the elongation rate and ultimately to the higher accessibility of weaker splice sites to the splicing machinery. During this time, weaker splice sites might be already accessible to splicing factors and thus are favoured over stronger, but not yet transcribed splice sites. These circumstances effectively give rise to alternative splicing of nascent pre-mRNAs. However, these alternative splice isoforms do not code for the "correctly" spliced transcript. They more likely either code for heavily truncated proteins or are non-protein-coding due to multiple premature termination codons. We tried to address the question whether these alternative splice isoforms have a function besides being degraded.

We first formulated this question when we observed a shift in alternative splicing of several SR pre-mRNAs, which happens along time after DNA has been damaged via UV-C irradiation (Figure 30). 30 minutes to one hour after UV-C treatment, the concentration of the correctly spliced isoform IS1 drops, while the alternative splice

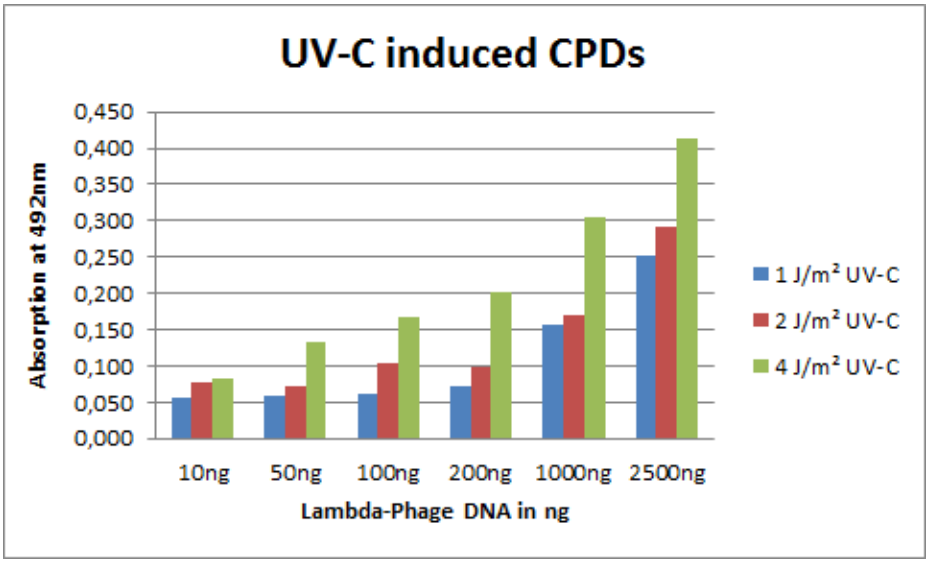

Figure 37: **Detection of UV-C induced CPDs in λ-Phage DNA.** Shown are ELISA-controls, carried out to determine the actual antibody-sensitivity. λ-Phage DNA was irradiated with 1, 2 and 4 J/m^2 of UV-C to induce the formation of CPDs. Radiation values are low due to the fact that naked DNA was used. Varying amounts of DNA were irradiated to verify the detection limit of the CPD-detecting antibody. It is evident that higher doses of UV-C radiation lead to more accurate detection results, especially when low amounts of DNA are used. Shown data represents 6 technical replicates.

isoform IS2 steadily increases. From four to 24 hours after UV-C irradiation, this trend reverts towards IS1 again. We hypothesized that DNA damage repair might coincide with the shift towards the correctly spliced isoform. However, this raises another question. If the Pol II is stalled at the site of transcription during DNA damage, why is this shift not happening immediately after the damage site is repaired? A possible explanation might be that the Pol II is continuously trying to transcribe as the damage site is being repaired base by base. During this phase, a feedback quality control mechanism might exist, which communicates between alternative splice isoforms and the Pol II. In this case, alternative splice isoforms would work as an indicator of the DNA repair progress for the Pol II. However, current debates evolve around the question whether the RNA polymerase II is ubiquitinylated and subsequently degraded upon stalling at the site of transcription, which would potentially negate the above stated idea. Further studies will be needed to resolve this problem.

Anyhow, to prove our own wild theory we first tried to monitor the repair of UV-C induced DNA damage along 24 hours by using CPD-binding antibodies in connection with ELISA (Figure 31). However, due to inaccurate protocol details we faced a

quite severe problem regarding DNA damage detection. Unfortunately, the detection sensitivity of the employed antibody was nowhere near the claimed accuracy level, even though we used 200 instead of 100 J/m^2 UV-C radiation, which already inflicts a higher amount of CPDs and thus should simplify the detection process in the first place. Figure 37 shows the detection of CPDs in λ-phage DNA control ELISAs. Only with an increasing dose of UV-C could we accurately detect CPDs in 50 ng DNA. For our main experiment we used 40 ng DNA per sample, which was already four times the amount the protocol suggested. To fully understand this dilemma, one should note that DNA isolation in plants is quite unprofitable, meaning that the isolated amounts are humble to say the least. Furthermore, one cannot simply increase the dose of UV-C radiation at will since this might inhibit DNA repair mechanisms or simply kill the plants immediately. Thus we were stuck with limited amounts of DNA, which were already irradiated to the limit. However, trends can be seen in the data we produced (Figure 31). Plants which were kept in the light clearly show a reduction of CPDs after 24 hours, indicating that repair mechanisms are indeed active and working. In contrast, CPD detection in plants kept in the dark after UV-C treatment stays approximately the same, indicating less effective repair mechanisms. This in turn might implicate that the DNA damage is being repaired by photoreactivation in light exposed samples. Additionally, we included different genetic backgrounds of *A.thaliana* for this experiment. At-RS31 has been shown to negatively regulate At-RAD1 (Kalyna et al., unpublished), therefore an overexpression of At-RS31 should result in hampered DNA repair through nucleotide excision. On the contrary, At-RS31 knockout should show an increase in DNA repair effectiveness since the negative regulation of At-RAD1 drops out. Last but not least we included *A.thaliana* plants defective in the expression of At-RAD1, which should result in severe DNA repair defects. Our ELISA readouts partially confirm these predictions. With the exception of dark exposed plants four hours after UV-C treatment, CPD intensity is highest in At-RAD1 knockout plants, followed by plants overexpressing At-RS31. However, our main interest lay on the coincidence of DNA damage repair and the appearance of shifting alternative splicing patterns towards the correctly spliced isoform. In fact, this interest has been cautiously satisfied, seeing as DNA damage is in fact being repaired within the time frame of 24 hours in light exposed as well as dark kept plants.

Simultaneously to the detection of CPDs via ELISA, we tried to analyse the phosphorylation status of the RNA polymerase II, since phosphorylation events are known

to dramatically alter the activity of the Pol II. UV-C radiation introduces DNA damage, which triggers a systemic response that, among other things, results in the hyperphosphorylation of the Pol II [96]. Thus, a stalled or slowed down Pol II should be distinguishable from an actively transcribing one through its phosphorylation status. Consequently, by using an antibody which binds to phosphorylation sites on the Pol II, it should be possible to determine when the DNA damage is being cleared and the Pol II resumes transcription. Additionally, current debates highlight the possibility of ubiquitinilation and subsequent degradation of the Pol II after UV induced damage. Thus, by using an antibody which recognizes the whole pool of RNA Pol II, we may be able to extract hints about the relation between the amount of Pol II and its phosphorylation status on one side, and alternative splicing patterns in connection to a drop down of gene expression on the other side.

Figure 32 summarizes the results of this experiment. Interestingly, UV-C treated samples show a steady decline in Pol II detection over time. This may indicate the degradation of the Pol II after UV irradiation, which would fit into the current debate on ubiquitinilation and subsequent degradation of the Pol II after UV treatment. We can state that 24 hours is not a sufficient amount of time for a complete recovery of the Pol II signal.

In summary, at this point our theory remains just that. However, by refining ELISA protocols and the addition of further experiments targeting the RNA polymerase II, some more much needed light will be surely shed on this topic.

5.6 Partial knockdown of At-SR30, At-RS41 and At-SC35 through amiRNAs

We were able to achieve a partial knockdown of At-SR30, At-RS41 and At-SC35 in the F1 generation in *A.thaliana* through the application of artificial microRNAs supplied by the Cold Spring Harbor Laboraties (Figure 35, 36). While knockdowns for At-RS41 and At-SC35 are not as prominent as for At-SR30, it should be mentioned that the F1 generations are only heterozygous regarding the stable insertions of these amiRNA constructs. Further efforts will give rise to homozygous F2 generations, which should show even more prominent knockdowns of these SR genes. While we

were not able to observe phenotypical changes for the *A.thaliana* lines CSHL_011244 and CSHL_078707, initial observations indicated that CSHL_082339 positive plants might be sterile. However, more transformed CSHL_082339 plants will have to be selected to prove this suspicion.

5.7 Outlook

After all the results presented here, interesting follow up studies will surely be launched. Our initial UV-C related studies in *A.thaliana* have uncovered fascinating feedback and regulatory mechanisms within the SR family. Through the realization of additional SR knockout and overexpression lines more interactions will be discovered, which will add to our understanding of the roles of SR proteins during constitutive and alternative splicing. Especially closely related paralogous genes will be an interesting subject of investigation, since their functions are often cryptic. Such genes most commonly emerge through genome duplication events. However, paralogous genes might slightly differ in their gene structure and thus have evolved diverging functions. Yet, to uncover the part they are playing, knockout approaches are often an ill choice since usually both genes are eliminated via such an approach exactly because of their close sequence relations. Therefore, (a)miRNA mediated knockdown approaches might prove extremely useful in this area of research. By applying specifically designed miRNAs it is possible to target sequence stretches which are unique to the one, but not the other closely related gene.

Another topic which might still hold luring secrets is the role non-protein-coding alternative splice isoforms play during RNA polymerase II stalling caused by DNA damage. Unfortunately, our initial experiments regarding this question were ill equipped. However, this should not discourage any follow up studies but rather motivate them to apply elaborate well thought out ideas to shed more light on this topic.

Besides our experiments dealing with *A.thaliana*, we also adapted a new lab pet, *Physcomitrella patens*. This extremely accessible ancient moss is an ideal, emerging model organism because of its unique features regarding gene targeting and evolution. Our results give rise to a plenitude of indications and potential goals for further studies. We were able to show that regulation of alternative splicing through SR

proteins might differ in certain aspects to *A.thaliana*, which might be due to specific adaptations caused by evolutionary pressure. Our lab was also able to establish stable knockout lines, making use of *P.patens* uncommonly high rate of homologous recombination. *P.patens* is still a young model organism, which holds a smorgasbord of questions and secrets which need to be uncovered. Therefore our work with this fascinating moss will surely continue.

Bibliography

[1] D. Adams. *The hitch hiker's guide to the galaxy: a trilogy in five parts*. Number 1. William Heinemann, 1997.

[2] S. Leonelli. Arabidopsis, the botanical drosophila: from mouse cress to model organism. *Endeavour*, 31(1):34–38, 2007.

[3] M. Koornneef and D. Meinke. The development of arabidopsis as a model plant. *The Plant Journal*, 61(6):909–921, 2010.

[4] C. Somerville and M. Koornneef. A fortunate choice: the history of arabidopsis as a model plant. *Nature Reviews Genetics*, 3(11):883–889, 2002.

[5] G.P. Redei. Arabidopsis as a genetic tool. *Annual review of genetics*, 9(1):111–127, 1975.

[6] E.M. Meyerowitz. *Arabidopsis*, volume 27. Cold Spring Harbor Laboratory Pr, 1994.

[7] D.W. Meinke, J.M. Cherry, C. Dean, S.D. Rounsley, and M. Koornneef. Arabidopsis thaliana: a model plant for genome analysis. *Science*, 282(5389):662, 1998.

[8] J.J. Doyle, L.E. Flagel, A.H. Paterson, R.A. Rapp, D.E. Soltis, P.S. Soltis, and J.F. Wendel. Evolutionary genetics of genome merger and doubling in plants. *Annual Review of Genetics*, 42:443–461, 2008.

[9] S.J. Clough and A.F. Bent. Floral dip: a simplified method foragrobacterium-mediated transformation ofarabidopsis thaliana. *The Plant Journal*, 16(6):735–743, 1998.

[10] M. Lagos-Quintana, R. Rauhut, W. Lendeckel, and T. Tuschl. Identification of novel genes coding for small expressed rnas. *Science*, 294(5543):853, 2001.

[11] N.C. Lau, L.P. Lim, E.G. Weinstein, and D.P. Bartel. An abundant class of tiny rnas with probable regulatory roles in caenorhabditis elegans. *Science*, 294(5543):858, 2001.

[12] R.C. Lee and V. Ambros. An extensive class of small rnas in caenorhabditis elegans. *Science*, 294(5543):862, 2001.

[13] S. Niemeier, L. Alves, and T. Merkle. Improvement of the design and generation of highly specific plant knockdown lines using primary synthetic micrornas (prismirnas). *BMC Research Notes*, 3(1):59, 2010.

[14] K. Kroemer, R. Reski, and W. Frank. Abiotic stress response in the moss physcomitrella patens: evidence for an evolutionary alteration in signaling pathways in land plants. *Plant Cell Reports*, 22(11):864–870, 2004.

[15] L. Wolf, L. Rizzini, R. Stracke, R. Ulm, and S.A. Rensing. The molecular and physiological responses of physcomitrella patens to ultraviolet-b radiation. *Plant physiology*, 153(3):1123, 2010.

[16] D. Lang, A.D. Zimmer, S.A. Rensing, and R. Reski. Exploring plant biodiversity: the physcomitrella genome and beyond. *Trends in plant science*, 13(10):542–549, 2008.

[17] D. Cove. The moss physcomitrella patens. *Annu. Rev. Genet.*, 39:339–358, 2005.

[18] S.F. McDaniel, M. Von Stackelberg, S. Richardt, R.S. Quatrano, R. Reski, and S.A. Rensing. The speciation history of the physcomitriumphyscomitrella species complex. *Evolution*, 64(1):217–231, 2010.

[19] P.P. Engel. The induction of biochemical and morphological mutants in the moss physcomitrella patens. *American Journal of Botany*, pages 438–446, 1968.

[20] M.J. Prigge and M. Bezanilla. Evolutionary crossroads in developmental biology: Physcomitrella patens. *Development*, 137(21):3535, 2010.

[21] S.A. Rensing, D. Lang, A.D. Zimmer, A. Terry, A. Salamov, H. Shapiro, T. Nishiyama, P.F. Perroud, E.A. Lindquist, Y. Kamisugi, et al. The physcomitrella genome reveals evolutionary insights into the conquest of land by plants. *Science*, 319(5859):64, 2008.

[22] S. Rensing, D. Fritzowsky, D. Lang, and R. Reski. Protein encoding genes in an ancient plant: analysis of codon usage, retained genes and splice sites in a moss, physcomitrella patens. *BMC genomics*, 6(1):43, 2005.

[23] G. Brücker, F. Mittmann, E. Hartmann, and T. Lamparter. Targeted site-directed mutagenesis of a heme oxygenase locus by gene replacement in the moss ceratodon purpureus. *Planta*, 220(6):864–874, 2005.

[24] W. Kammerer and D.J. Cove. Genetic analysis of the effects of re-transformation of transgenic lines of the mossphyscomitrella patens. *Molecular and General Genetics MGG*, 250(3):380–382, 1996.

[25] D.G. Schaefer and J.P. Zrÿd. Efficient gene targeting in the moss physcomitrella patens. *The Plant Journal*, 11(6):1195–1206, 1997.

[26] R. Strepp, S. Scholz, S. Kruse, V. Speth, and R. Reski. Plant nuclear gene knockout reveals a role in plastid division for the homolog of the bacterial cell division protein ftsz, an ancestral tubulin. *Proceedings of the National Academy of Sciences*, 95(8):4368, 1998.

[27] L.T. Chow, R.E. Gelinas, T.R. Broker, and R.J. Roberts. An amazing sequence arrangement at the 5'ends of adenovirus 2 messenger rna. *Cell*, 12(1):1–8, 1977.

[28] S.M. Berget, C. Moore, and P.A. Sharp. Spliced segments at the 5'terminus of adenovirus 2 late mrna. *Proceedings of the National Academy of Sciences*, 74(8):3171, 1977.

[29] A.J. Matlin, F. Clark, and C.W.J. Smith. Understanding alternative splicing: towards a cellular code. *Nature Reviews Molecular Cell Biology*, 6(5):386–398, 2005.

[30] A. Barta and D. Schümperli. Editorial on alternative splicing and disease. *RNA biology*, 7(4):388, 2010.

[31] A.S.N. Reddy. Alternative splicing of pre-messenger rnas in plants in the genomic era. *Annu. Rev. Plant Biol.*, 58:267–294, 2007.

[32] M.C. Wahl, C.L. Will, and R. Lührmann. The spliceosome: design principles of a dynamic rnp machine. *Cell*, 136(4):701–718, 2009.

[33] D.L. Black. Mechanisms of alternative pre-messenger rna splicing. *Annual review of biochemistry*, 72(1):291–336, 2003.

[34] N. Toor, K.S. Keating, S.D. Taylor, and A.M. Pyle. Crystal structure of a self-spliced group ii intron. *Science*, 320(5872):77, 2008.

[35] A.A. Patel and J.A. Steitz. Splicing double: insights from the second spliceosome. *Nature Reviews Molecular Cell Biology*, 4(12):960–970, 2003.

[36] M.M. Konarska, J. Vilardell, and C.C. Query. Repositioning of the reaction intermediate within the catalytic center of the spliceosome. *Molecular cell*, 21(4):543–553, 2006.

[37] B. Modrek and C. Lee. A genomic view of alternative splicing. *Nature genetics*, 30(1):13–19, 2002.

[38] H. Keren, G. Lev-Maor, and G. Ast. Alternative splicing and evolution: diversification, exon definition and function. *Nat Rev Genet*, 11(5):345–355, 2010.

[39] B.P. Lewis, R.E. Green, and S.E. Brenner. Evidence for the widespread coupling of alternative splicing and nonsense-mediated mrna decay in humans. *Proceedings of the National Academy of Sciences*, 100(1):189, 2003.

[40] D.A.W. Soergel, L.F. Lareau, and S.E. Brenner. Regulation of gene expression by coupling of alternative splicing and nmd. *Nonsense-mediated mRNA decay*, pages 175–96, 2006.

[41] S.A. Filichkin, H.D. Priest, S.A. Givan, R. Shen, D.W. Bryant, S.E. Fox, W.K. Wong, and T.C. Mockler. Genome-wide mapping of alternative splicing in arabidopsis thaliana. *Genome research*, 20(1):45, 2010.

[42] D. Schmucker and J.G. Flanagan. Generation of recognition diversity in the nervous system. *Neuron*, 44(2):219–222, 2004.

[43] R.F. Luco, M. Allo, I.E. Schor, A.R. Kornblihtt, and T. Misteli. Epigenetics in alternative pre-mrna splicing. *Cell*, 144(1):16–26, 2011.

[44] SP Dinesh-Kumar and B.J. Baker. Alternatively spliced n resistance gene transcripts: their possible role in tobacco mosaic virus resistance. *Proceedings of the National Academy of Sciences*, 97(4):1908, 2000.

[45] X.C. Zhang and W. Gassmann. Rps4-mediated disease resistance requires the combined presence of rps4 transcripts with full-length and truncated open reading frames. *The Plant Cell Online*, 15(10):2333, 2003.

[46] S.G. Palusa, G.S. Ali, and A.S.N. Reddy. Alternative splicing of pre-mrnas of arabidopsis serine/arginine-rich proteins: regulation by hormones and stresses. *The Plant Journal*, 49(6):1091–1107, 2007.

[47] ASN Reddy. Nuclear pre-mrna splicing in plants. *Critical reviews in plant sciences*, 20(6):523–571, 2001.

[48] N. Hopf, N. Plesofsky-Vig, and R. Brambl. The heat shock response of pollen and other tissues of maize. *Plant molecular biology*, 19(4):623–630, 1992.

[49] M. Kalyna, S. Lopato, and A. Barta. Ectopic expression of atrsz33 reveals its function in splicing and causes pleiotropic changes in development. *Molecular biology of the cell*, 14(9):3565, 2003.

[50] S. Lopato, M. Kalyna, S. Dorner, R. Kobayashi, A.R. Krainer, and A. Barta. atsrp30, one of two sf2/asf-like proteins from arabidopsis thaliana, regulates splicing of specific plant genes. *Genes & development*, 13(8):987, 1999.

[51] X.Y. Zhong, P. Wang, J. Han, M.G. Rosenfeld, and X.D. Fu. Sr proteins in vertical integration of gene expression from transcription to rna processing to translation. *Molecular cell*, 35(1):1–10, 2009.

[52] M.B. Roth, C. Murphy, and J.G. Gall. A monoclonal antibody that recognizes a phosphorylated epitope stains lampbrush chromosome loops and small granules in the amphibian germinal vesicle. *The Journal of cell biology*, 111(6):2217, 1990.

[53] Y. Huang and J.A. Steitz. Srprises along a messenger's journey. *Molecular cell*, 17(5):613–615, 2005.

[54] J. Long and J. Caceres. The sr protein family of splicing factors: master regulators of gene expression. *Biochem. J*, 417:15–27, 2009.

[55] C.F. Bourgeois, F. Lejeune, and J. Stevenin. Broad specificity of sr (serinearginine) proteins in the regulation of alternative splicing of pre-messenger rna. *Progress in nucleic acid research and molecular biology*, 78:37–88, 2004.

[56] S.F. van Bentem, D. Anrather, E. Roitinger, A. Djamei, T. Hufnagl, A. Barta, E. Csaszar, I. Dohnal, D. Lecourieux, and H. Hirt. Phosphoproteomics reveals extensive in vivo phosphorylation of arabidopsis proteins involved in rna metabolism. *Nucleic acids research*, 34(11):3267, 2006.

[57] T. Feilner, C. Hultschig, J. Lee, S. Meyer, R.G.H. Immink, A. Koenig, A. Possling, H. Seitz, A. Beveridge, D. Scheel, et al. High throughput identification of potential arabidopsis mitogen-activated protein kinases substrates. *Molecular & Cellular Proteomics*, 4(10):1558, 2005.

[58] M. Golovkin and A.S.N. Reddy. An sc35-like protein and a novel serine/arginine-rich protein interact with arabidopsis u1-70k protein. *Journal of Biological Chemistry*, 274(51):36428, 1999.

[59] S. Savaldi-Goldstein, D. Aviv, O. Davydov, and R. Fluhr. Alternative splicing modulation by a lammer kinase impinges on developmental and transcriptome expression. *The Plant Cell Online*, 15(4):926, 2003.

[60] H. Shen and M.R. Green. Rs domains contact splicing signalsand promote splicing by a commonmechanism in yeast through humans. *Genes & development*, 20(13):1755, 2006.

[61] S. Lopato, A. Mayeda, A.R. Krainer, and A. Barta. Pre-mrna splicing in plants: characterization of ser/arg splicing factors. *Proceedings of the National Academy of Sciences*, 93(7):3074, 1996.

[62] A. Barta, M. Kalyna, and A.S.N. Reddy. Implementing a rational and consistent nomenclature for serine/arginine-rich protein splicing factors (sr proteins) in plants. *The Plant Cell Online*, 22(9):2926, 2010.

[63] K. Iida and M. Go. Survey of conserved alternative splicing events of mrnas encoding sr proteins in land plants. *Molecular biology and evolution*, 23(5):1085, 2006.

[64] M. Isshiki, A. Tsumoto, and K. Shimamoto. The serine/arginine-rich protein family in rice plays important roles in constitutive and alternative splicing of pre-mrna. *The Plant Cell Online*, 18(1):146, 2006.

[65] A.S.N. Reddy. Plant serine/arginine-rich proteins and their role in pre-mrna splicing. *Trends in plant science*, 9(11):541–547, 2004.

[66] M. Kalyna and A. Barta. A plethora of plant serine/arginine-rich proteins: redundancy or evolution of novel gene functions? *Biochemical Society Transactions*, 32(Pt 4):561, 2004.

[67] C. Simillion, K. Vandepoele, M.C.E. Van Montagu, M. Zabeau, and Y. Van de Peer. The hidden duplication past of arabidopsisthaliana. *Proceedings of the National Academy of Sciences of the United States of America*, 99(21):13627, 2002.

[68] A. Barta, M. Kalyna, and ZJ Lorković. Plant sr proteins and their functions. *Nuclear pre-mRNA Processing in Plants*, pages 83–102, 2008.

[69] M. Golovkin and A.S.N. Reddy. The plant u1 small nuclear ribonucleoprotein particle 70k protein interacts with two novel serine/arginine–rich proteins. *The Plant Cell Online*, 10(10):1637, 1998.

[70] G. Lazar, T. Schaal, T. Maniatis, and H.M. Goodman. Identification of a plant serine-arginine-rich protein similar to the mammalian splicing factor sf2/asf. *Proceedings of the National Academy of Sciences*, 92(17):7672, 1995.

[71] S. Lopato, R. Gattoni, G. Fabini, J. Stevenin, and A. Barta. A novel family of plant splicing factors with a zn knuckle motif: examination of rna binding and splicing activities. *Plant molecular biology*, 39(4):761–773, 1999.

[72] S. Lopato, C. Forstner, M. Kalyna, J. Hilscher, U. Langhammer, K. Indrapichate, Z.J. Lorković, and A. Barta. Network of interactions of a novel plant-specific arg/ser-rich protein, atrsz33, with atsc35-like splicing factors. *Journal of Biological Chemistry*, 277(42):39989, 2002.

[73] Z.J. Lorković and A. Barta. Genome analysis: Rna recognition motif (rrm) and k homology (kh) domain rna-binding proteins from the flowering plant arabidopsis thaliana. *Nucleic acids research*, 30(3):623, 2002.

[74] G. Lazar and H.M. Goodman. The arabidopsis splicing factor sr1 is regulated by alternative splicing. *Plant molecular biology*, 42(4):571–581, 2000.

[75] M. Kalyna, S. Lopato, V. Voronin, and A. Barta. Evolutionary conservation and regulation of particular alternative splicing events in plant sr proteins. *Nucleic acids research*, 34(16):4395, 2006.

[76] B.B. Wang and V. Brendel. Genomewide comparative analysis of alternative splicing in plants. National Acad Sciences, 2006.

[77] S. Lopato, E. Waigmann, and A. Barta. Characterization of a novel arginine/serine-rich splicing factor in arabidopsis. *The Plant Cell Online*, 8(12):2255, 1996.

[78] T. Jordan, S. Schornack, and T. Lahaye. Alternative splicing of transcripts encoding toll-like plant resistance proteins-what's the functional relevance to innate immunity? *Trends in plant science*, 7(9):392–398, 2002.

[79] K.R. Luehrsen, S. Taha, and V. Walbot. Nuclear pre-mrna processing in higher plants. *Progress in nucleic acid research and molecular biology*, 47:149–193, 1994.

[80] K. Iida, M. Seki, T. Sakurai, M. Satou, K. Akiyama, T. Toyoda, A. Konagaya, and K. Shinozaki. Genome-wide analysis of alternative pre-mrna splicing in arabidopsis thaliana based on full-length cdna sequences. *Nucleic acids research*, 32(17):5096, 2004.

[81] Y. Fang, S. Hearn, and D.L. Spector. Tissue-specific expression and dynamic organization of sr splicing factors in arabidopsis. *Molecular biology of the cell*, 15(6):2664, 2004.

[82] D. Longman, I.L. Johnstone, and J.F. Cáceres. Functional characterization of sr and sr-related genes in caenorhabditis elegans. *The EMBO journal*, 19(7):1625–1637, 2000.

[83] Z.J. Lorkovic and A. Barta. Compartmentalization of the splicing machinery in plant cell nuclei. *Trends in plant science*, 9(12):565–568, 2004.

[84] AL Beyer and YN Osheim. Splice site selection, rate of splicing, and alternative splicing on nascent transcripts. *Genes & development*, 2(6):754, 1988.

[85] G. Bird, D.A.R. Zorio, and D.L. Bentley. Rna polymerase ii carboxy-terminal domain phosphorylation is required for cotranscriptional pre-mrna splicing and 3'-end formation. *Molecular and cellular biology*, 24(20):8963, 2004.

[86] T. Misteli and D.L. Spector. Rna polymerase ii targets pre-mrna splicing factors to transcription sites in vivo. *Molecular cell*, 3(6):697–705, 1999.

[87] C. Attanasio, A. David, and M. Neerman-Arbez. Outcome of donor splice site mutations accounting for congenital afibrinogenemia reflects order of intron removal in the fibrinogen alpha gene (fga). *Blood*, 101(5):1851, 2003.

[88] G. Baurén and L. Wieslander. Splicing of balbiani ring 1 gene pre-mrna occurs simultaneously with transcription. *Cell*, 76(1):183–192, 1994.

[89] O. Kessler, Y. Jiang, and LA Chasin. Order of intron removal during splicing of endogenous adenine phosphoribosyltransferase and dihydrofolate reductase pre-mrna. *Molecular and cellular biology*, 13(10):6211, 1993.

[90] M.F. LeMaire and C.S. Thummel. Splicing precedes polyadenylation during drosophila e74a transcription. *Molecular and cellular biology*, 10(11):6059, 1990.

[91] L.P. Eperon, I.R. Graham, A.D. Griffiths, and I.C. Eperon. Effects of rna secondary structure on alternative splicing of pre-mrna: is folding limited to a region behind the transcribing rna polymerase? *Cell*, 54(3):393–401, 1988.

[92] G.C. Roberts, C. Gooding, H.Y. Mak, C.W.J. Smith, and N.J. Proudfoot. Co-transcriptional commitment to alternative splice site selection. *Nucleic acids research*, 26(24):5568, 1998.

[93] P. Cramer, C.G. Pesce, F.E. Baralle, and A.R. Kornblihtt. Functional association between promoter structure and transcript alternative splicing. *Proceedings of the National Academy of Sciences*, 94(21):11456, 1997.

[94] P. Cramer, J.F. Cáceres, D. Cazalla, S. Kadener, A.F. Muro, F.E. Baralle, and A.R. Kornblihtt. Coupling of transcription with alternative splicing:: Rna pol ii promoters modulate sf2/asf and 9g8 effects on an exonic splicing enhancer. *Molecular cell*, 4(2):251–258, 1999.

[95] A.R. Kornblihtt. Promoter usage and alternative splicing. *Current opinion in cell biology*, 17(3):262–268, 2005.

[96] M.J. Muñoz, M. Santangelo, M.P. Paronetto, M. de la Mata, F. Pelisch, S. Boireau, K. Glover-Cutter, C. Ben-Dov, M. Blaustein, J.J. Lozano, et al. Dna damage regulates alternative splicing through inhibition of rna polymerase ii elongation. *Cell*, 137(4):708–720, 2009.

[97] N. Tuteja, P. Ahmad, B.B. Panda, and R. Tuteja. Genotoxic stress in plants: shedding light on dna damage, repair and dna repair helicases. *Mutation Research/Reviews in Mutation Research*, 681(2-3):134–149, 2009.

[98] S. Mahajan and N. Tuteja. Cold, salinity and drought stresses: an overview. *Archives of Biochemistry and Biophysics*, 444(2):139–158, 2005.

[99] E.A. Bray, J. Bailey-Serres, and E. Weretilnyk. Responses to abiotic stresses. *Biochemistry and molecular biology of plants*, pages 1158–1203, 2000.

[100] A.B. Britt. Molecular genetics of dna repair in higher plants. *Trends in plant science*, 4(1):20–25, 1999.

[101] N. Tuteja, M.B. Singh, M.K. Misra, P.L. Bhalla, and R. Tuteja. Molecular mechanisms of dna damage and repair: Progress in plants. *Critical Reviews in Biochemistry and Molecular Biology*, 36(4):337–397, 2001.

[102] C.M. Bray and C.E. West. Dna repair mechanisms in plants: crucial sensors and effectors for the maintenance of genome integrity. *New phytologist*, 168(3):511–528, 2005.

[103] D.L. Mitchell and R.S. Nairn. The biology of the (6-4) photoproduct. *Photochemistry and photobiology*, 49(6):805, 1989.

[104] W.G. McGregor. Dna repair, dna replication, and uv mutagenesis. In *Journal of Investigative Dermatology Symposium Proceedings*, volume 4, pages 1–5. Nature Publishing Group, 1999.

[105] B. Demple and L. Harrison. Repair of oxidative damage to dna: enzymology and biology. *Annual Review of Biochemistry*, 63(1):915–948, 1994.

[106] D.M. Hodges, C.J. Andrews, D.A. Johnson, and R.I. Hamilton. Antioxidant enzyme and compound responses to chilling stress and their combining abilities in differentially sensitive maize hybrids. *Crop science*, 37(3):857–863, 1997.

[107] R.R. Wise and A.W. Naylor. Chilling-enhanced photooxidation: the peroxidative destruction of lipids during chilling injury to photosynthesis and ultrastructure. *Plant Physiology*, 83(2):272, 1987.

[108] L.O. Björn. Effects of ozone depletion and increased uv-b on terrestrial ecosystems. *International journal of environmental studies*, 51(3):217–243, 1996.

[109] G.I. Jenkins. Signal transduction in responses to uv-b radiation. *Annual Review of Plant Biology*, 60:407–431, 2009.

[110] L. Rizzini, J.J. Favory, C. Cloix, D. Faggionato, A. OHara, E. Kaiserli, R. Baumeister, E. Schäfer, F. Nagy, G.I. Jenkins, et al. Perception of uv-b by the arabidopsis uvr8 protein. *Science*, 332(6025):103, 2011.

[111] B.A. Brown, C. Cloix, G.H. Jiang, E. Kaiserli, P. Herzyk, D.J. Kliebenstein, and G.I. Jenkins. A uv-b-specific signaling component orchestrates plant uv protection. *Proceedings of the National Academy of Sciences of the United States of America*, 102(50):18225, 2005.

[112] B.A. Brown and G.I. Jenkins. Uv-b signaling pathways with different fluence-rate response profiles are distinguished in mature arabidopsis leaf tissue by requirement for uvr8, hy5, and hyh. *Plant physiology*, 146(2):576, 2008.

[113] A. Oravecz, A. Baumann, Z. Máté, A. Brzezinska, J. Molinier, E.J. Oakeley, É. Ádám, E. Schäfer, F. Nagy, and R. Ulm. Constitutively photomorphogenic1 is required for the uv-b response in arabidopsis. *The Plant Cell Online*, 18(8):1975, 2006.

[114] S.H.A. Mackerness. Plant responses to ultraviolet-b (uv-b: 280–320 nm) stress: What are the key regulators? *Plant Growth Regulation*, 32(1):27–39, 2000.

[115] M. Brosche and Å. Strid. Molecular events following perception of ultraviolet-b radiation by plants. *Physiologia Plantarum*, 117(1):1–10, 2003.

[116] B. Thomas. Ultraviolet-b-induced stress and changes in gene expression in arabidopsis thaliana: role of signaling pathways controlled by jasmonic acid, ethylene and reactive oxygen species. *Plant, Cell and Environment*, 22:1413–1423, 1999.

[117] SL Surplus, BR Jordan, AM Murphy, JP Carr, B. Thomas, and S.A.H. Mackerness. Ultraviolet-b-induced responses in arabidopsis thaliana: role of salicylic acid and reactive oxygen species in the regulation of transcripts encoding photosynthetic and acidic pathogenesis-related proteins. *Plant, Cell & Environment*, 21(7):685–694, 1998.

[118] A. Sancar, L.A. Lindsey-Boltz, K. Ünsal-Kaçmaz, and S. Linn. Molecular mechanisms of mammalian dna repair and the dna damage checkpoints. *Annual review of biochemistry*, 73(1):39–85, 2004.

[119] JF Bornman, S. Reuber, and YP Cen. Weissenbock, g.(1997). ultraviolet radiation as a stress factor and the role of protective pigments. *Plants and UV-B: responses to environmental changes, 157û168. Cambridge University Press, Cambridge*.

[120] AE Stapleton, CS Thornber, and V. Walbot. Uv-b component of sunlight causes measurable damage in field-grown maize (zea mays l.): developmental and cellular heterogeneity of damage and repair. *Plant Cell and Environment*, 20(3):279–290, 1997.

[121] B.B.S. Zhou and S.J. Elledge. The dna damage response: putting checkpoints in perspective. *Nature*, pages 433–439, 2000.

[122] S. Panda, A. Isbatan, and G.R. Adami. Modification of the atm/atr directed dna damage response state with aging and long after hepatocyte senescence induction in vivo. *Mechanisms of ageing and development*, 129(6):332–340, 2008.

[123] P. Herrlich, M. Karin, and C. Weiss. Supreme enlightenment: damage recognition and signaling in the mammalian uv response. *Molecular cell*, 29(3):279–290, 2008.

[124] C. Schwerk and K. Schulze-Osthoff. Regulation of apoptosis by alternative pre-mrna splicing. *Molecular cell*, 19(1):1–13, 2005.

[125] D.A.P. Rockx, R. Mason, A. Van Hoffen, M.C. Barton, E. Citterio, D.B. Bregman, A.A. Van Zeeland, H. Vrieling, and L.H.F. Mullenders. Uv-induced inhibition of transcription involves repression of transcription initiation and phospho-

rylation of rna polymerase ii. *Proceedings of the National Academy of Sciences*, 97(19):10503, 2000.

[126] M. de la Mata, C.R. Alonso, S. Kadener, J.P. Fededa, M. Blaustein, F. Pelisch, P. Cramer, D. Bentley, and A.R. Kornblihtt. A slow rna polymerase ii affects alternative splicing in vivo. *Molecular cell*, 12(2):525–532, 2003.

[127] A. Yasui and APM Eker. Dna photolyases. *DNA damage and repair*, 2:9–32, 1998.

[128] S. Kimura, Y. Tahira, T. Ishibashi, Y. Mori, T. Mori, J. Hashimoto, and K. Sakaguchi. Dna repair in higher plants; photoreactivation is the major dna repair pathway in non-proliferating cells while excision repair (nucleotide excision repair and base excision repair) is active in proliferating cells. *Nucleic acids research*, 32(9):2760, 2004.

[129] G.B. Sancar. Dna photolyases: physical properties, action mechanism, and roles in dark repair. *Mutation Research/DNA Repair*, 236(2-3):147–160, 1990.

[130] T. Todo. Functional diversity of the dna photolyase/blue light receptor family. *Mutation research. DNA repair*, 434(2):89–97, 1999.

[131] D.P. Batty and R.D. Wood. Damage recognition in nucleotide excision repair of dna. *Gene*, 241(2):193–204, 2000.

[132] O. Maillard, U. Camenisch, K.B. Blagoev, and H. Naegeli. Versatile protection from mutagenic dna lesions conferred by bipartite recognition in nucleotide excision repair. *Mutation Research/Reviews in Mutation Research*, 658(3):271–286, 2008.

[133] D. Mu and A. Sancar. Model for xpc-independent transcription-coupled repair of pyrimidine dimers in humans. *Journal of Biological Chemistry*, 272(12):7570, 1997.

[134] A. Britt. Repair of damaged bases. *The Arabidopsis Book*, 2002.

[135] H. Xu, I. Swoboda, P.L. Bhalla, A.M. Sijbers, C. Zhao, E. Ong, J.H.J. Hoeijmakers, and M.B. Singh. Plant homologue of human excision repair gene ercc1 points to conservation of dna repair mechanisms. *The Plant Journal*, 13(6):823–829, 1998.

[136] Z. Liu, G.S. Hossain, M.A. Islas-Osuna, D.L. Mitchell, and D.W. Mount. Repair of uv damage in plants by nucleotide excision repair: Arabidopsis uvh1 dna repair gene is a homolog of saccharomyces cerevisiae rad1. *The Plant Journal*, 21(6):519–528, 2000.

[137] A. Vidal, N. Abril, and C. Pueyo. Dna repair by ogt alkyltransferase influences ems mutational specificity. *Carcinogenesis*, 16(4):817, 1995.

[138] E.A. Greene, C.A. Codomo, N.E. Taylor, J.G. Henikoff, B.J. Till, S.H. Reynolds, L.C. Enns, C. Burtner, J.E. Johnson, A.R. Odden, et al. Spectrum of chemically induced mutations from a large-scale reverse-genetic screen in arabidopsis. *Genetics*, 164(2):731, 2003.

[139] T. Lindahl and R.D. Wood. Quality control by dna repair. *Science*, 286(5446):1897, 1999.

[140] K.W. Caldecott. Mammalian dna single-strand break repair: an x-ra (y) ted affair. *Bioessays*, 23(5):447–455, 2001.

[141] J.C. Fromme, A. Banerjee, and G.L. Verdine. Dna glycosylase recognition and catalysis. *Current opinion in structural biology*, 14(1):43–49, 2004.

[142] K. Sakumi and M. Sekiguchi. Structures and functions of dna glycosylases. *Mutation research*, 236(2-3):161, 1990.

[143] Y. Matsumoto and K. Kim. Excision of deoxyribose phosphate residues by dna polymerase beta during dna repair. *Science*, 269(5224):699, 1995.

[144] P. Fortini, B. Pascucci, E. Parlanti, R.W. Sobol, S.H. Wilson, and E. Dogliotti. Different dna polymerases are involved in the short-and long-patch base excision repair in mammalian cells. *Biochemistry*, 37(11):3575–3580, 1998.

[145] Y. Nakabeppu, T. Ohtsubo, O. Matsuda, K. Iba, and M. Sekiguchi. Direct submission. *GenBank Accession AB010690*, 1998.

[146] T. Ohtsubo, O. Matsuda, K. Iba, I. Terashima, M. Sekiguchi, and Y. Nakabeppu. Molecular cloning of atmmh, an arabidopsis thaliana ortholog of the escherichia coli mutm gene, and analysis of functional domains of its product. *Molecular and General Genetics MGG*, 259(6):577–590, 1998.

[147] TM Murphy and MJ Gao. Two cdnas encoding arabidopsis thaliana homologs of bacterial formamidopyrimidine-dna glycosylase genes are produced by alternative processing (accession nos. af099970 and af099971). *Plant Physiol*, 118:1535, 1998.

[148] TM Murphy and M.J. Gao. Multiple forms of formamidopyrimidine-dna glycosylase produced by alternative splicing in arabidopsis thaliana. *Journal of Photochemistry and Photobiology B: Biology*, 61(3):87–93, 2001.

[149] D. Valvekens, M.V. Montagu, and M.V. Lijsebettens. Agrobacterium tumefaciens-mediated transformation of arabidopsis thaliana root explants by using kanamycin selection. *Proceedings of the National Academy of Sciences*, 85(15):5536, 1988.

[150] H. Inoue, H. Nojima, and H. Okayama. High efficiency transformation of escherichia coli with plasmids. *Gene*, 96(1):23–28, 1990.

[151] G.R. Harlow, M.E. Jenkins, T.S. Pittalwala, and D.W. Mount. Isolation of uvh1, an arabidopsis mutant hypersensitive to ultraviolet light and ionizing radiation. *The Plant Cell Online*, 6(2):227, 1994.

[152] D. Schaefer, J.P. Zryd, CD Knight, and DJ Cove. Stable transformation of the moss physcomitrella patens. *Molecular and General Genetics MGG*, 226(3):418–424, 1991.

[153] C.G. Simpson, J. Fuller, M. Maronova, M. Kalyna, D. Davidson, J. McNicol, A. Barta, and J.W.S. Brown. Monitoring changes in alternative precursor messenger rna splicing in multiple gene transcripts. *The Plant Journal*, 53(6):1035–1048, 2008.

[154] A. Nakagawa, N. Kobayashi, T. Muramatsu, Y. Yamashina, T. Shirai, M.W. Hashimoto, M. Ikenaga, and T. Mori. Three-dimensional visualization of ultraviolet-induced dna damage and its repair in human cell nuclei. *Journal of investigative dermatology*, 110(2):143–148, 1998.

[155] I.R. Kirsch, E.D. Green, R. Yonescu, R. Strausberg, N. Carter, D. Bentley, M.A. Leversha, I. Dunham, V.V. Braden, E. Hilgenfeld, et al. Isis, the intron information system, reveals the high frequency of alternative splicing in the human genome. *Nature genetics*, 24:341, 2000.

[156] Q. Pan, O. Shai, L.J. Lee, B.J. Frey, and B.J. Blencowe. Deep surveying of alternative splicing complexity in the human transcriptome by high-throughput sequencing. *Nat Genet*, 40(12):1413–1415, 2008.

[157] E.T. Wang, R. Sandberg, S. Luo, I. Khrebtukova, L. Zhang, C. Mayr, S.F. Kingsmore, G.P. Schroth, and C.B. Burge. Alternative isoform regulation in human tissue transcriptomes. *Nature*, 456(7221):470, 2008.

[158] J.F. Cáceres and A.R. Kornblihtt. Alternative splicing: multiple control mechanisms and involvement in human disease. *TRENDS in Genetics*, 18(4):186–193, 2002.

[159] T.A. Cooper, L. Wan, and G. Dreyfuss. Rna and disease. *Cell*, 136(4):777–793, 2009.

[160] E.S. Lander, L.M. Linton, B. Birren, C. Nusbaum, M.C. Zody, J. Baldwin, K. Devon, K. Dewar, M. Doyle, W. FitzHugh, et al. Initial sequencing and analysis of the human genome. *Nature*, 409(6822):860–921, 2001.

[161] A.S.N. Reddy. Extensive coupling of alternative splicing of pre-mrnas of serine/arginine (sr) genes with nonsense-mediated decay. *New Phytologist*, page 1, 2009.

[162] W. Qin, M. Chachich, M. Lane, G. Roth, M. Bryant, R. de Cabo, M.A. Ottinger, J. Mattison, D. Ingram, S. Gandy, et al. Calorie restriction attenuates alzheimer's disease type brain amyloidosis in squirrel monkeys (saimiri sciureus). *Journal of Alzheimer's Disease*, 10(4):417–422, 2006.

Appendix A

Supplementary Data

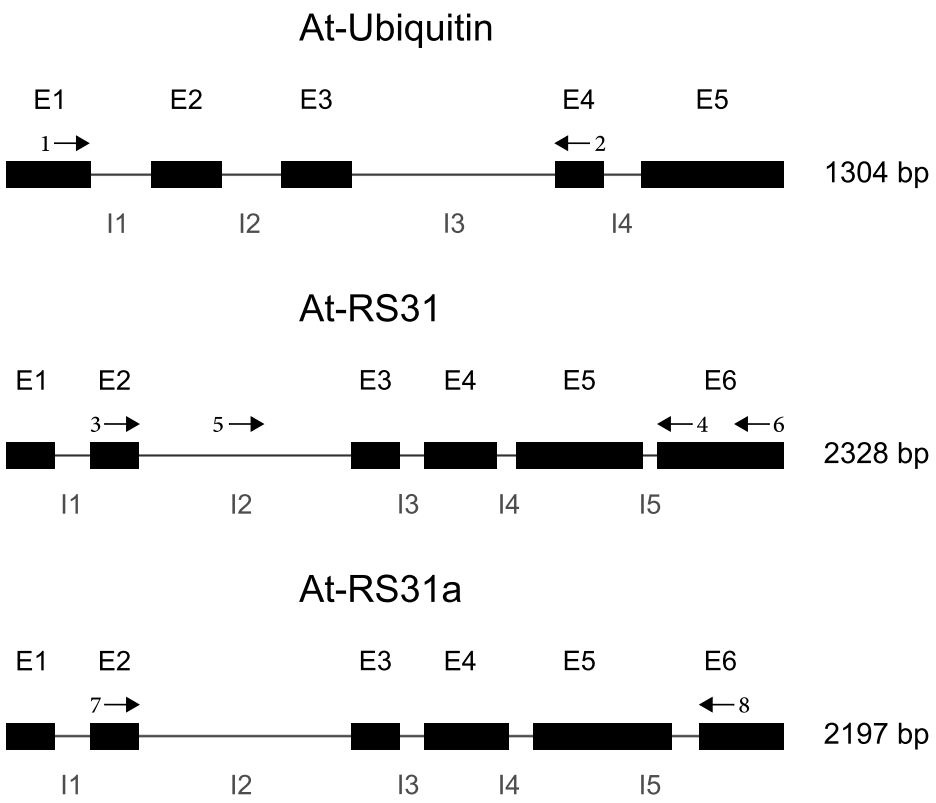

Figure 38: **Gene schemes and primer locations.** Shown are the gene schemes and according primer locations described in the materials section. Black boxes depict exons while intervening lines depict introns. Black arrows point to the location of the primers, numbers next to the arrows correspond to the respective primers, numbered in the materials section. Gene size is indicated by the number on the right side of the gene scheme. Schemes are not in size to actual gene size. Abbrevations: At - *A.thaliana*; Pp - *P.patens*; E - Exon; I - Intron; bp - base pairs

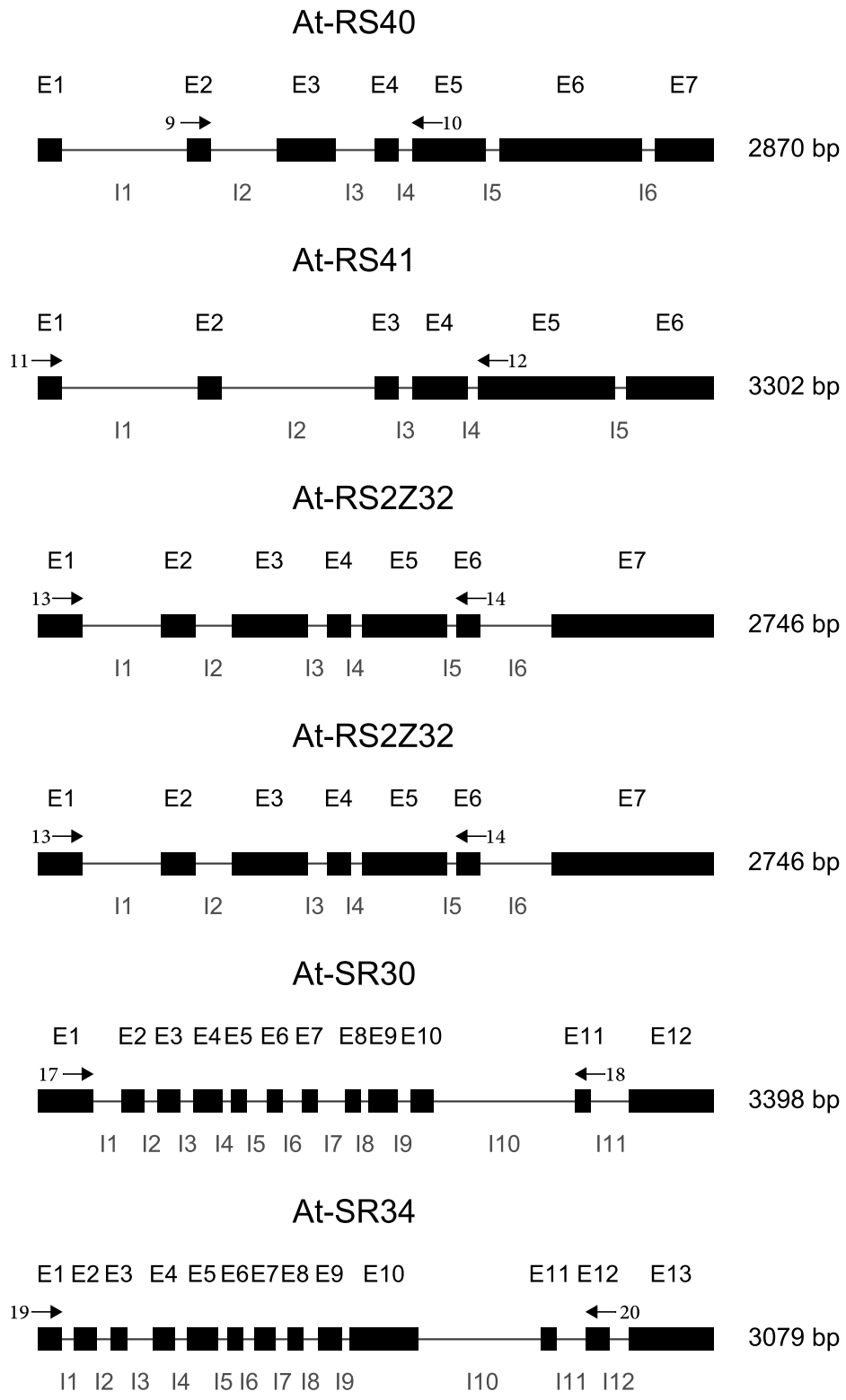

Figure 39: **Gene schemes and primer locations**

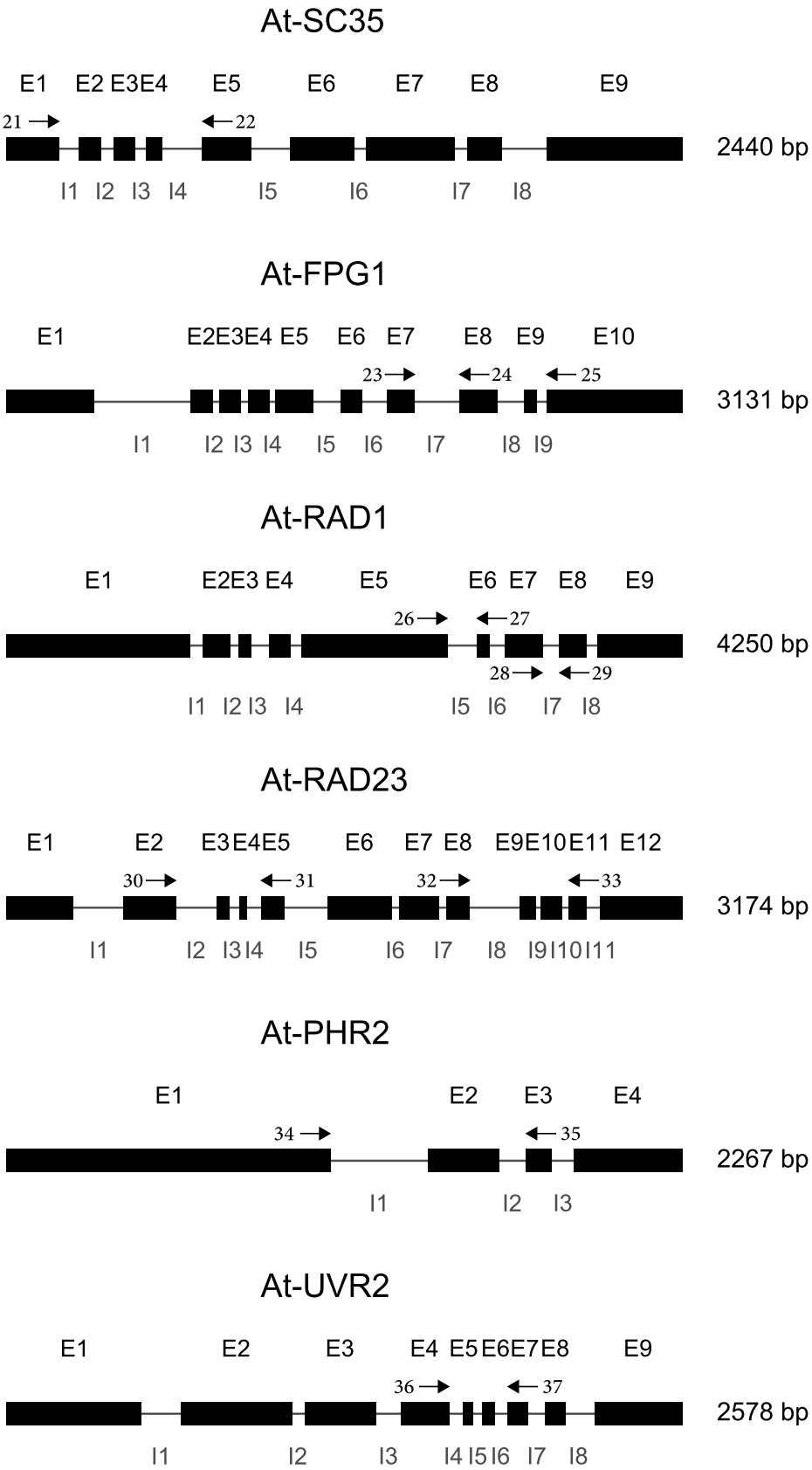

Figure 40: **Gene schemes and primer locations**

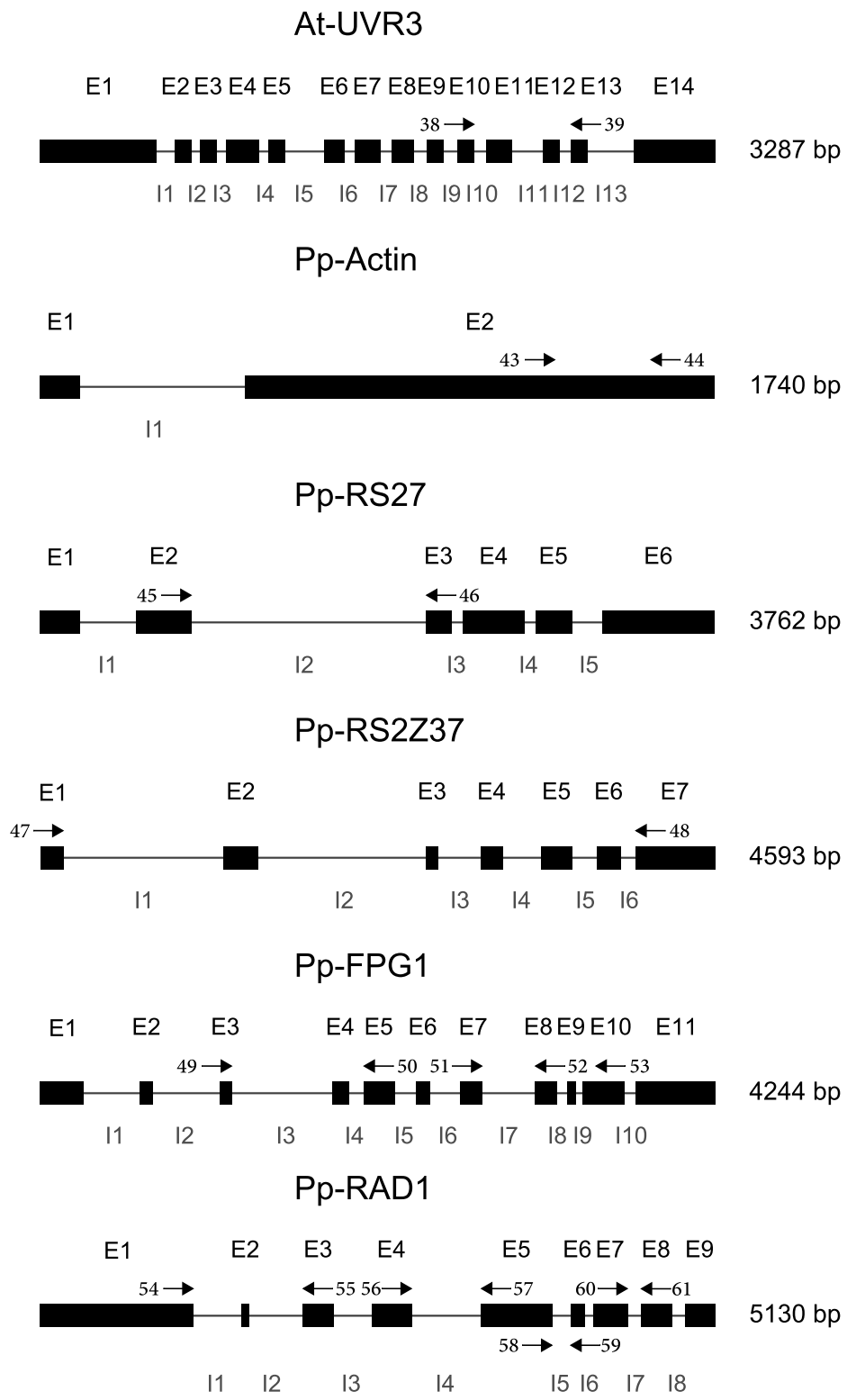

Figure 41: **Gene schemes and primer locations**

Appendix B

Curriculum Vitae

Personal data

Name	Armin Fuchs
Date of birth	28.01.1986
Place of birth	Hall (Tirol, Austria)

Scientific career

Since March 2010	Master's thesis with the title "The effects of UV irradiation on alternative splicing in *A.thaliana* and *P.patens*" in the group of Prof. Barta at the University of Vienna / MFPL

Education

2008 - 2011	Master studies "Molecular Microbiology and Immunobiology" at the University of Vienna (2009/2010 - Performance scholarship; 2011 - Tutor in the practical course of Prof. Meskiene)
2004 - 2008	Bachelor studies "Biology" at the University of Innsbruck
2000 - 2004	Private academic high school (PORG) with special emphasis on ecology, completed with the formal exam "Matura", Volders

Scientific projects / collaborations

May - September 2011	Identification of bacteria in industrially used water - Collaboration of the University of Innsbruck and the company Swarovski, Wattens

Appendix C

Lebenslauf

Persönliche Daten

Name	Armin Fuchs
Geburtsdatum	28.01.1986
Geburtsort	Hall (Tirol, Österreich)

Wissenschaftlicher Werdegang

Seit März 2010	Masterarbeit mit dem Titel "The effects of UV irradiation on alternative splicing in *A.thaliana* and *P.patens*" in der Gruppe von Prof. Barta an der Universität Wien / MFPL

Ausbildung

2008 - 2011	Masterstudium "Molekulare Mikrobiologie und Immunbiologie" an der Universität Wien (2009/2010 - Leistungsstipendium; 2011 - Tutor in den molekularbiologischen Übungen von Prof. Meskiene)
2004 - 2008	Bakkalaureatsstudium "Biologie" an der Universität Innsbruck
2000 - 2004	Privates Oberstufenrealgymnasium (PORG Volders) mit Schwerpunkt Ökologie, Abschluss mit Matura

Wissenschaftliche Projekte / Kollaborationen

Mai - September 2011	Identifizierung von Bakterien in industriell belastetem Wasser - Kollaboration der Universität Innsbruck mit der Firma Swarovski, Wattens